VOL.107 NO.GT3. MARCH 1981

JOURNAL OF THE GEOTECHNICAL ENGINEERING DIVISION

PROCEEDINGS OF
THE AMERICAN SOCIETY
OF CIVIL ENGINEERS

VOL.107 NO.GT3. MARCH 1981

JOURNAL OF THE GEOTECHNICAL ENGINEERING DIVISION

PROCEEDINGS OF
THE AMERICAN SOCIETY
OF CIVIL ENGINEERS

Copyright© 1981 by
American Society
of Civil Engineers
All Rights Reserved
ISSN 0093-6405

AMERICAN SOCIETY OF CIVIL ENGINEERS

BOARD OF DIRECTION

President
Irvan F. Mendenhall

Past President
Joseph S. Ward

President Elect
James R. Sims

Vice Presidents
Robert D. Bay — Lyman R. Gillis
Francis J. Connell — Albert A. Grant

Directors
Martin G. Abegg — Paul R. Munger
Floyd A. Bishop — William R. Neuman
L. Gary Byrd — Leonard S. Oberman
Larry J. Feeser — John D. Parkhurst
John A. Focht, Jr. — Celestino R. Pennoni
Sergio Gonzalez-Karg — Robert B. Rhode
James E. Humphrey, Jr. — S. Russell Stearns
Richard W. Karn — William H. Taylor
Leon D. Luck — Stafford E. Thornton
Arthur R. McDaniel — Robert E. Whiteside
Richard S. Woodruff

EXECUTIVE OFFICERS

Eugene Zwoyer, *Executive Director*
Julie E. Gibouleau, *Assistant to the Executive Director*
Louis L. Meier, *Washington Counsel/Assistant Secretary*
William H. Wisely, *Executive Director Emeritus*
Michael N. Salgo, *Treasurer*
Elmer B. Isaak, *Assistant Treasurer*

STAFF DIRECTORS

Donald A. Buzzell, *Managing Director for Education and Professional Affairs*
Robert A. Crist, Jr., *Managing Director for Publications and Technical Affairs*
Alexander Korwek, *Managing Director for Finance and Administrative Services*
Alexandra Bellow, *Director, Human Resources*
David Dresia, *Director, Publications Production and Marketing*
Barker D. Herr, *Director, Membership*
Richard A. Jeffers, *Controller*
Carl E. Nelson, *Director, Field Services*
Don P. Reynolds, *Director, Policy, Planning and Public Affairs*
Bruce Rickerson, *Director, Legislative Services*
James M. Shea, *Director, Public Communications*
Albert W. Turchick, *Director, Technical Services*
George K. Wadlin, *Director, Education Services*
R. Lawrence Whipple, *Director, Engineering Management Services*

COMMITTEE ON PUBLICATIONS

Stafford E. Thornton, *Chairman*
Martin G. Abegg — Richard W. Karn
John A. Focht, Jr. — Paul R. Munger
William R. Neuman

GEOTECHNICAL ENGINEERING DIVISION

Executive Committee
Robert Schuster, *Chairman*
Ernest T. Selig, *Vice Chairman*
William F. Swiger — Harvey E. Wahls
Robert T. Darragh, Jr., *Secretary*
Elio D'Appolonia, *Management Group E Contact Member*

Publications Committee
William F. Marcuson III, ***Chairman***
O. B. Andersland — Fred H. Kulhawy
Warren J. Baker — C. C. Ladd
Don C. Banks — Poul V. Lade
James M. Bell — Leonard J. Langfelder
Chandra S. Brahama — Felipe A. Len-Rios
John T. Christian — Gholamreza Mesri
G. W. Clough — Donald J. Murphy
Tuncer B. Edil — S. V. Nathan
Herbert H. Einstein — Thom L. Neff
Arley G. Franklin — Michael W. O'Neill
D. H. Gray — Jean H. Prevost
Bobby Hardin — Adel Saada
Cornelius J. Higgins — Surendra K. Saxena
William H. Highter — Robert L. Schiffman
Robert D. Holtz — Woodland G. Schockley
Izzat M. Idriss — Marshall L. Silver
L. H. Irwin — Glen S. Tarbox
Reuben H. Karol — G. R. Thiers
H. Y. Ko — D. D. Treadwell
William D. Kovacs — Charles R. Ulrich
Leland M. Kraft — J. Lawrence Von Thun
Raymond J. Krizek — R. N. Yong
E. T. Selig, *Exec. Comm. Contact Member*

PUBLICATION SERVICES DEPARTMENT

David Dresia, *Director, Publications Production and Marketing*

Technical and Professional Publications

Richard R. Torrens, *Manager*
Joseph P. Cerami, *Chief Copy Editor*
Linda Ellington, *Copy Editor*
Thea C. Feldman, *Copy Editor*
Meryl Mandle, *Copy Editor*
Joshua Spieler, *Copy Editor*
Shiela Menaker, *Production Co-ordinator*
Richard C. Scheblein, *Draftsman*

Information Services

Elan Garonzik, *Editor*

PERMISSION TO PHOTOCOPY JOURNAL PAPERS

Permission to photocopy for personal or internal reference beyond the limits in Sections 107 and 108 of the U.S. Copyright Law is granted by the American Society of Civil Engineers for libraries and other users registered with the Copyright Clearance Center, 21 Congress Street, Salem, Mass. 01970, provided the appropriate fee is paid to the CCC for all articles bearing the CCC code. Requests for special permission or bulk copying should be addressed to the Manager of Technical and Professional Publications, American Society of Civil Engineers.

CONTENTS

Vibration Tests of Full-Scale Earth Dam
by Ahmed M. Abdel-Ghaffar and Ronald F. Scott 241

Comparative Study of Dynamic Response of Earth Dam
by Ahmed M. Abdel-Ghaffar and Ronald F. Scott 271

Probabilistic Evaluation of Loads
by Wilson H. Tang 287

Design Considerations for Collapsible Soils
by Samuel P. Clemence and Albert O. Finbarr 305

Geotechnical Considerations for Construction in Saudi Arabia
by Issa Oweis and John Bowman 319

Safety of a Constructed Facility: Geotechnical Aspects
by T. William Lambe, W. Allen Marr, and Francisco Silva 339

This Journal is published monthly by the American Society of Civil Engineers. Publications office is at 345 East 47th Street, New York, N.Y. 10017. Address all ASCE correspondence to the Editorial and General Offices at 345 East 47th Street, New York, N.Y. 10017. Allow six weeks for change of address to become effective. Subscription price to members is $16.00. Nonmember subscriptions available; prices obtainable on request. Second-class postage paid at New York, N.Y. and at additional mailing offices. GT.

The Society is not responsible for any statement made or opinion expressed in its publications.

TECHNICAL NOTES

Proc. Paper 16073

Microgravity Surveys for Evaluation of Elevation Changes Due to Reservoir Impoundment
by Dwain K. Butler 355

DISCUSSION

Proc. Paper 16066

Strength and Deformability of Highly Fractured Rock,* by Jerome M. Raphael and Richard E. Goodman (Nov., 1979).
by J. Laginha Serafim 365
closure 366

Cyclic Shear Resistance of Noncohesive Soils,* by Edward G. Prater (Jan., 1980).
by Yoshiharu Moriwaki and Maurice S. Power 367
closure 370

Self-Boring Pressuremeter Study of San Francisco Bay Mud,* by G. Wayne Clough and Gordon M. Denby (Jan., 1980).
by Thomas C. Anderson and Robert G. Lukas 372
by J. C. P. Dalton 374
closure 375

Settlement Comparison Used in Tank-Failure Study,* by Roy A. Bell and Jun Iwakiri (Feb., 1980).
by Robert E. Bigham 377
closure 379

Repeated Loading on Single Piles in Sand,* by Sin-Fatt Chan and Thomas H. Hanna (Feb., 1980).
by N. K. Jain and Gopal Ranjan 380
closure 380

*Discussion period closed for this paper. Any other discussion received during this discussion period will be published in subsequent Journals.

16096 VIBRATION TESTS OF FULL-SCALE EARTH DAM

KEY WORDS: **Dams (earth); Dynamic characteristics; Dynamic stability;** Dynamic tests; Earth fills; Excitation; Experimental data; Measuring instruments; Natural frequency; Pressure waves; **Vibration measurement;** Vibration response; **Vibration tests**

ABSTRACT: Extensive full-scale dynamic tests, including ambient (unique in earth dam research) and forced vibration as well as popper tests were conducted on the Santa Felicia earth dam in Southern California. For the forced vibration tests, the dam was excited into resonance in both the upstream-downstream and longitudinal directions. During the ambient test, the naturally occurring vibrations of the dam were measured. The popper test involved the use of pressure waves originating from a controlled, submerged release of gas. During the tests, three-dimensional measurements of the motions of approximately 25 stations along the crest and seven stations on the downstream slope were recorded and then analyzed in both time and frequency domains. Modes of vibrations and associated natural frequencies as well as damping ratios were determined.

REFERENCE: Abdel-Ghaffar, Ahmed M., and Scott, Ronald F., "Vibration Tests of Full-Scale Earth Dam," *Journal of the Geotechnical Engineering Division,* ASCE, Vol. 107, No. GT3, **Proc. Paper 16096**, March, 1981, pp. 241-269

16097 DYNAMIC RESPONSE OF EARTH DAM

KEY WORDS: Damping; **Dams (earth); Dynamic characteristics; Dynamic response; Dynamic tests;** Earth fills; Earthquakes; Experimental data; Mathematical models; Natural frequency; Shear modulus; Shear strain; **Vibration tests**

ABSTRACT: Full-scale experimentally determined dynamic characteristics of an earth dam determined from imposed dynamic forces are compared with those estimated from earthquake responses. The measured frequencies and modes of upstream-downstream vibrations are compared with those predicted by an existing two-dimensional shear-beam model. Shear strains and shear moduli were estimated from the full-scale tests and were plotted along with those estimated from the earthquake response analysis. The same procedure was followed for damping versus shear strain at different levels. Then the combined results were interpolated and extrapolated. The dynamic properties of the dam's constituent materials estimated from low-strain full-scale tests are consistent with those determined from relatively large strains induced by the two earthquakes. Also the tests revealed substantial change in the dynamic properties of the dam; the behavior is typical of a yielding dynamic system.

REFERENCE: Abdel-Ghaffar, Ahmed M., and Scott, Ronald F., "Comparative Study of Dynamic Response of Earth Dam," *Journal of the Geotechnical Engineering Division,* ASCE, Vol. 107, No. GT3, **Proc. Paper 16097**, March, 1981, pp. 271-286

16100 PROBABILITIC EVALUATION OF LOADS

KEY WORDS: Dead loads; Earth pressure; **Earthquakes; Liquefaction;** Live loads; Offshore structures; Pore pressure; **Probability theory;** Random vibration; **Statistical analysis;** Wind forces

ABSTRACT: The loads that effect geotechnical designs are reviewed, characterizing the uncertainties in each load component. Probabilistic models for evaluating each component are examined. Whenever data are available, the level of variabilities and uncertainties associated with the effect of each component on the foundation is assessed. Satisfactory performance of a geotechnical system relies, in part, on a good understanding of the characteristics of the loads and environments to which the system is subjected. Uncertainties do exist in these factors. For dynamic loads due to earthquake excitation and wave action, both their magnitude and frequencies of occurrences over the expected duration of the system could not be known. The long-term stability of soil slope would also be dependent on stochastic fluctuation of the pore pressure due to seasonal variation and other temporal changes in the environment.

REFERENCE: Tang, Wilson H., "Probabilistic Evaluation of Loads," *Journal of the Geotechnical Engineering Division,* ASCE, Vol. 107, No. GT3, **Proc. Paper 16100**, March, 1981, pp. 287-304

16106 DESIGN CONSIDERATIONS FOR COLLAPSIBLE SOILS

KEY WORDS: Bearing capacity; **Collapsible soils; Design; Design practices; Foundation design;** Loess; Settlement analysis; Shallow foundations; Stabilization

ABSTRACT: Metastable or collapsible soils are defined as any unsaturated soil that goes through a radical rearrangement of particles and great loss of volume upon wetting, with or without additional loading. The existing types of collapsible soils and theories developed to explain collapse phenomenon are reviewed, as are the methods of recognizing collapsible soils in the field and laboratory. Prediction techniques for the magnitude of collapse are presented and summarized; current foundation design methods on collapsible soils are explored. Finally, present methods for the stabilization of collapsible soils and possible future methods of treatment are reviewed.

REFERENCE: Clemence, Samuel P., and Finbarr, Albert O., "Design Considerations for Collapsible Soils," *Journal of the Geotechnical Engineering Division,* ASCE, Vol. 107, No. GT3, **Proc. Paper 16106**, March, 1981, pp. 305-317

16092 GEOTECHNICAL CONSIDERATIONS IN SAUDI ARABIA

KEY WORDS: **Construction materials; Construction planning; Construction procedure;** Corrosion; Foundations; **Geological surveys; Geotechnical engineering;** Rocks; Salinity; **Saudi Arabia; Soil mechanics**

ABSTRACT: Several geologic environments prevail in Saudi Arabia. Problems in design and construction are intimately related to the environment at particular locations. Coastal areas are generally characterized by particularly soft and loose corrosive soils. Limestones in the interior are characterized by the potential for the presence of dry cavities and solution channels. Igneous and metamorphic rocks of good bearing quality characterize the high mountains overlooking the west coast; superimposed areas of sand dunes and salt flats could present special foundation problems. The availability of construction materials depends on bedrock geology and varies from relatively good in the western areas to poor in the eastern region. Offshore conditions in western coastal areas are characterized by varied subsurface conditions at relatively short distances, affecting the design of offshore facilities.

REFERENCE: Oweis, Issa, and Bowman, John, "Geotechnical Considerations for Construction in Saudi Arabia," *Journal of the Geotechnical Engineering Division,* ASCE, Vol. 107, No. GT3, **Proc. Paper 16092**, March, 1981, pp. 319-338

16107 GEOTECHNICAL ASPECTS OF FACILITY SAFETY

KEY WORDS: Earth dams; Earth dam seepage; **Facilities; Geotechnical engineering;** Pore water pressure; Risk prediction (accidents); **Safety;** Safety design; **Safety engineering;** Safety research; **Stability**

ABSTRACT: An approach is presented to ensure the safety of a constructed facility by outlining, discussing, and illustrating various components of a comprehensive safety program. When dealing with important complex geotechnical facilities, experience clearly shows that the geotechnical profession cannot feasibly create a facility which completely fulfills all performance criteria for the entire life of the facility. Rather, the only logical approach is to engineer a facility for its design life, i.e., create a reasonable design, construct the facility according to the design, and then execute an appropriate ongoing safety program. The comprehensive safety program consists of nine components. These components are described, and several are illustrated, using experience from actual project.

REFERENCE: Lambe, T. William, Marr, W. Allen, and Silva, Franciso, "Safety of a Constructed Facility: Geotechnical Aspects," *Journal of the Geotechnical Engineering Division,* ASCE, Vol. 107, No. GT3, **Proc. Paper 16107**, March, 1981, pp. 339-352

JOURNAL OF THE GEOTECHNICAL ENGINEERING DIVISION

VIBRATION TESTS OF FULL-SCALE EARTH DAM

By Ahmed M. Abdel-Ghaffar,[1] A. M. ASCE and Ronald F. Scott,[2] M. ASCE

INTRODUCTION

Full-scale experimentally determined dynamic characteristics are required both to improve the techniques by which such properties are calculated for purposes of analysis and design, and to permit interpretation of the measured response of earth dams in the event of a strong earthquake. In addition, as information on the dynamic characteristics of dams and their earthquake response accumulates, it should be possible to develop better procedures for determining the appropriate levels of earthquake loading for design.

This paper concerns full-scale dynamic tests, including ambient (unique in earth dam research) and forced vibration as well as popper tests (12), that were carried out on Santa Felicia Dam in southern California subsequent to the study of the dam's response to two earthquakes (3 and 4). A description of the dynamic field tests and a review of the results are briefly presented; a companion paper (2) compares the dynamic properties determined herein from the full-scale tests and those estimated previously from the measured responses to the two earthquakes (3 and 4).

Some notable improvements in these tests, added since most previous earth dam tests (6, 10, 11, and 13) were made, are: (1) Ambient vibration measurements; (2) the popper test (previously proved very efficient in testing arch and gravity dams); (3) longitudinal shaking of the dam, and determination of the dynamic properties in the longitudinal direction not only from the forced vibration tests but also from the ambient tests (the data obtained have great potential for future research); (4) measurement of the modal three-dimensional response of the dam; and (5) availability of usable earthquake response records to compare with the full-scale low-level induced response measurements. A detailed de-

[1] Asst. Prof., Civ. Engrg. Dept., Princeton Univ., Princeton, N.J. 08544.
[2] Prof. of Civ. Engrg., California Inst. of Tech., Pasadena, Calif.

Note.—Discussion open until August 1, 1981. Separate discussions should be submitted for the individual papers in this symposium. To extend the closing date one month, a written request must be filed with the Manager of Technical and Professional Publications, ASCE. Manuscript was submitted for review for possible publication on April 17, 1980. This paper is part of the Journal of the Geotechnical Engineering Division, Proceedings of the American Society of Civil Engineers, ©ASCE, Vol. 107, No. GT3, March, 1981. ISSN 0093-6405/81/0003-0241/$01.00.

scription of the vibration tests presented herein can be found in the original report (1).

Description of Dam

Santa Felicia Dam (Figs. 1 and 2) is a modern rolled-fill embankment built in 1955. It is 273 ft (83 m) high above its lowest foundation and 200 ft (61 m) above the original stream bed; it is 450 ft (137 m) long across the valley at the base and 1,275 ft (389 m) long at the crest. The dam has a central impervious core and pervious shells upstream and downstream. The core and shell materials are basically alluvial, consisting of clays, sands, gravel, and boulders. A more complete description of the dam is given in Refs. 1 and 3.

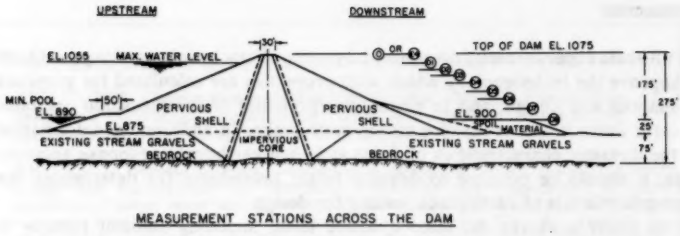

FIG. 1.—Cross Section of Santa Felicia Dam Showing Measurement Stations on Downstream Face (1 ft = 0.305 m)

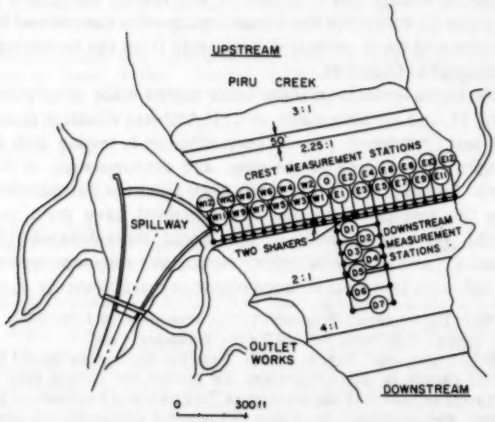

FIG. 2.—Plan View Showing Measurement Stations and Location of Two Shakers (1 ft = 0.305 m)

Description of Instrumentation

The essential features of the instrumentation are substantially the same as those used in previous full-scale tests and have been described in detail in other references (8, 9, 10, and 11). It basically consists of: (1) Motion sensing transducers (SS-1 seismometers by Kinemetrics, Inc.); (2) recording instruments including signal conditioners (SC-1 also by Kinemetrics, Inc.), and oscillograph recorder (7418A by Hewlett-Packard), and instrumentation tape recorders (3460A by Hewlett-Packard); (3) force generating systems or shaking machines capable of producing a force up to 10,000 lbs (44,500 N) [designed at California Institute of Technology (Caltech) and manufactured by Kinemetrics, Inc.]; and (4) data processing instruments including an electronic analog-digital converter (DDS-1103 by Kinemetrics) and a digital signal processor (SD360 manufactured by Spectral Dynamics Corp.).

Experimental Setup

The crest was apportioned into 25 measurement stations at intervals of approx 50 ft (15 m) (Fig. 1); these stations were designated by E1–E12 for the eastern half and W1–W12 for the western half, with the center station designated 0. There were two arrays of measurement stations on the downstream slope (Figs. 1 and 2), each consisting of seven stations [at intervals of approx 50 ft (15 m) along the slope]; one array was along the midpoint cross section, for measurement of symmetric modes, while the other was even with station E4, for measurement of antisymmetric modes. One vibration generator was mounted at station E2, and the other was placed at station W2 [the two stations were 200 ft (61 m) apart, Fig. 2]. The aforementioned recording instruments were placed in the central region of the crest between the two shakers (close to station 0).

Forced Vibration Test

Upstream-Downstream Vibration

Experimental Procedure and Results.—The dam was excited into resonance in various modes in the upstream-downstream (U-D) direction by the coupled pair of mechanical shakers. Symmetric and antisymmetric vibrations were obtained by synchronizing the two shakers to run in-phase and 180° out-of-phase, respectively, with the aid of a precise and stable control system. The measurements taken (in the frequency range 1.0 Hz–6.0 Hz) on the dam included, as a first step, the determination of the natural frequencies (via frequency sweeps), preliminary modal damping ratios and mode shapes along the crest and the downstream face. Eight seismometers, located at selected measurement stations to cover the entire dam crest and downstream face, were used to pick up the steady-state vibrations of the dam; they were oriented in the direction of the exciting harmonic force. In addition to the measurement of 17 modes in the U-D direction, eight modes of vibration of the dam's three-dimensional (3-D) response were measured using six seismometers (three were placed at the reference station W1, where they remained throughout the tests while the other three were moved from station to station). Fig. 3 summarizes the instrumen-

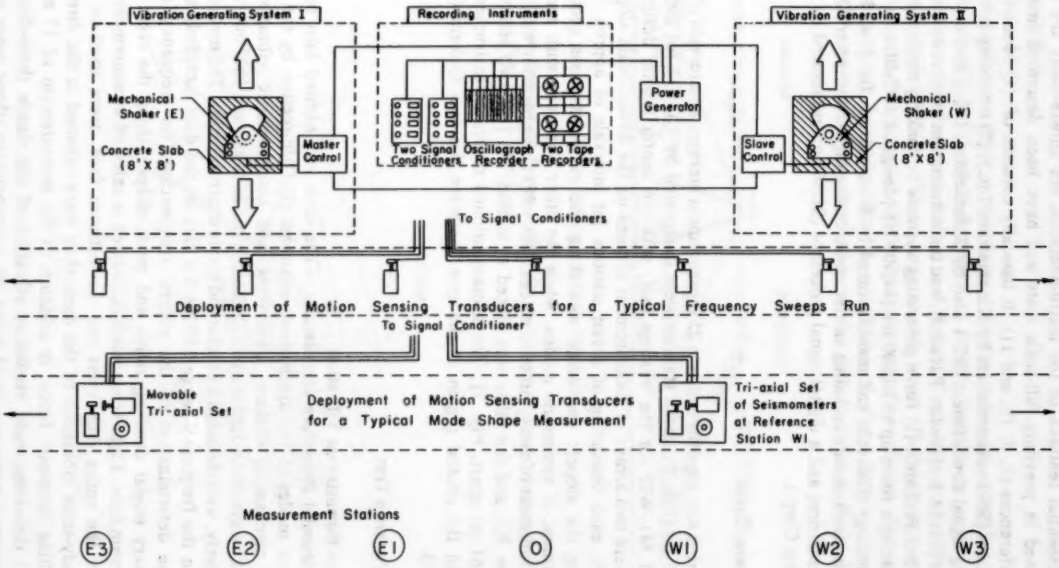

FIG. 3.—Schematical Diagram Showing Experimental Setup

tation used in the tests, the measuring procedures and the experimental setup of the frequency sweeps as well as the 3-D mode measurements on the dam.

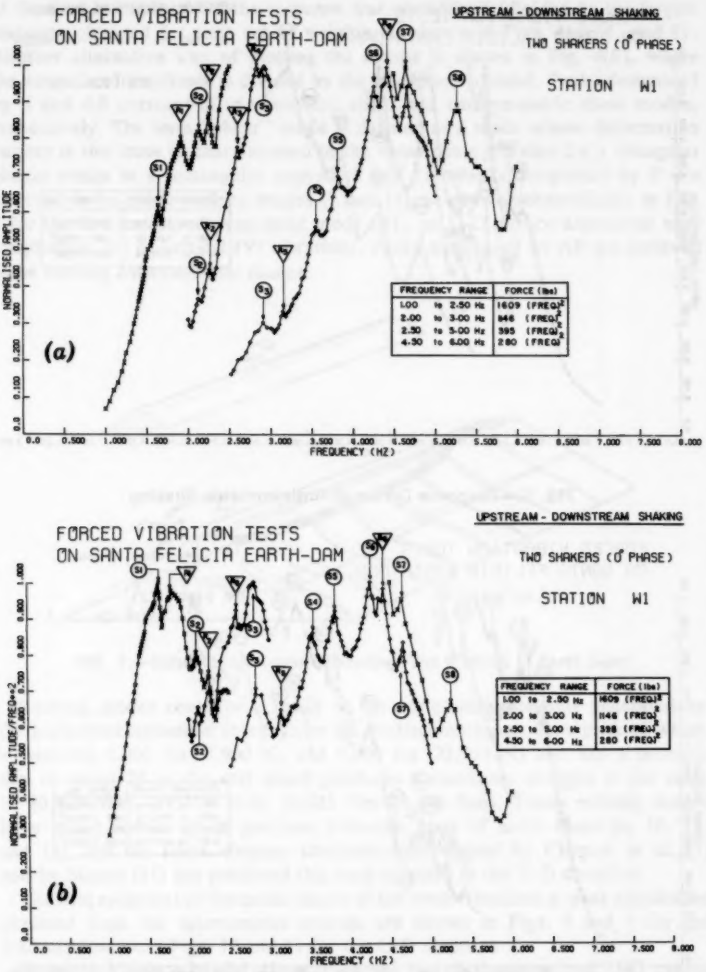

FIG. 4.—Symmetric Shaking: (*a*) Response Curves; (*b*) Normalized Response Curves

Resonance Curves and Modes of Vibration.—Figs. 4, 5, and 6 show some of the resonance curves determined for three selected stations. Discontinuities

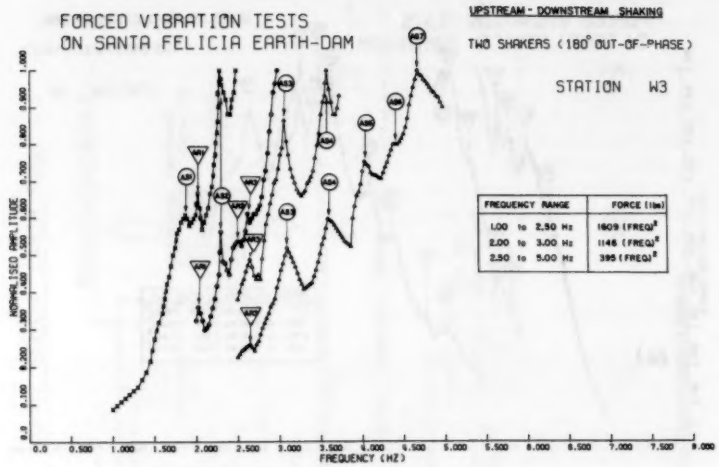

FIG. 5.—Response Curves of Antisymmetric Shaking

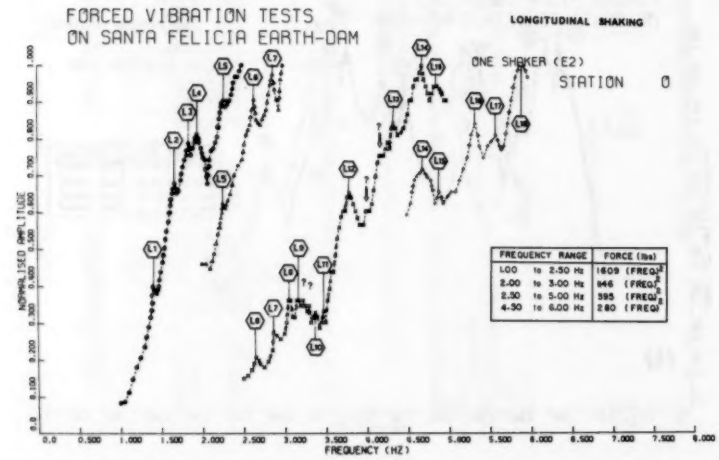

FIG. 6.—Response Curves of Longitudinal Shaking

in these curves resulted when changes were made in the weight combinations used in the shakers; the force level (or the weight combinations) for each segment of the curves is indicated on the figures. In plotting these curves, the magnitude of the double-amplitude of the response was normalized [divided by the largest response obtained for each set of weights, as shown in Figs. 4(*a*), 5, and 6]. Another alternative way of plotting the results is shown in Fig. 4(*b*), where the normalized amplitude is divided by the frequency squared. Peaks designated by S and AS correspond to symmetric shear and antisymmetric shear modes, respectively. The term "shear" mode is defined as a mode whose deformation pattern is the same as that assumed in the shear-beam theories for a triangular elastic wedge in a rectangular canyon (5 and 11). Peaks designated by R are believed to be either rocking modes (7 and 11), as shown schematically in Fig. 7 for the first measured symmetric mode (R1), or U-D motion associated with longitudinal (L) or vertical (V) vibrations. Peaks designated by AR are believed to be rocking antisymmetric modes.

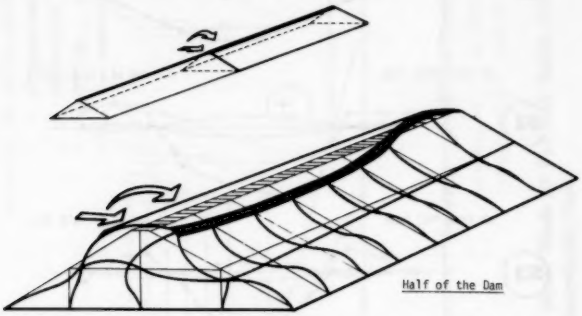

FIG. 7.—Schematic Diagram Showing First R Mode of Earth Dam

Rocking modes could be a result of the vibrational moments generated by the horizontal sinusoidal forces from the shaking machines, each peak of which is between 2,000 lbs (8,900 N) and 5,000 lbs (22,250 N) and has a moment arm of about 20 in. (51 cm) which produces a maximum moment at the crest of 80,000 lb-in.–200,000 lb-in. (2,035 Nm–22,606 Nm). These rocking modes have never shown up in previous full-scale tests of earth dams (6, 10, 11, and 13), but the finite element idealization developed by Chopra, et al. (7) and by Martin (11) has predicted this kind of mode in the U-D direction.

The best estimates of the mode shapes of the crest vibrations at peak amplitudes obtained from the seismometer records are shown in Figs. 8 and 9 for the 3-D response, and Figs. 10 and 11 for the U-D response.

Damping Values.—Modal damping values for all the measured U-D modes were determined by the logarithmic decrement method, applied to recordings of the damped free vibration of the dam (immediately after discontinuing the power to the vibration generating system). This method was used because the width of the modal peaks of the resonance curves were generally not suitable for the determination of modal damping values by the half-power band width

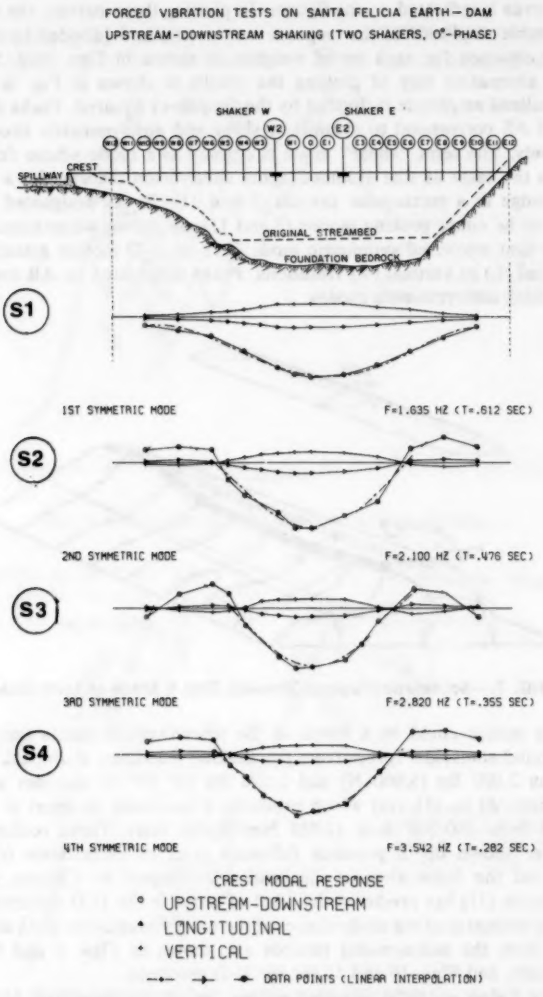

FIG. 8(*a*).—First Four Measured S Shear Mode Shapes (Note: Mode S2 Has Two Nodes along Crest, while Mode S3 Has Four Nodes along Crest): Three-Dimensional Measurements along Crest

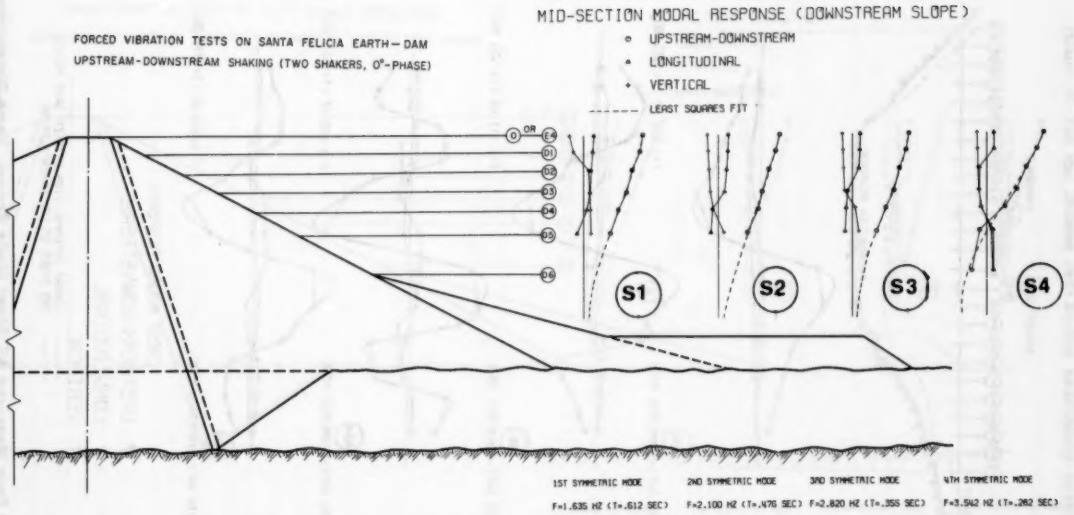

FIG. 8(*b*).—First Four Measured S Shear Mode Shapes (Note: Mode S2 Has Two Nodes along Crest, while Mode S3 Has Four Nodes along Crest): Three-Dimensional Measurements along Downstream Face

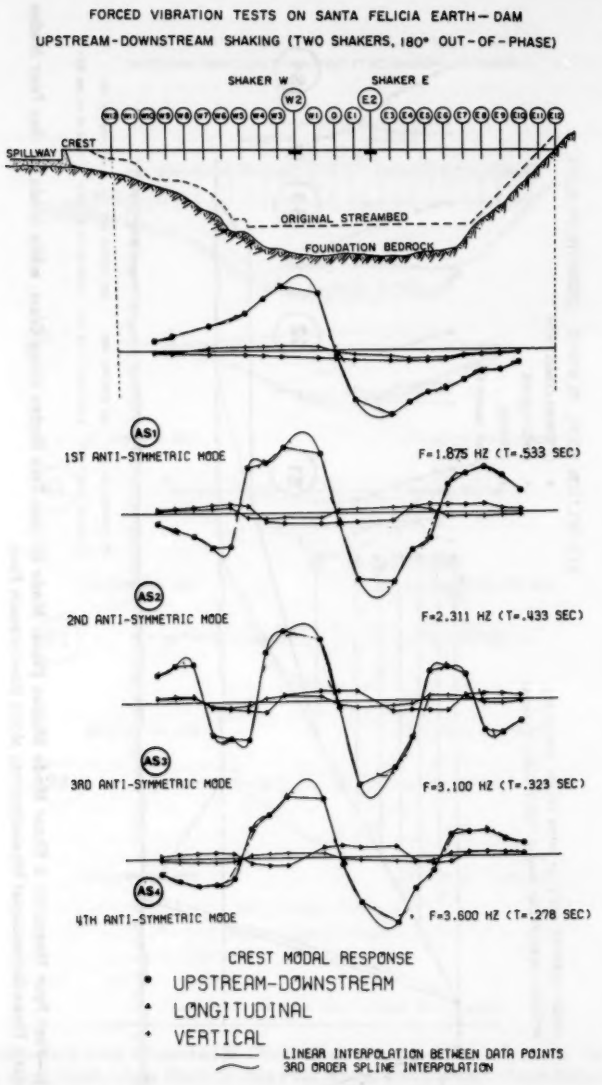

FIG. 9(*a*).—First Four Measured AS Shear Mode Shapes: Three-Dimensional Measurements along Crest

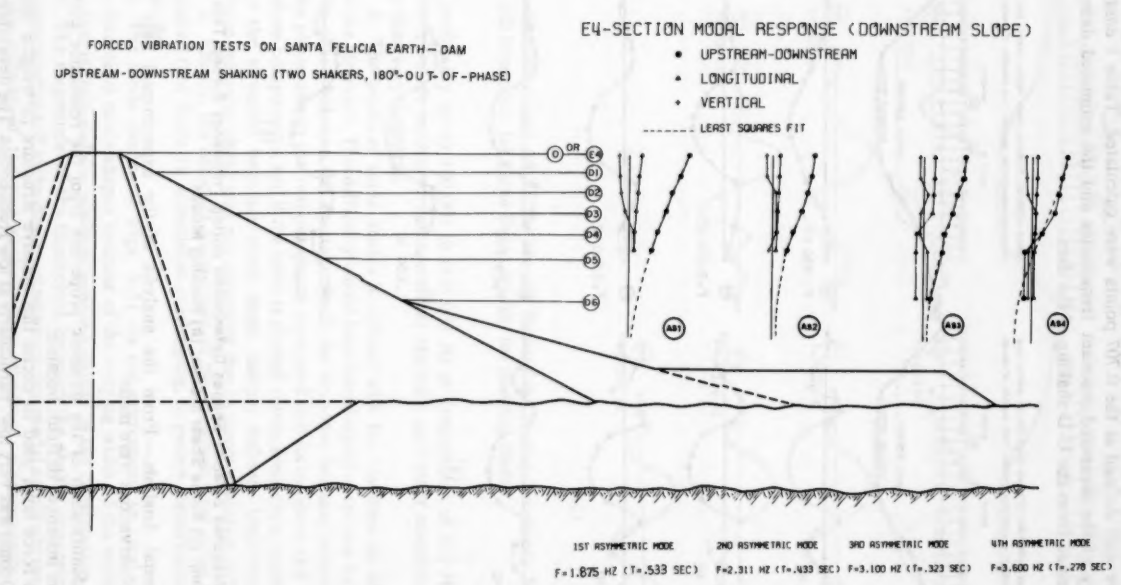

FIG. 9(*b*).—First Four Measured AS Shear Mode Shapes: Three-Dimensional Measured along Downstream Face

method. However, modal damping for a few modes where the spectral or modal peaks were well defined at the 0.707 points were calculated. Table 1 contains a summary of the measured resonant frequencies and the estimated damping ratios obtained from the U-D shaking of the dam.

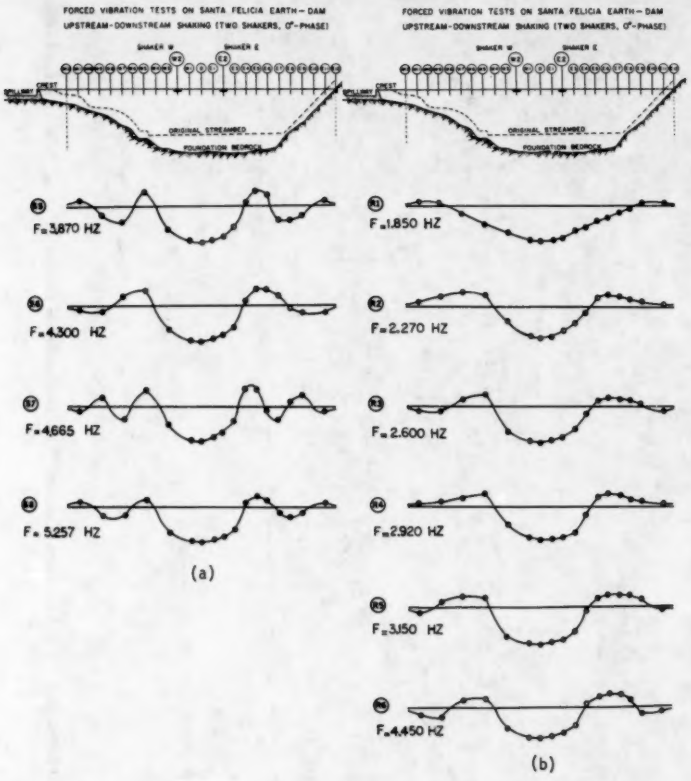

FIG. 10.—Measured S Mode Shapes Determined during Frequency Sweep Test (in U-D Direction): (*a*) Some Shear Modes; (*b*) Rocking Modes

Experimental Analysis.—From the analysis of the experimental data the following observations were made:

1. The identification of the dynamic properties from the resonance curves was in some instances difficult because:

a. The force level used to excite this massive structure (it weights about 6,000,000 tons) was very low, particularly at low frequencies. The development of a new, large vibration generator capable of producing very large forces

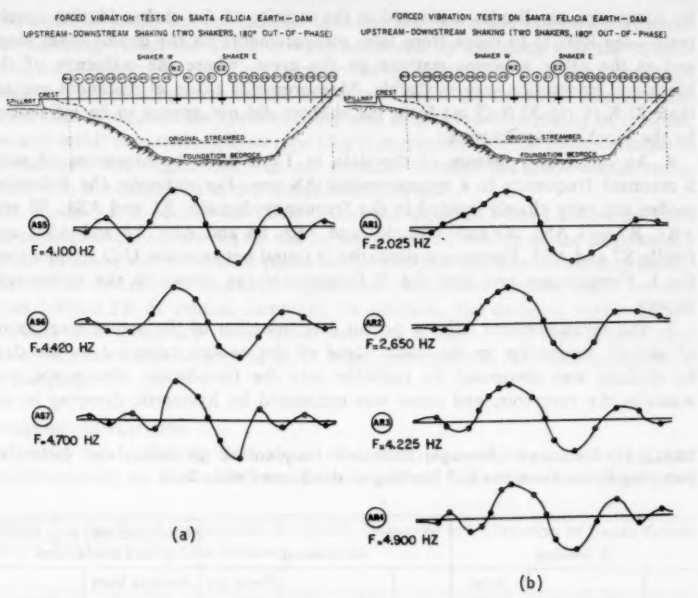

FIG. 11.—Measured AS Mode Shapes Determined during Frequency Sweep Test (in U-D Direction): (*a*) Some Shear Modes; (*b*) Rocking Modes

[preferably up to 100,000 lb (445,000 N) at frequencies of 0.3 Hz–2.0 Hz] for full-scale testing of dams, nuclear reactors, and other massive structures is thus very desirable.

b. The peaks of some modes interfered with the response at other modes of the structure. This difficulty would have been largely overcome by measuring the phase between the excitation and the response because measurement of the phase allows the response to be separated into its in-phase and 90°-out-of-phase components, and if the latter is plotted versus frequency, each resonance of the structure becomes much more sharply defined. Unfortunately, this force-response phase was not measured due to instrumentation difficulties.

c. Finally, the resonant frequencies of the structure were often too closely spaced (see Table 1), sometimes overlapping, to permit identification of every mode.

2. The mode shapes of Figs. 8–11 do not correspond to ideal versions of the sinusoidal mode shapes because of the varying width of the valley in which the dam is built and the nonhomogeneous nature of the construction materials.

3. The magnitude of the interaction between the shaker concrete block and the surrounding soil in the dam crest was such that modal amplitude measurements in the vicinity of the two shakers were distorted. Consequently, the modal amplitudes of Figs. 8–11 at shaker Stations E2 and W2 were modified (reduced)

by comparing amplitudes measured in the vicinity of the shaker (during special tests—see Ref. 1) to those from later measurements on the downstream slope and at the other adjacent stations on the crest, where the influence of the block-soil interaction was negligible. Measurements taken at distances greater than 20 ft (6 m)–30 ft (9 m) from the shakers did not appear to be influenced by the block-soil interaction.

4. An interesting feature of the data in Table 1 is the closeness of each S resonant frequency to a corresponding AS one. For example, the following modes are very closely spaced in the frequency domain: R1 and AS1, S2 and AR1, R2 and AS2, S3 and AR2, R5 and AS3, S4 and AS4, R6 and AS6, and finally S7 and AS7. Frequency similarity is found between the U-D frequencies, the L Frequencies and also the V frequencies (as shown in the companion paper).

5. The measurements did not permit determination of the actual mechanism of energy dissipation in the dam. Some of the energy imparted to the dam by shaking was dissipated by radiation into the foundation, abutments, and water in the reservoir, and some was consumed by hysteretic damping in the

TABLE 1.—Measured (Average) Resonant Frequencies (in Hertz) and Estimated Damping Ratios from the U-D Shaking of the Santa Felicia Dam

S Shaking			AS Shaking			Measured Damping Ratio, as a percentage	
Mode (1)	Measured frequency, in Hertz (2)	Total force, in pounds (3)	Mode (4)	Measured frequency, in Hertz (5)	Force per shaker, in pounds (6)	Average from damped free vibration (7)	From response curves (8)
S1	1.64	4,301	—	—	—	3.2	—
R1	1.85	5,507	—	—	—	3.1	—
—	—	—	AS1	1.88	2,829	3.0	—
—	—	—	AR1	2.03	3,299	3.1	—
S2	2.10	7,096	—	—	—	2.9	4.5
R2	2.27	8,291	—	—	—	3.0	—
—	—	—	AS2	2.30	4,256	2.9	4.9
R3	2.60	7,747	—	—	—	2.7	—
—	—	—	AR2	2.65	4,024	2.8	4.7
S3	2.84	9,243	—	—	—	2.6	4.8
R4	2.92	9,771	—	—	—	2.7	—
—	—	—	AS3	3.10	1,898	2.7	4.8
R5	3.15	3,919	—	—	—	2.6	—
S4	3.55	4,978	—	—	—	2.5	3.5
—	—	—	AS4	3.60	2,555	2.4	3.8
S5	3.87	5,915	—	—	—	2.3	3.9
—	—	—	AS5	4.10	3,320	2.5	—
—	—	—	AR3	4.23	3,526	2.3	—
S6	4.30	7,304	—	—	—	2.2	—
—	—	—	AS6	4.42	3,859	2.1	—
R6	4.45	7,822	—	—	—	2.2	—
S7	4.67	8,578	—	—	—	2.0	2.7
—	—	—	AS7	4.70	4,363	1.8	2.7
—	—	—	AR4	4.90	4,742	2.0	—
S8	5.26	7,738	—	—	—	1.9	3.8

dam material itself, but the relation between the two could not be determined. The damping values (of Table 1) were estimated by assuming that the system is basically linear. In order to estimate the damping of a nonlinear dam-type structure, the exciting force should be plotted against the structural displacement of the dam to produce the hysteretic response at the modal frequency of interest; the area inside the resulting hysteretic loop is proportional to the energy dissipated by the structure. Again this was not possible because the force-displacement phase was not measured in the forced vibration test.

6. Finally, it is seen from Table 1 that the damping values estimated from the resonance curves are higher and so less reliable (because of the interference of the in-phase and 90°-out-of-phase modal components mentioned previously) than those determined from the logarithmic decrement method (seen to vary from 1.8%–3.2% of critical damping). In addition, the damping ratios do not increase with frequency (they rather decrease a little). This may suggest that the hysteretic contribution was more important than the radiation contribution to damping.

Longitudinal Vibration

During the L shaking (last phase of testing) one of the two shakers was malfunctioning so the other one was used alone; also, time was limited due

TABLE 2.—Resonant Frequencies (in Hertz), Observed in L Direction of Santa Felicia Dam (L Shaking Using One Shaker)

Representative natural frequency, in Hertz (1)	Designation (2)	Total force, in pounds (3)
1.43	L1	1,634
1.68	L2	2,257
1.85	L3	2,753
1.95	L4	3,059
2.16	L5	3,736
2.28	possible	4,164
2.43	possible	4,731
2.63	L6	3,948
2.88	L7	4,736
3.05	L8	1,837
3.15	L9	1,960
3.23	possible	2,061
3.35	L10	2,216
3.48	L11	2,392
3.78	L12	2,815
4.03	possible	3,199
4.18	possible	3,443
4.37	L13	3,772
4.70	L14	4,363
4.88	L15	4,694
5.35	L16	4,007
5.60	L17	4,390
5.90	L18	4,873

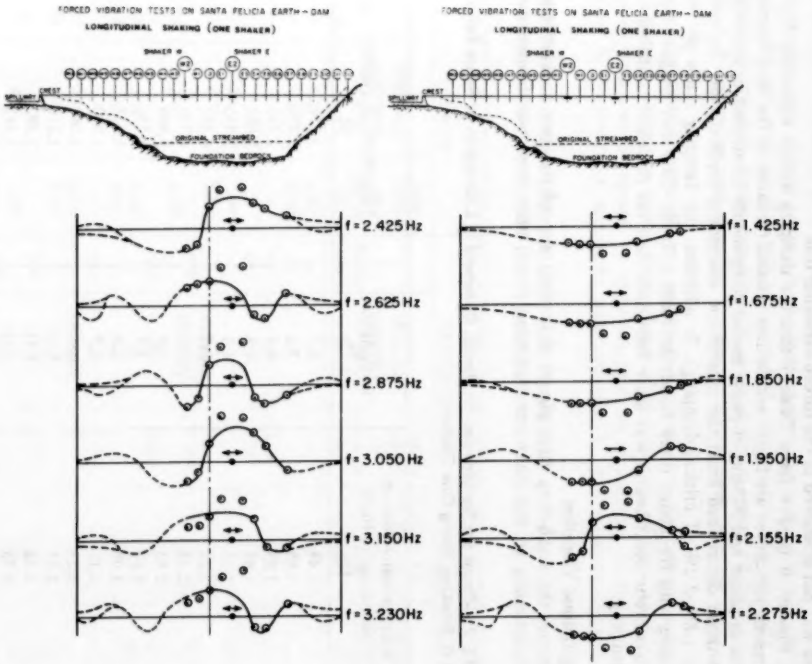

FIG. 12.—Estimation of Some of Resonating Modes Obtained during L Frequency Sweeps (One Shaker Was Used)

to expiration of the test permit, so the measurements of L shaking (unique in earth dam research) were not extensive. Nonetheless, the resonance curves and the preliminary modes (of about half the dam crest) were useful. Table 2 summarizes all resonant frequencies of major peaks recorded at selected stations; because only eight seismometers were used during this shaking, it was difficult to completely determine several modes corresponding to the resonant frequencies of Table 2. In addition, it was not possible to distinguish between S and AS mode shapes. However, Fig. 12 shows estimations of some of the modes (up to about 3.0 Hz) obtained during the L frequency sweeps (the solid lines connecting the data points of Fig. 12 are estimates of the modal configuration, while the dashed lines represent possible extrapolations); the local magnification effect of the soil surrounding the shaker block is also shown.

From Table 2 and Fig. 12 the following observations can be made:

1. There are many closely spaced resonant frequencies in the L direction. And, some L resonant frequencies are very close (even identical) to some of the U-D frequencies. Examples of these are: L2(1.675) and S1(1.635); L3(1.850) and R1(1.850); L(2.275) and R2(2.270) and AS2(2.30); L6(2.625) and R3(2.60) and AR2(2.650); L7(2.875) and R4(2.920); and L8(3.05) and AS3(3.100). (Frequencies separated by 0.05 Hz or less are defined as "close.") This proximity may suggest a strong coupling between the U-D and L vibrations, or it may suggest that due to both the eccentricity of the single shaker (it was not located on the L-axis of the dam) and the fact that the dam is not symmetrical, the U-D modes containing significant L motions were excited.
2. Some of the incomplete L mode shapes are similar to the L components of the 3-D motions recorded during the U-D shaking; examples of these are: L2(1.675) and S1(1.635), L3(1.850) and AS1(1.875), L4(1.950) and S2(2.100), L(2.275) and AS2(2.300), L6(2.625) and S3(2.82), L9(3.150) and AS3(3.100), and finally L12(3.775) and both S4(3.540) and AS4(3.600).

It is apparent from these observations that it was very difficult to tell, from the data available, whether a given mode was purely L, associated with a U-D mode, or a 3-D mode.

Ambient Vibration Tests

Fourier Amplitude Spectra (FAS).—The naturally occurring vibrations of the dam (U-D as well as 3-D motions) caused by strong winds (of speeds ranging from 10 mph–40 mph) and by the spilling of the reservoir, were measured during the ambient tests. These ambient tests were conducted over 7 days, which allowed the stationarity of the records to be examined. Samples of the Fourier amplitude spectra (FAS) of the recorded motions (at different stations and on different days) are shown in Figs. 13, 14, and 15. These figures have been chosen as best exemplifying the basic trends seen in all the analyses and comparisons (for more detail see Ref. 1); the frequency resolution in all the FAS was 0.0073 Hz which proved to be high resolution. Phase, cross power, and cross correlation spectra (obtained by the digital signal processor) between different stations were used to determine the sign (in-phase or 180°-out-of-phase) of the modal amplitudes, facilitating identification of the modes of vibration

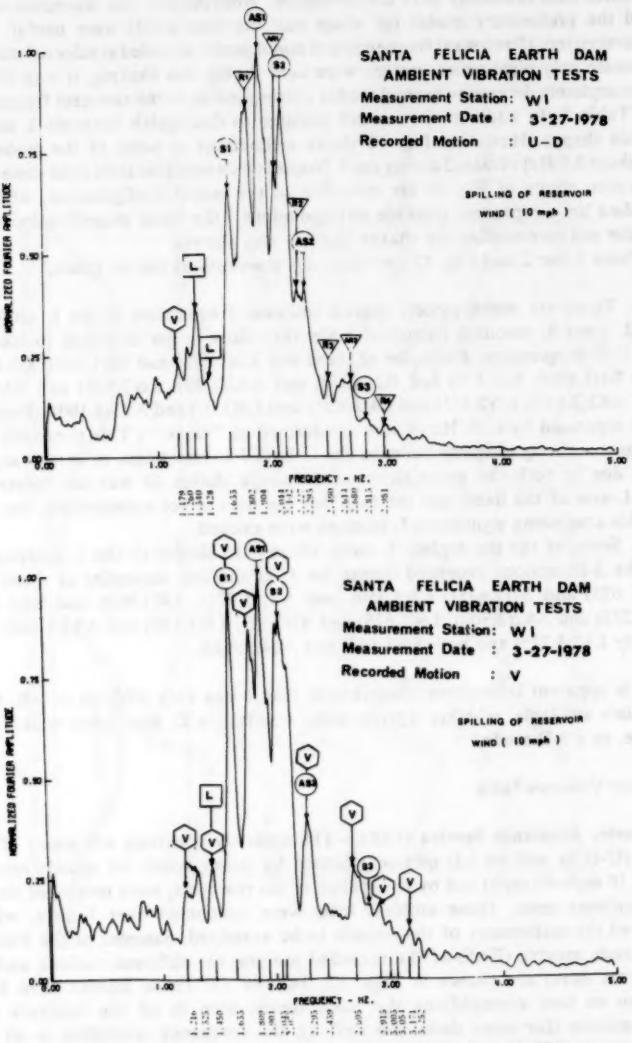

FIG. 13.—FAS of Velocity Proportional Response of Three Orthogonal Directional Motions Recorded, Simultaneously, at Station W1 on Crest of Dam

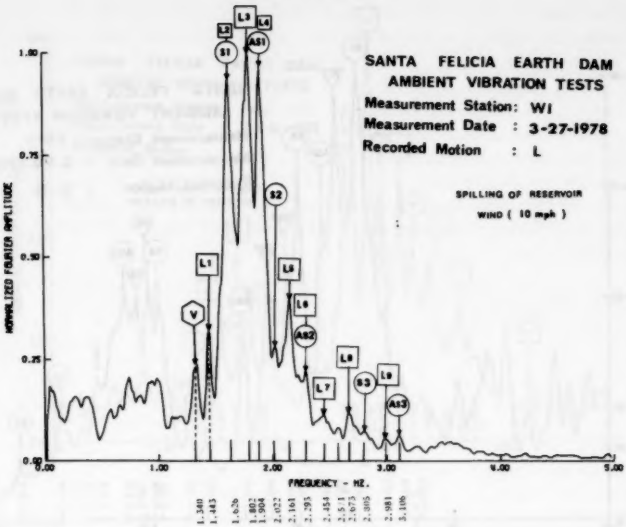

FIG. 13.—*Continued*

as shown in Figs. 13, 14, and 15. Table 3 summarizes the average resonant frequencies for the dam in the three orthogonal directions; although the differences of the frequency values in this table are small, they are distinct. The table also contains the estimated damping ratios for the U-D direction.

Analysis.—From the analysis of the ambient vibration results, the following observations can be made:

1. Most of the FAS contain peaks at common frequencies, but there are some exceptions. One possible explanation is that several modes of vibration were excited in varying degrees from one test (or station) to the other because of the random nature of wind loads (distributed over the surface of the structure) and the water flowing over the spillway. As will be covered in the companion paper, the natural frequencies and modes of vibration are influenced by the point of application of the loading (as well as by its magnitude). Also, changes in frequency due to structural nonlinearity are quite noticeable when comparing ambient with forced vibrations, but from one ambient level of excitation to another these changes are relatively very small (less than 10%).

2. The ambient vibration mode shapes were determined in the same way as were the forced vibration mode shapes, and these modes were almost identical to those resulting from the forced vibration tests, so only the natural frequencies (which did vary with the level of excitation) of the ambient modes are presented here.

3. Often the FAS obtained appear to have common spectral peaks in the three orthogonal directions (U-D, L, and V); i.e., during the ambient vibration

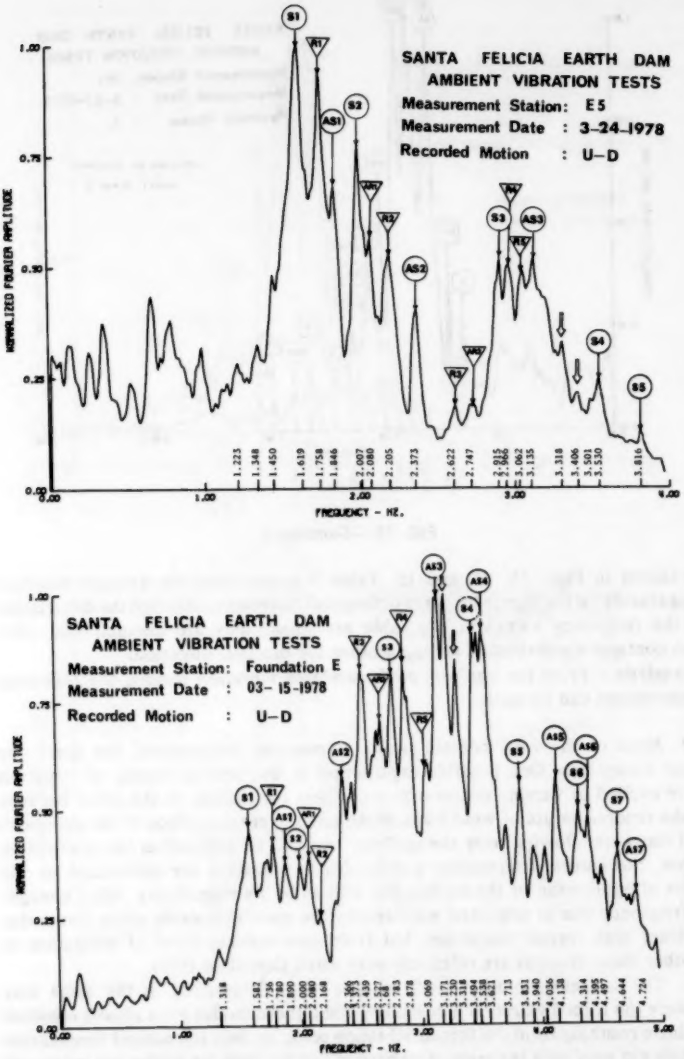

FIG. 14.—FAS of U-D Motion Recorded at Different Stations on Two Different Days

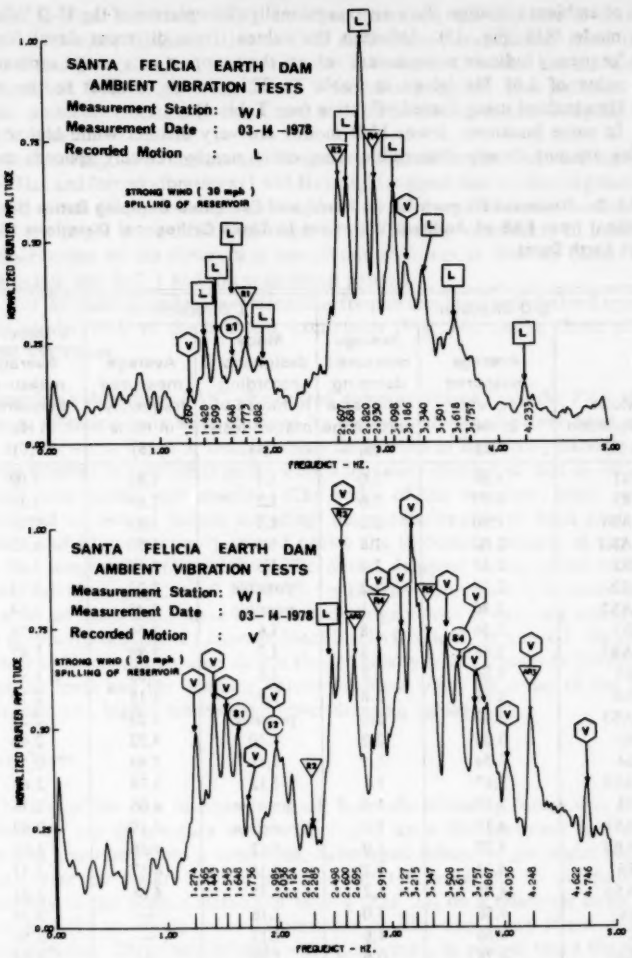

FIG. 15.—FAS of L and V Motions Recorded Simultaneously at Same Station

excitations the dam sometimes exhibited motion which dominated all three orthogonal directions (Fig. 13). The V component in most cases shows a more complicated spectral pattern than the two horizontal components, exhibiting several major peaks in addition to those common to the horizontal directions (Fig. 15).

4. Unlike the results obtained from resonant curves of forced vibration, the

FAS of ambient vibration show an exceptionally clear picture of the U-D "shear" first mode (S1) (Fig. 15). Although the values (from different days) for the first frequency indicate nonconstant values, they support an average representative value of 1.61 Hz (given in Table 3). This is very similiar to the value 1.64 Hz obtained using forced vibration (see Table 1).

5. In some instances, lower U-D modes are very distinct while higher U-D modes are not clearly discernible from other nearby (closely spaced) modes

TABLE 3.—Resonant Frequencies (in Hertz) and Estimated Damping Ratios (for U-D Direction) from FAS of Ambient Vibrations in Three Orthogonal Directions (Santa Felicia Earth Dam)

U-D Direction			L Direction		V Direction
Mode designation (1)	Average measured frequency, in Hertz (2)	Average measured damping ratio, as a percentage (3)	Mode designation according to forced vibration tests (4)	Average measured frequency, in Hertz (5)	Average measured frequency, in Hertz (6)
S1	1.61	3.0	L1	1.45	1.00
R1	1.77	2.6	L2	1.64	1.13
AS1	1.90	2.5	L3	1.85	1.26
AR1	2.02	1.9	L4	1.99	1.35
S2	2.10	2.4	L5	2.18	1.46
R2	2.21	2.2	possible	2.32	1.54
AS2	2.36	2.1	possible	2.45	1.64
R3	2.56	1.8	L6	2.64	1.76
AR2	2.68	1.8	L7	2.88	1.87
S3	2.84	1.6	L8	3.03	1.98
R4	2.98	1.8	L9	3.15	2.10
AS3	3.17	2.0	possible	3.23	2.26
R5	3.23	2.2	L10	3.32	2.40
S4	3.54	1.5	L11	3.49	2.52
AS4	3.67	1.1	L12	3.78	2.64
S5	3.87	1.4	possible	4.05	2.76
AS5	4.15	1.2	possible	4.19	2.92
AR3	4.22	1.0	L13	4.36	3.04
S6	4.33	1.2	L14	4.67	3.11
AS6	4.45	1.2	L15	4.88	3.21
R6	4.56	1.0	L16	—	3.35
S7	4.65	1.0	L17	—	3.50
AS7	4.78	0.9	L18	—	3.64
AR4	4.97	—			3.77
S8	5.14	1.0			3.88
					3.99
					4.17
					4.28
					4.39
					4.65
					4.76
					4.84

as seen in Figs. 13(*a*) and 15(*a*). In other instances, the opposite is true. In addition, in some instances, lower U-D modes are very distinct from those lower L and V modes, and in other instances lower U-D modes are not clearly distinguished from neighboring L and V modal amplitudes. This indicates that in the ambient vibration tests, there was both strong modal coupling and interference.

6. Incidentally, the fundamental frequency (S1) difference between ambient (1.614 Hz) and forced vibrations (1.635 Hz) might suggest that the forces generated by wind [from 10 mph–40 mph (16 km/h–64 km/h)] on the dam's downstream face were larger than those generated by the shaking machines; in addition, the distribution of the forces was completely different in the two cases. (For more detail, see Ref. 1 and the companion paper.)

7. For the rocking modes, several natural frequencies have well-defined spectral peaks in the FAS of the ambient excitations (Fig. 14), unlike those of the forced vibrations.

Damping Values from FAS.—Estimated damping values from the FAS of the ambient vibration tests were obtained by the method of half-power band width and are shown in Table 3. Despite some difficulties in measuring band widths, a large number of individual peaks were adequately defined so that an estimate of half-point width was possible. (The width of the resonance peak can be influenced by several factors including: the nonstationarity of wind loads, the presence of adjacent closely spaced peaks, the smoothing process of the FAS and the structural nonlinearities.) The modal damping values given in Table 3 have values ranging from 2.3%–3.6% for the first symmetric U-D shear mode. Even for an earth dam, these are relatively large values of damping considering that they were determined from ambient level vibrations. In general, the results show that the damping values do not change greatly with a change in the ambient vibration level and the damping values decrease when the order of the mode increases; i.e., higher modes have lower damping values.

Popper Tests

The test of the dam response to small hydraulic actuating forces was accomplished by use of pressure waves, impinging upon the upstream face of the dam and generated from a controlled, submerged release of gas under pressure in the reservoir water. The purposes of this test were: (1) To determine the feasibility of the popper method of testing (Ref. 12) on a relatively large earth dam; and (2) to obtain more information on the dam's low-strain dynamic characteristics. Three sets of tests were performed; in popper test I the source of energy release was placed 10 ft–20 ft (3 m–6 m) away from the dam in the central region. In popper test II, the source was moved along a line in the central region of the dam perpendicular to the longitudinal axis, and energy was released at various points from 10 ft–60 ft (3 m–18 m) away. In popper test III, the boat which released the popper traversed half of the dam length (starting from the east abutment), and energy was released at every other measurement station.

During all three tests, some seismometers were oriented (at selected stations) only in the U-D direction to gain the maximum amount of information about

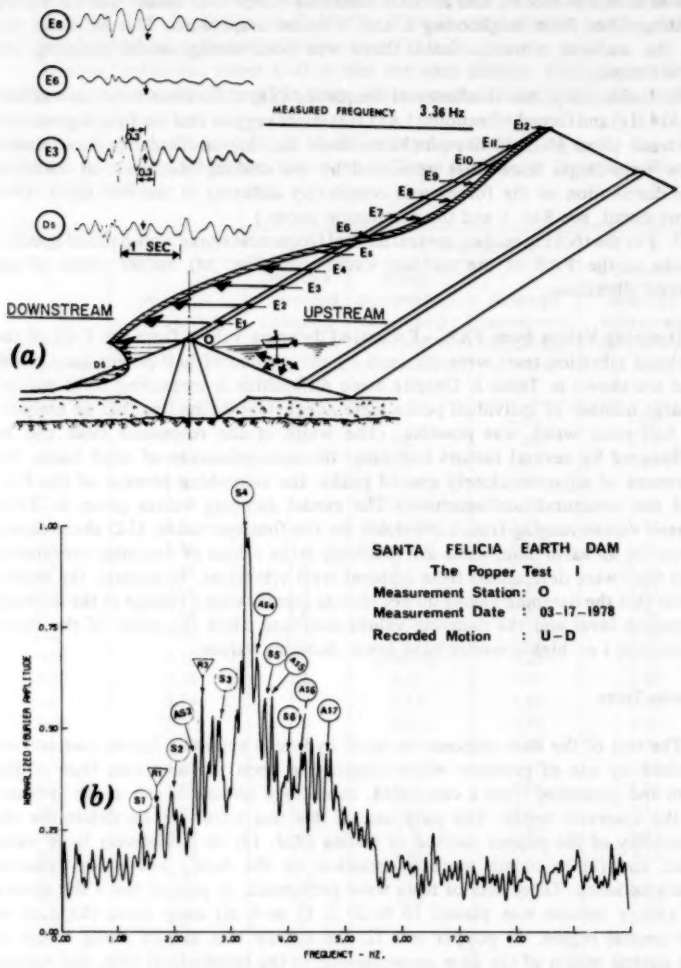

FIG. 16.—(*a*) Schematical Diagram Showing Excitation of Dam's 4th S Shear Mode, S4 (Popper Opposite Dam's Center Line); (*b*) FAS of Velocity Proportional Response of U-D Motion during Popper Test I

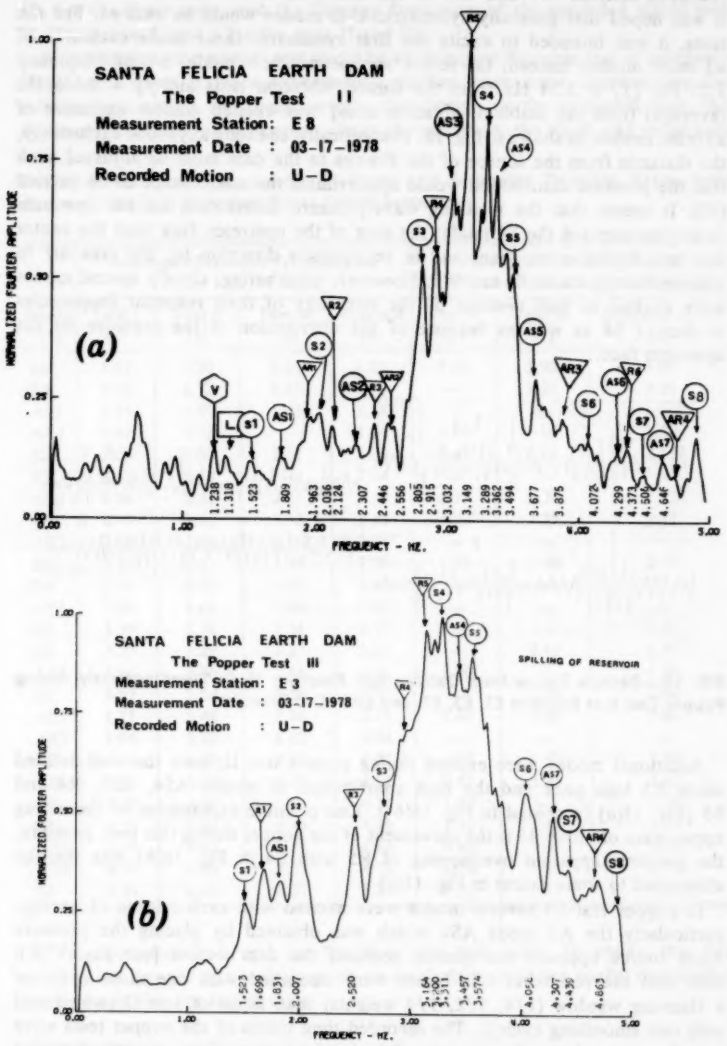

FIG. 17.—FAS: (*a*) Popper Test II; (*b*) Popper Test III

the U-D modal configurations. Also, by loading mostly the central portion (between stations W1 and E1) of the dam's upstream face (tests I and II), it was hoped that generally symmetric U-D modes would be excited. For the tests, it was intended to excite the first symmetric shear mode exclusive of all other modes; instead, the fourth symmetric shear mode, S4, of frequency 3.27 Hz [f_4 = 3.54 Hz from the forced vibration tests and f_4 = 3.665 Hz (average) from the ambient vibration tests] was excited, almost exclusive of all other modes, as shown in Fig. 16. Theoretically, to excite any mode exclusively, the distance from the source of the P-wave to the dam must be adjusted such that the pressure distribution would approximate the mode shape to be excited (10). It seems that the resulting wave-pressure distribution on the upstream face approximated the S4 mode; the area of the upstream face near the center line was loaded more than, and in an opposite direction to, the area off to either side of stations E6 and W6. However, neighboring, closely spaced modes were excited as well because of the proximity of their resonant frequencies to that of S4 as well as because of the distribution of the pressure on the upstream face.

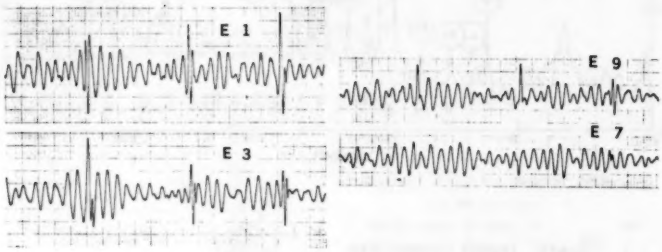

FIG. 18.—Sample Traces from Oscillograph Recorder Made Simultaneously during Popper Test II at Stations E1, E3, E7, and E9 in U-D Direction

Additional modes were excited during popper test II; note the well-defined mode R5 high peak and the high contribution of modes AS4, AS3, R4 and S5 [Fig. 17(*a*) compared to Fig. 16(*b*)]. One possible explanation of the strong appearance of mode R5 is the movement of the popper during this test; possibly, the previous apparent overlapping of R5 with S4 in Fig. 16(*b*) was thereby eliminated to some extent in Fig. 17(*a*).

In popper test III several modes were excited with each release of energy, particularly the AS mode AS1 which was obtained by placing the pressure wave source opposite the quarter point of the dam's crest [see Fig. 17(*b*); note that the results of this figure were smoothed with one more cycle of a Hanning window (1/4, 1/2, 1/4 weights) than those of test II (which had only one smoothing cycle)]. The recorded time traces of the popper tests were not clear enough to allow meaningful visual interpretation; only the S4 (and perhaps the R5) mode shape, frequency, and damping value could be determined visually (Fig. 18).

Table 4 gives a summary of the average resonant frequencies of the U-D

direction from the three popper tests as well as estimated damping values obtained from the FAS curves. Note that the frequency resolution was taken to be 0.0073 Hz for the three tests, and the filtering frequency of the recorded signal was 10 Hz for test I, and 5 Hz for tests II and III.

In conclusion, the popper test could be an effective dynamic test of relatively large earth dams if more experimental studies were done, emphasizing the relationships among the pressure-wave distribution on the upstream face, the distance of the source (or popper) from the structure, the slope and roughness

TABLE 4.—Resonant Frequencies (in Hertz) and Estimated Damping Ratios from Popper Tests (U-D Direction) Santa Felicia Earth Dam

	Average Measured Frequencies From FAS, in Hertz				Estimated Damping Ratios From FAS, as a percentage		
Mode (1)	Test I (2)	Test II (3)	Test III (4)	Average (5)	Test II (6)	Test III (7)	Average value (8)
S1	1.51	1.50	1.51	1.51	3.30	3.90	3.60
R1	1.73	1.72	1.68	1.71	—	3.25	3.25
AS1	1.89	1.80	1.83	1.84	—	—	—
AR1	1.95	1.92	—	1.94	2.60	—	2.60
S2	2.06	2.03	2.02	2.04	2.07	3.43	2.75
R2	2.13	2.14	—	2.14	—	—	—
AS2	2.36	2.31	2.35	2.34	1.73	3.30	2.52
R3	2.49	2.52	2.52	2.51	1.50	2.35	1.93
AR2	2.66	2.60	2.66	2.64	—	—	—
S3	2.78	2.81	2.74	2.73	1.73	2.60	2.17
R4	2.95	2.92	2.90	2.92	—	—	—
AS3	3.09	3.06	3.06	3.07	—	—	—
R5	3.19	3.16	3.16	3.17	1.05	—	1.05
S4	3.25	3.29	3.27	3.27	—	2.83	2.83
AS4	3.46	3.36	3.44	3.42	1.20	—	1.20
S5	3.57	3.50	3.59	3.55	—	2.40	2.40
AS5	3.71	3.68	3.74	3.71	1.40	1.80	1.60
AR3	3.94	3.89	4.00	3.94	—	—	—
S6	4.09	4.09	4.07	4.08	1.00	1.95	1.48
AS6	4.23	4.26	4.29	4.26	0.87	1.38	1.12
R6	4.40	4.36	—	4.38	1.10	—	1.10
S7	4.52	4.51	4.44	4.49	1.10	1.80	1.45
AS7	4.66	4.62	4.61	4.63	0.90	—	0.90
AR4	4.75	4.69	4.71	4.72	0.70	—	0.70
S8	4.85	4.83	4.87	4.85	1.00	—	1.00

of the upstream face, and the length of the dam crest. However, this first trial of the popper test technique on an earth dam provided useful information and a beginning for future tests.

Conclusions

From the information outlined in this paper and from extensive analysis of the entire full-scale dynamic test results, the following conclusions may be drawn.

1. Existing, low-strain, mechanical vibration generators can be used effectively in earth dam tests but should be developed further to produce much larger oscillating forces, particularly at low frequencies.
2. It is recommended that ambient vibration tests should be performed on important earth and concrete dams in areas susceptible to earthquakes in order to roughly estimate the structures' dynamic properties at this low level of excitation prior to any high-level seismic event.
3. The results obtained via the popper test proved to be very informative.
4. Values of the observed resonant frequencies from the forced vibration tests vary slightly from those determined from the ambient vibration and popper tests.
5. For the geometry of the dam studied, the shear modes contain significant L as well as V deformations, so mathematical models to represent the prototype realistically in both L and V directions are needed.
6. The L vibration data obtained from both the forced and ambient vibration tests have great potential for future research.
7. Further work is needed to better understand the energy dissipation mechanism.

Acknowledgments

This research was supported by grants from the National Science Foundation and the Earthquake Engineering Research Affiliates program at Caltech. The data reduction, interpretation and analysis were carried out in the Department of Materials Engineering at the University of Illinois at Chicago Circle and in the Civil Engineering Department at Princeton University. The assistance provided by both departments is greatly appreciated. The field program was carried out with the assistance of R. Relles and M. J. Craig. The help provided by both Kinemetrics, Inc. of Pasadena and the United Water Conservation District of Ventura County, Calif. is also greatly appreciated. Finally, Dennis Ostrom of Southern California Edison took an active interest in trying the popper tests on the dam.

Appendix.—References

1. Abdel-Ghaffar, A. M., Scott, R. F., and Craig, M. J., "Full Scale Experimental Investigation of a Modern Earth Dam," *EERL-80-01*, California Institute of Technology, Pasadena, Calif., Feb., 1980.
2. Abdel-Ghaffar, A. M., and Scott, R. F., "Comparative Study of Dynamic Response of an Earth Dam," *Journal of the Geotechnical Engineering Division*, ASCE, Vol. 107, No. GT3, Proc. Paper 16097, Mar., 1981, pp. 271–286.
3. Abdel-Ghaffar, A. M., and Scott, R. F., "Analysis of Earth Dam Response to Earthquakes," *Journal of the Geotechnical Engineering Division*, ASCE, Vol. 105, No. GT12, Proc. Paper 15033, Dec., 1979, pp. 1379–1404.
4. Abdel-Ghaffar, A. M., and Scott, R. F., "Shear Moduli and Damping Factors of Earth Dam," *Journal of the Geotechnical Engineering Division*, ASCE, Vol. 105, No. GT12, Proc. Paper 15034, Dec., 1979, pp. 1405–1426.
5. Ambraseys, N. N., "On the Shear Response of a Two Dimensional Wedge Subjected to an Arbitrary Disturbance," *Bulletin of the Seismological Society of America*, Vol. 50, Jan., 1960, pp. 45–56.
6. Calcialti, F., Castoldi, A., Fanelli, M., and Mazzieri, C., "In Site Tests for the Determination of the Dynamic Characteristics of Some Italian Dams," *Proceedings*,

Sixth World Conference on Earthquake Engineering, Jan., 1977, Part 9, pp. 9-119–9-124.

7. Chopra, A. K., Dibaj, M., Clough, R. W., Penzin, J., and Seed, H. B., "Earthquake Analysis of Earth Dams," *Proceedings,* Fourth World Conference on Earthquake Engineering, Jan., 1969.
8. Foutch, D. A., "A Study of the Vibrational Characteristics of Two Multistory Buildings," *EERL 76-03,* California Institute of Technology, Pasadena, Calif., Sept., 1976.
9. Hudson, D. E., "Synchronized Vibration Generators for Dynamic Tests of Full-Scale Structures," California Institute of Technology, Pasadena, Calif., 1962.
10. Keightley, W. O., "Vibrational Characteristics of an Earth Dam," *Bulletin of the Seismological Society of America,* Vol. 56, No. 6, Dec., 1966, pp. 1207–1226.
11. Martin, G. R., "The Response of Earth Dams to Earthquakes," thesis presented to the University of California, in Berkeley, Calif., in 1965, in partial fulfillment of the requirements for the degree of Doctor of Philosophy.
12. Ostrom, D. K., and Kelly, T. A., "Method for Dynamic Testing of Dams," *Journal of the Power Division,* ASCE, Vol. 103, No. PO1, Proc. Paper 13044, July, 1977, pp. 27–36.
13. Paskalov, T. A., Petrovski, J. T., Jurukovski, D. V., and Taskoyski, B. M., "Forced Vibration Full-Scale Tests on Earth-Fill and Rock-Fill Dams," *Proceedings,* Sixth World Conference on Earthquake Engineering, Part 9, Jan., 1977, pp. 9-125–9-130.

JOURNAL OF THE GEOTECHNICAL ENGINEERING DIVISION

COMPARATIVE STUDY OF DYNAMIC RESPONSE OF EARTH DAM

By Ahmed M. Abdel-Ghaffar,[1] A. M. ASCE and Ronald F. Scott,[2] M. ASCE

INTRODUCTION

The full-scale experimental work reported in the companion paper (2) and which provided data for this one was conducted not just to investigate the Santa Felicia earth dam itself, but rather to gather experimental data concerning its low-level dynamic characteristics which could then be used to compare with the relatively high-level characteristics resulting from the analysis of the dam's structrual performance during two actual earthquake conditions (3,4). In addition, the data was gathered to be used to test and develop various analytical and numerical methods for computing the natural frequencies and mode shapes of earth dams in general, for the purpose of predicting earthquake responses.

This paper, the second of a two paper sequence describing the results and analyses of a full-scale experimental investigation of an earth dam, compares the measured frequencies and modes of upstream-downstream (U-D) vibration resulting from the forced, ambient, and popper vibration tests (in the companion paper) with those predicted by an existing two-dimensional (2-D) shear-beam theory (5,6,9). Furthermore, the dynamic characteristics estimated from the measured response of the dam to the dynamic tests are compared with those from two earthquakes.

Also in the present paper, the shear strains and shear moduli are estimated from the full-scale tests and are plotted along with those estimated from the earthquake response analysis (4). The same procedure was followed for damping versus shear strain at various levels. Then the combined results are interpolated and extrapolated to provide a general guide to the material properties of rolled-fill earth dams for both earthquake and geotechnical engineers. Additional details

[1]Asst. Prof., Civ. Engrg. Dept., Princeton Univ., Princeton, N.J. 08544.
[2]Prof. of Civ. Engrg., California Inst. of Tech., Pasadena, Calif.

Note.—Discussion open until August 1, 1981. Separate discussions should be submitted for the individual papers in this symposium. To extend the closing date one month, a written request must be filed with the Manager of Technical and Professional Publications, ASCE. Manuscript was submitted for review for possible publication on March 17, 1980. This paper is part of the Journal of the Geotechnical Engineering Division, Proceedings of the American Society of Civil Engineers, ©ASCE, Vol. 107, No. GT3, March, 1981. ISSN 0093-6405/81/0003-0271/$01.00.

of the study presented herein can be found in the original report (1).

Comparison Between Results of U-D Shaking And Those of 2-D Shear-Beam Theory.—To estimate the shear-wave velocity within the dam material from the observed resonant frequencies and to check the values of the measured resonant frequencies, a 2-D homogeneous medium shear-beam theory was used. The natural frequencies and modes of shear vibration determined from this theory are given by (5,6,8,9)

$$\omega_{n,r} = \frac{v_s}{h}\left[\beta_n^2 + \left(\frac{r\pi h}{l}\right)^2\right]^{1/2}, \quad n, r = 1, 2, 3, \ldots \quad \ldots\ldots\ldots\ldots\ldots (1)$$

and $$\phi_{n,r}(y, z) = J_0\left(\beta_n \frac{y}{h}\right) \sin\left(\frac{r\pi z}{l}\right), \quad n, r = 1, 2, 3, \ldots \quad \ldots\ldots\ldots (2)$$

in which $\omega_{n,r}$ = the (n,r)th natural frequency; v_s = the shear-wave velocity within the dam ($v_s = \sqrt{G/\rho}$ where G = the shear modulus of the dam material; and ρ = the mass density); h = the height of the dam; β_n, n = 1, 2, 3, ... are the roots of the Bessel function of zero order of the first kind, $J_0(\beta_n)$; l = the length of the dam (a rectangular canyon is assumed); y = the depth coordinate; and z = the length coordinate.

For symmetric (S) modes, n = 1, 2, 3, 4, ... and r = 1, 3, 5, 7, ..., while for antisymmetric (AS) modes, n = 1, 2, 3, 4, ... and r = 2, 4, 6, 8, ... For this 2-D theory of a triangular wedge in a rectangular canyon, the trapezoidal canyon of Santa Felicia Dam is represented by an equivalent rectangle of length l equal to the average of the crest length and the length of the base, i.e., $l = 0.5 \times (1{,}275 + 450) = 913$ ft (278.3 m). Substituting this value of l, and values of h = 237 ft (72 m) and $f_{1,1} = \omega_{1,1}/2\pi = 1.64$ Hz (the measured frequency of the first U-D shear mode from the forced vibration test) in Eq. 1, gives a value of v_s equal to 957 fps (292 m/s). This is fairly close to the value obtained by in-situ wave-velocity measurements on the dam (3) which show that there is a shear-velocity variation as the depth changes, but that a range of v_s between 850 fps (259 m/s) and about 1,070 fps (326 m/s) is representative of the dam material. Also, by substituting the value of the measured first AS shear frequency $f_{1,2} = \omega_{2,1}/2\pi = 1.875$ Hz in Eq. 1, the resulting v_s is equal to 959 fps (292.5 m/s) which is very close to that from the first S mode.

The values of higher frequencies ($>f_{1,1}$ or $>f_{1,2}$) were therefore computed by substituting the value of v_s = 958 fps (292 m/s) in Eq. 1; these computed natural frequencies are listed in Table 1 where they are compared with those observed from the U-D forced vibrations. Only the frequencies of the observed shear modes (taken from the companion paper, Ref. 2) have been shown in Table 1 ("shear" modes are those which are similar in configuration to the ones predicted by Eq. 2).

On the basis of the information contained in Table 1 as well as in the resonance curves, the plots of U-D mode shapes (both shear and rocking modes), and the plots of 3-D components of shear modes (all in the companion paper) the following conclusions may be drawn:

1. Values of the observed resonant (shear) frequencies vary slightly from

those predicted by Eq. 1 (the measured frequencies are lower than the computed frequencies by from 3%–17%, but overall it is fair to say that the correspondence between the observations and Eq. 1 is good over the entire frequency range evaluated. The computations were based on the assumptions of an empty reservoir, a rectangular foundation for the dam, a rectangular canyon 913 ft long, an average value for the shear wave velocity of 958 fps (292 m/s), and only elastic shear (low-strain level) deformations in the horizontal direction (U-D).

2. Because of the selected deployment of the two shakers, it was possible to excite pure first (1, 1) modal response (response characterized by all points in the dam moving in the same phase). Several trials were made in the field to measure modes (2, 1) and (2, 2) which have similar configurations to the first S mode (1, 1) and the first AS mode (1, 2) along the crest and have a node along a vertical (V) section [like modes (2, 3) and (2, 4)]. Unfortunately, these modes were never excited or measured during the forced vibration tests. Nor have these modes ever been measured and reported in the literature (6,8,9).

TABLE 1.—Comparison between Observed Resonant Frequencies (from U-D Shaking) and Those Computed by 2-D Shear-Beam Theory (Eq. 1): Santa Felicia Earth Dam

SYMMETRIC VIBRATION							ANTISYMMETRIC VIBRATION						
2-D SHEAR-BEAM THEORY (Based on the Observed First Frequency 1.635 Hz)		Symmetric Shaking		Error Percent	Mode Shape as Predicted by the 2-D Shear-Beam Theory		2-D SHEAR-BEAM THEORY (Based on the Observed First Frequency 1.635 Hz)		Antisymmetric Shaking		Error Percent	Mode Shape as Predicted by the 2-D Shear-Beam Theory	
Mode n_x, r	Frequency $f_{n_x,r}$	Measured Frequency (Hz)	Designation		Along the Crest	Along the Downstream Side	Mode n_x, r	Frequency $f_{n_x,r}$	Measured Frequency (Hz)	Designation		Along the Crest	Along the Downstream Side
1,1	1.635	1.635	S1(1,1)	0.0			1,2	1.872	1.675	AS1(1,2)	0.3		
1,3	2.300	2.100	S2(1,3)	9.2			1,4	2.610	2.300	AS2(1,4)	13.5		
1,5	3.040	2.940	S3(1,5)	7.3			1,6	3.320	3.100	AS3(1,6)	13.2		
2,1	3.195	NOT	NOT				2,2	3.710	NOT	NOT	NOT		
2,3	3.695	3.550	S4(2,3)	9.6			2,4	4.131	3.660	AS4(2,4)	10.8		
1,7	3.987	3.670	S5(1,7)	8.0			1,8	4.476	4.100	AS5(1,8)	9.2		
2,5	4.421	4.300	S6(2,5)	2.8			2,6	4.752	4.420	AS6(2,6)	7.5		
1,9	4.971	4.660	S7(1,9)	6.6			1,10	5.470	4.700	AS7(1,10)	16.4		
2,7	5.115	5.257	S8(2,7)	2.7									

Instrumentation which would accurately (and less laboriously) measure the phase between the excitation and the response would be of great help in exploring these unmeasured modes.

3. If the total measured amplitude at each station is resolved into two components, one in phase with the exciting force, and one at 90° out-of-phase to the exciting force, and if the dam were to behave as a linear structure, then all of the response of the resonating mode would appear in the component at 90° out-of-phase to the exciting force. However, as a result of damping, all of the other modes of the dam would respond at phase angles other than 0° or 180° to the exciting force, and therefore they would appear to some extent in the component of response at 90° out-of-phase, depending on the amount of damping, the spacing of the natural frequencies, and the location of the exciting force on the dam.

4. The shear-beam theory (low levels of strain), although in reasonably good agreement with predominantly shear-like modes, does not predict all U-D motion modes, indicating the inadequacy of the theory for earthquake response (high

TABLE 2.—Comparison between Resonant Frequencies from Earthquake Records, Dam), U-D Direction

EARTHQUAKE RECORDS		2-D Shear Beam Theory (Based on Observed First Frequency 1.45 Hz)		FORCED VIBRATION TESTS					
				S Shaking			AS Shaking		
San Fernando Earthquake, 1971	Southern California Earthquake, 1976	Mode	Frequency $f_{n,r}$, in Hertz	Measured frequency, in Hertz	Designation	Remarks	Measured frequency, in Hertz	Designation	Remarks
Observed frequency, in Hertz (1)	Observed frequency, in Hertz (2)	n, r (3)	(4)	(5)	(6)	(7)	(8)	(9)	(10)
1.44	1.46	1, 1	1.45	1.635	S1(1, 1)	Shear	—	—	—
—	1.66	—	—	1.850	R1	Rocking	—	—	—
1.81	1.86	1, 2	1.67	—	—	—	1.875	AS1(1, 2)	Shear
—	—	—	—	—	—	—	2.025	AR1	Rocking
2.03	2.08	1, 3	1.95	2.100	S2(1, 3)	Shear	—	—	—
—	—	—	—	2.270	R2	Rocking	—	—	—
2.27	2.25	1, 4	2.32	—	—	—	2.300	AS2(1, 4)	Shear
2.47	—	—	—	2.600	R3	Rocking	—	—	—
—	—	—	—	—	—	—	2.650	AR2	Rocking
2.88	2.73	1, 5	2.71	2.840	S3(1, 5)	Shear	—	—	—
—	—	—	—	2.920	R4	Rocking	—	—	—
3.10	3.13	1, 6	3.11	—	—	—	3.100	AS3(1, 6)	Shear
—	—	2, 1	3.21	3.150	R5	Rocking	—	—	—
3.47	3.61	2, 2	3.33	3.550	S4(2, 3)	Shear	—	—	—
—	—	2, 3	3.48	—	—	—	3.600	AS4(2, 4)	Shear
—	—	1, 7	3.54	3.870	S5(1, 7)	Shear	—	—	—
3.93	3.81	2, 4	3.68	—	—	—	4.100	AS5(1, 8)	Shear
—	—	2, 5	3.96	—	—	—	4.225	AR3	Rocking
—	—	1, 8	3.97	4.300	S6(2, 5)	Shear	—	—	—
4.25	4.00	2, 6	4.25	—	—	—	4.420	AS6(2, 6)	Shear
—	—	1, 9	4.41	4.450	R6	Rocking	—	—	—
—	—	2, 7	4.54	4.665	S7(1, 9)	Shear	—	—	—
4.90	—	1, 10	4.87	—	—	—	4.700	AS7(1, 10)	Shear
—	—	2, 8	4.90	—	—	—	4.900	AR4	Rocking
5.08	—	3, 1	5.14	5.257	S8(2, 7)	Shear	—	—	—
5.32	—	2, 9	5.28	—	—	—	—	—	—

levels of strain) computations. In order to achieve agreement between the computed and all of the observed frequencies, it appears that a representation of the dam more sophisticated than that provided by shear-beam (or wedge) theory is needed, and possibly a more accurate knowledge of the physical properties of the soil in the dam is also required. Perhaps more accurate dynamic properties, using a 2-D shear-beam theory with nonuniform soil properties along the dam depth, may be attained by assuming for instance, that the shear modulus G varies with depth (say, $G \propto y^{1/3}$ or $G \propto y^{2/5}$); this has not been tried in this investigation.

5. From the shapes of the first four measured S (and AS shear modes at peak amplitudes, obtained from the simultaneously recorded three components (U-D, L, and V shown in Ref. 2), it is seen that the U-D modal motions are accompanied by contributions from the longitudinal (L) as well as the V motions; these contributions range between 10% and 25%. For S vibration, the L and V motions along the crest are similar to the U-D configuration, while along the downstream slope there is some disagreement. For AS vibration, the configuration of the L component is similar to that of the U-D but the V component is completely different along the crest. And again, there are disagreements among the three components along the downstream face. This leads to the conclusion that although a (3-D) representation of the dam is costly, it would provide

Full-Scale Dynamic Tests and Existing Shear-Beam Theories (Santa Felicia Earth

2-D Shear Beam Theory (Based on Observed First Frequency, 1.635 Hz)		AMBIENT VIBRATION MEASUREMENTS								POPPER TESTS			
		Average Measured Frequency From Fourier Amplitude Spectra, in Hertz							Average measured frequency, in Hertz "7 days"	Average Measured Frequencies From Fourier Amplitude Spectra, in Hertz			
Mode n, r (11)	Frequency $f_{n,r}$, in Hertz (12)	3/13/78 (13)	3/14/78 (14)	3/15/78 (15)	3/16/78 (16)	3/17/78 (17)	3/24/78 (18)	3/27/78 (19)	(20)	Test I (21)	Test II (22)	Test III (23)	Average (24)
1, 1	1.635	1.620	1.621	1.586	1.619	1.603	1.620	1.626	1.614	1.513	1.503	1.512	1.509
—	—	1.753	1.779	1.792	1.773	1.745	1.787	1.780	1.773	1.727	1.719	1.677	1.708
1, 2	1.872	1.934	1.884	1.924	1.835	1.916	1.881	1.924	1.900	1.892	1.802	1.831	1.842
—	—	2.025	2.020	2.030	1.978	—	2.035	2.044	2.022	1.954	1.922	—	1.938
1, 3	2.209	2.130	2.130	2.097	2.044	2.050	2.111	2.119	2.097	2.062	2.027	2.027	2.037
—	—	2.224	2.244	2.168	2.161	2.225	2.237	2.229	2.213	2.133	2.141	—	2.137
1, 4	2.610	2.368	2.350	2.395	2.333	2.377	2.367	2.320	2.359	2.355	2.307	2.354	2.339
—	—	2.591	2.611	2.549	2.540	2.587	2.568	2.500	2.564	2.489	2.522	2.520	2.510
—	—	2.680	2.693	2.680	2.695	2.632	2.699	2.646	2.675	2.659	2.604	2.659	2.641
1, 5	3.048	2.900	2.809	2.783	—	2.842	2.869	2.859	2.844	2.778	2.805	2.735	2.773
—	—	3.010	2.942	2.903	—	3.038	2.970	2.989	2.975	2.954	2.920	2.897	2.924
1, 6	3.510	3.091	3.230	3.128	—	3.190	3.214	3.135	3.165	3.093	3.057	3.062	3.071
2, 1	3.595	3.157	3.348	3.230	—	3.289	3.105	—	3.226	3.186	3.157	3.157	3.167
2, 2	3.710	—	3.606	3.474	—	3.480	3.539	3.582	3.536	3.246	3.289	3.270	3.268
2, 3	3.891	—	3.745	3.641	—	3.515	3.704	3.669	3.665	3.457	3.362	3.435	3.418
1, 7	3.987	—	3.943	3.853	—	3.847	3.866	3.830	3.868	3.569	3.496	3.589	3.551
2, 4	4.131	—	4.146	4.136	—	4.124	4.181	—	4.147	3.706	3.675	3.735	3.705
2, 5	4.421	—	4.241	4.197	—	4.243	4.204	—	4.221	3.935	3.890	3.999	3.941
1, 8	4.476	—	4.360	4.282	—	4.339	4.325	—	4.327	4.093	4.093	4.065	4.084
2, 6	4.752	—	4.472	4.398	—	4.433	4.476	—	4.445	4.230	4.256	4.292	4.259
1, 9	4.971	—	4.594	4.516	—	—	—	—	4.555	4.400	4.364	—	4.382
2, 7	5.115	—	4.695	4.656	—	4.636	4.598	—	4.646	4.517	4.507	4.444	4.489
1, 10	5.470	—	4.780	4.749	—	4.804	4.790	—	4.781	4.662	4.616	4.607	4.628
—	—	—	—	—	—	—	4.973	—	4.973	4.745	4.693	4.706	4.715
—	—	—	—	—	—	—	5.140	—	5.140	4.851	4.831	4.867	4.850
—	—	—	—	—	—	—	—	—	—	—	—	—	—

the most informative description of the dam's vibrations.

Comparison Between Results of Full-Scale Dynamic Tests and Dam's Earthquake Responses.—Tables 2, 3, 4 contain summaries of comparisons made between resonant frequencies measured (in the U-D, L, and V directions, respectively) in the dynamic tests and those determined from the spectral analysis of the dam's two earthquake responses (3).

The time history as well as spectral analyses of the dam's earthquake responses (3) indicated that the structure responded primarily in its fundamental U-D shear mode with apparent natural frequency of 1.45 Hz (0.70 secs). However, the response in the L direction showed significant contribution from higher as well as lower modes; the V component indicated a very complex response. Furthermore, the earthquake-response analysis indicated that a modern rolled-fill earth dam undergoes rather small relative displacements of its crest at a moderate intensity of shaking; the peak accelerations recorded during the 1971 earthquake were 0.22 *g* on the abutment and 0.21 *g* on the crest.

U-D Direction.—Based on the results of Table 2 the following observations relating to the U-D motion from the dynamic tests and from the earthquakes can be drawn:

Observation 1.—By comparing the resonant frequency of the first U-D S

shear mode determined from various full-scale tests and that estimated from the response of the dam during the two earthquakes, it is seen that the natural period was longer during the earthquakes (f_1 = 1.45 Hz or T_1 = 0.69 sec)

TABLE 3.—Comparison between Resonant Frequencies from Earthquake Records and Full-Scale Dynamic Tests (Santa Felicia Earth Dam): L Direction

EARTHQUAKE RECORDS		FORCED VIBRATION TESTS		AMBIENT VIBRATION MEASUREMENTS					
		One Shaker Only		Measured Frequencies From Fourier Amplitude Spectra, in Hertz					Average Measured frequency, in Hertz
San Fernando Earthquake 1971	Southern California Earthquake 1976	Measured frequency, in Hertz							
Observed frequency, in Hertz (1)	Observed frequency, in Hertz (2)	Measured frequency, in Hertz (3)	Remarks (4)	3/13 (5)	3/14 (6)	3/15 (7)	3/16 (8)	3/27 (9)	"5 days" (10)
0.99	—	—	—	—	—	—	—	—	—
1.35	1.27	1.43	L1	1.50	1.42	1.47	1.41	1.43	1.45
1.70	1.66	1.68	L2	1.67	1.63	1.66	1.58	1.65	1.64
1.86	1.86	1.85	L3	1.88	1.88	1.87	1.81	1.80	1.85
—	—	1.95	L4	2.03	1.98	1.95	2.04	1.92	1.99
2.15	2.15	2.16	L5	2.23	2.15	2.18	2.16	2.16	2.18
2.32	—	2.28	Possible	2.36	2.36	2.33	2.24	2.27	2.32
—	—	2.43	Possible	2.44	2.48	2.49	2.40	2.45	2.45
—	2.64	2.63	L6	2.65	2.66	2.62	2.67	2.60	2.64
2.91	—	2.88	L7	2.87	2.93	2.85	2.94	2.81	2.88
—	—	3.05	L8	3.06	3.08	3.01	—	2.98	3.03
3.15	—	3.15	L9	3.15	3.16	3.16	—	3.13	3.15
—	3.22	3.23	Possible	3.21	3.21	3.24	—	3.26	3.23
—	—	3.35	L10	3.35	3.33	—	—	3.38	3.32
3.49	—	3.48	L11	3.49	3.49	3.46	—	3.50	3.49
3.85	3.71	3.78	L12	3.75	3.80	3.82	3.70	3.81	3.78
4.03	—	4.03	Possible	4.06	4.04	4.07	—	4.03	4.05
—	4.20	4.18	Possible	4.17	4.22	4.16	—	4.22	4.19
4.42	—	4.37	L13	4.37	4.37	4.33	—	4.37	4.36
—	4.59	4.70	L14	—	4.64	4.70	—	4.66	4.67
4.88	—	4.88	L15	—	4.92	4.86	—	4.85	4.88
5.44	—	5.35	L16	—	—	—	—	—	—
	5.57	5.60	L17	—	—	—	—	—	—
5.98	6.05	5.90	L18	—	—	—	—	—	—

than it was during the tests (forced: f_1 = 1.635 Hz or T_1 = 0.61 sec; ambient: f_1 = 1.614 Hz or T_1 = 0.62 sec; popper: f_1 = 1.509 Hz or T_1 = 0.66 sec).

TABLE 4.—Comparison between Resonant Frequencies from Earthquake Records and Ambient Vibration Tests (Santa Felicia Earth Dam): V Direction

EARTHQUAKE RECORDS		AMBIENT VIBRATION MEASUREMENTS					
San Fernando Earthquake 1971	Southern California Earthquake 1976	Measured Frequencies From Fourier Amplitude Spectra, in Hertz					Average measured frequency, in Hertz "5 days" (8)
Observed frequency, in Hertz (1)	Observed frequency, in Hertz (2)	3/13/78 (3)	3/14/78 (4)	3/15/78 (5)	3/16/78 (6)	3/27/78 (7)	
0.95	0.98	1.00	0.99	1.00	1.02	1.00	1.00
		1.15	1.08	1.12	1.11	1.17	1.13
		1.29	1.28	1.24	1.23	1.25	1.26
1.37	1.46	1.33	1.38	1.34	1.34	1.34	1.35
		1.48	1.47	1.48	1.43	1.44	1.46
		1.55	1.56	—	1.53	1.53	1.54
1.78	1.76	1.64	1.63	1.66	1.63	1.63	1.64
		1.77	1.77	1.76	1.73	1.77	1.76
		1.88	1.87	1.84	1.84	1.92	1.87
		1.98	1.96	1.99	1.93	2.04	1.98
2.20	2.25	2.11	2.09	2.13	2.06	2.09	2.10
		2.19	2.22	2.39	2.23	2.29	2.26
		2.37	2.35	2.43	2.39	2.44	2.40
2.34	2.64	2.45	2.50	2.56	2.55	—	2.52
		2.64	2.63	2.65	2.65	2.63	2.64
		2.72	2.77	—	2.77	2.76	2.76
2.91	3.03	2.91	2.92	2.92	2.90	2.93	2.92
		3.03	3.06	3.06	3.00	3.03	3.04
		3.14	3.13	—	3.13	3.05	3.11
3.20	3.22	3.22	3.22	3.24	3.19	3.19	3.21
			3.37	3.36	3.35	3.33	3.35
3.54	3.52		3.53	3.52	3.44	3.51	3.50
			3.64	3.66	3.61	3.66	3.64
3.64	3.71		3.77	3.79	3.73	3.78	3.77
			3.88	3.87	3.86	3.92	3.88
			4.01	3.95		4.02	3.99
3.93	4.10		4.18	4.16		—	4.17
			4.26	4.28		4.29	4.28
			4.34	4.44		4.39	4.39
4.59	—		4.65	4.67		4.64	4.65
			4.77	—		4.74	4.76
			4.86	4.82			4.84

The lengthening of the first S shear period during earthquakes by factors of 1.13 (as compared to forced tests), 1.12 (ambient), and 1.04 (popper) corresponds to a decrease in overall stiffness by factors of 1.28, 1.25, and 1.08, respectively.

This behavior is typical of a yielding dynamic system such as the soil of an earth dam which is known to be extremely nonlinear. However, in assessing this variability of the dam's dynamic characteristics one has to be very careful about concluding whether these changes in frequency are caused solely by a change in the stiffness due to different excitation levels of the dam material or by other factors as well. For example, this variability could be partially due to an increase in the vibrating mass of the dam caused by an increase in the level of the reservoir water, or it could be partly due to the nature of the dynamic excitations which varied greatly in their time history characteristics, spatial distributions, and intensities.

During the full-scale measurements, the water level in the reservoir was at the same maximum (spilling) level throughout the tests; during the 1971 earthquake the reservoir level was quite high but not at its maximum level. The virtual additional mass could have had some effect, but it is believed that such effect would be very slight and probably unnoticeable (because of the massiveness of the structure and the flatness of the upstream face, Ref. 7). Thus, the data presented here seems to imply that changes in dynamic characteristics observed during the tests were mainly the result of the loss in stiffness due to the nonlinear behavior of the dam materials and less significantly due to the nature of the dynamic loadings.

Observation 2.—The frequency difference between the first S shear mode in the U-D direction from the ambient tests (1.614 Hz) and that from the forced vibration tests (1.635 Hz) might suggest that the forces generated by the wind (from 10 mph–40 mph) on the dam's downstream face were larger than those generated by the shaking machines. (During some forced vibration tests, the wind prevented measurement of the steady-state response of the dam, but during most of the testing this was not a factor). An estimate of the wind forces acting on the dam can be made by using the dynamic pressure expression (usually used for calcalating wind loads on structures) $p = 0.00256\ C_s\ V^2$ (in pounds per square ft; 1 psf = 47.9 Pa) in which C_s = the shape factor; and V = the wind velocity, in miles per hour. Now, assume $C_s \simeq 1.0$ (a convenient assumption for the rectangular horizontal projection area of the downstream face) and assume an average velocity of 20 mph; then, the foregoing expression gives $p = 1.024$ psf. The exposed effective area (horizontal projection) of the downstream face can be estimated to be 100 ft (depth) times 800 ft (average length); this value produces a total wind force of $F_w = 1.024 \times 100 \times 800 = 81{,}920.0$ lb.

If one assumes that the wind was not really perpendicular to the downstream face, then the aforementioned value can be reduced by, say, 40%; this gives a total wind force of 29,152 lb, which is approximately five times larger than the average steady-state sinusoidal force. Thus, the total amount of energy imparted to the dam by the wind, very likely, was greater than that produced by the shaking machines.

Finally, comparison also indicates that, in exciting the first S shear mode S1, the force generated by the popper (at 1.509 Hz) was more than that generated during the ambient and mechanical-shaking tests. Unfortunately, there were

no dynamic pressure transducers mounted on the upstream face to provide the order of magnitude of the popper forces.

Observation 3.—During the two earthquakes, very few high modes (shear or rocking) were excited in the U-D direction (the response was primarily from the first mode), whereas, contrarily, the higher modes were excited efficiently and clearly by the three dynamic tests. In addition, the identification of some of the higher modes excited during the earthquakes was not reliable. As a result, it is difficult to make any reliable comparison based on a frequency-to-frequency analysis.

Observation 4.—Looking at the frequencies of the first AS shear mode, AS1, (1.81 Hz "1971 earthquake," 1.86 Hz "1976 earthquake," 1.875 Hz "forced," 1.900 Hz "ambient," and 1.842 Hz "popper"), it is seen that there is a maximum difference of only 5% which may suggest that the AS1 mode may not have been excited effectively by the two earthquakes (the participation factors of other modes excited during the two earthquakes are presented in Ref. 3). Reasons this mode may not have been excited effectively are: (1) The uniformity of ground shaking at the dam causing S modes to be excited more effectively; and (2) the location of the crest accelerograph in the central region (about 50 ft away from the crest midpoint), i.e., in a position more likely to pick up the dominant S motions since this region represents nodes of AS modes.

Observation 5.—Some of the lower U-D rocking modes were not excited during the shaking of the two earthquakes; examples of these modes are AR1, R2, AR2, and R4. Apparently the first R mode, R1, was excited during the 1976 earthquake (with frequency 1.66 Hz); this frequency was increased by 3% (1.708 Hz) during the popper tests, by 7% (1.773 Hz) during the ambient tests and by 11% (1.850 Hz) during the forced vibration tests. The third S rocking mode, R3, was excited during the 1971 earthquake at a frequency of 2.47 Hz compared to frequencies of 2.510 Hz (2% increase) from the popper tests, 2.564 Hz (4% increase) from the ambient tests, and 2.600 Hz (5% increase) from the forced tests. Finally, the resonant frequencies of the rocking modes AR1, R2, and AR2 resulting from the full-scale tests vary slightly from one type of test to another; the variation ranges from 1%–5% as indicated by Table 2.

Observation 6.—The frequencies of S and AS shear modes S2, AS2, and AS3 also vary only slightly from the earthquake responses to the full-scale tests. However, the third S shear mode S3 was excited more strongly during the small earthquake of 1976 (frequency 2.71 Hz) than during the large earthquake of 1971 (frequency 2.88 Hz); the frequencies from the tests were 2.840 Hz, 2.844 Hz, and 2.773 Hz from forced, ambient, and popper tests, respectively. This just demonstrates that greater shaking does not always excite all modes more strongly.

Observation 7.—It is interesting to compare the frequencies of the fourth S shear mode, S4, resulting from the different tests and the two earthquakes since the mode associated with this frequency was excited very effectively by the popper test (2). The frequency determined from the 1971 earthquake response was 3.470 Hz, then it increased to 3.610 Hz from the 1976 earthquake response. The popper tests provided a frequency of 3.268 Hz while the frequencies from the forced and ambient vibration tests were 3.550 Hz and 3.536 Hz, respectively. Note that the popper test excited the S4 mode more strongly than even the strong earthquake. This observation is not a surprising one since the

dam responded mainly in its fundamental S shear mode during the two earthquakes, while during the popper test the dam was excited, exclusive of all other modes, in mode S4.

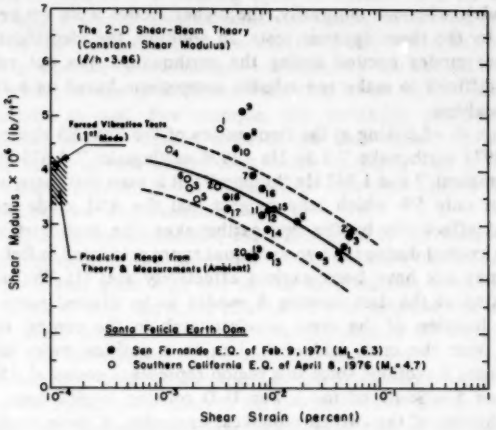
The 2-D Shear-Beam Theory
(Constant Shear Modulus)
(ℓ/h=3.86)
Forced Vibration Tests
(1st Mode)
Predicted Range from
Theory & Measurements (Ambient)
Santa Felicia Earth Dam
San Fernando E.Q. of Feb. 9, 1971 (ML=6.3)
Southern California E.Q. of April 8, 1976 (ML=4.7)
Shear Modulus × 10⁶ (lb/ft²)
Shear Strain (percent)

FIG. 1.—Estimated Shear Moduli and Corresponding Dynamic Shear Strains (Evaluated from Hysteretic Response of Two Earthquakes as well as from Full-Scale Dynamic Tests)

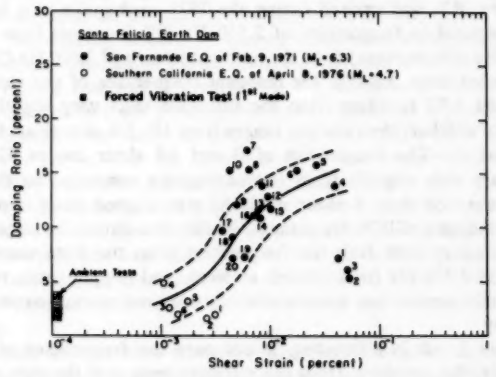
Santa Felicia Earth Dam
San Fernando E.Q. of Feb. 9, 1971 (ML=6.3)
Southern California E.Q. of April 8, 1976 (ML=4.7)
Forced Vibration Test (1st Mode)
Ambient Tests
Damping Ratio (percent)
Shear Strain (percent)

FIG. 2.—Estimated Damping Factors and Corresponding Dynamic Shear Strains (Evaluated from Hysteretic Response of Two Earthquakes as well as from Full-Scale Dynamic Tests)

Observation 8.—The dynamic shear moduli and damping factors of the dam's material were estimated from the measured responses (the hysteretic responses of the first S shear mode) to the two earthquakes. Both dynamic properties

were determined as functions of the induced dynamic strains (for more details see Ref. 4). The relationships between each dynamic property and the induced dynamic strain are shown by the semilog plots of Figs. 1 and 2 for the first 20 sec of the 1971 earthquake and the first 6 sec of the 1976 earthquake.

In order to reveal any change in the dynamic properties of the dam, the estimated shear moduli and damping factors from the full-scale tests are also shown in Figs. 1 and 2. In addition, Table 5 shows some of these dynamic properties associated with various levels of response. Both the figures and the table indicate that the dynamic properties of the dam's constituent materials

TABLE 5.—Comparison between Dynamic Properties (of Earth Dam) Estimated from Earthquake Records and Those Determined from Full-Scale Dynamic Tests

Source of data (different levels of excitation) (1)	U-D DIRECTION: S Vibration: First shear frequency, in Hertz (2)	U-D DIRECTION: S Vibration: Estimated shear modulus, in pounds per square inch (3)	U-D DIRECTION: S Vibration: Estimated shear strain as a percentage (4)	U-D DIRECTION: S Vibration: Estimated damping factor as a percentage (5)	U-D DIRECTION: S Vibration: Maximum acceleration at crest, as a percentage of g (6)	U-D DIRECTION: S Vibration: Maximum displacement at crest, in millimeters (7)	U-D DIRECTION: AS Vibration: First shear frequency, in Hertz (8)	Longitudinal Direction: Natural (first) frequency, in Hertz (9)
1971 San Fernando earthquake $M_L = 6.3$	1.440	Ranges from 2.4×10^5–4.5×10^5	Ranges from 0.4×10^{-2}–5.5×10^{-2}	Ranges from 5.0–15.0	20	13.30	1.81	1.35
1976 Southern California earthquake $M_L = 4.7$	1.460	Ranges from 3.4×10^5–4.8×10^5	Ranges from 0.10×10^{-2}–0.40×10^{-2}	Ranges from 1.5–5.0	5	0.85	1.86	1.27
Forced vibration tests (mechanical shaking)	1.635	4.10×10^5	0.716×10^{-3}	3.0	0.0037	0.00336	1.875	1.425
Ambient vibration tests (wind and spilling of reservoir)	Ranges from 1.570–1.670	Ranges from 3.6×10^5–4.3×10^5	—	Ranges from 2.3–3.6	—	—	Ranges from 1.85–1.95	Ranges from 1.44–1.48
Hydrodynamically generated force (popper tests)	Ranges from 1.50–1.63	—	—	Ranges from 2.9–4.2	—	—	Ranges from 1.76–1.93	—

Note: 1 psf = 47.9 Pa.

estimated from low-strain full-scale tests are consistent with those determined from the relatively larger strains induced by the two earthquakes.

By interpolating and extrapolating the data of Figs. 1 and 2, Figs. 3 and 4, accordingly, are proposed to provide reasonable estimates of the dynamic properties of the dam's constituent material; these estimates would be useful for any study of the dam's U-D earthquake-response characteristics. In addition, the variation of material properties with depth should be taken into account for any realistic dynamics study; the variation of the shear modulus of the dam material with depth is proposed in Fig. 5, which is based on an in-situ wave velocity measurement as well as on the analysis of the two earthquake responses (3). Figs. 3, 4, and 5 should provide a good guide to the material

properties in the dynamic analysis of any earth dam composed predominantly of rolled-fill, essentially cohesionless material, with or without a relatively thin core.

L and V Directions.—With the exception of the first three L frequencies observed during the two earthquakes (at 1.35 Hz, 1.70 Hz, and 1.86 Hz), it is difficult to make any reliable comparison with the values of the resonant

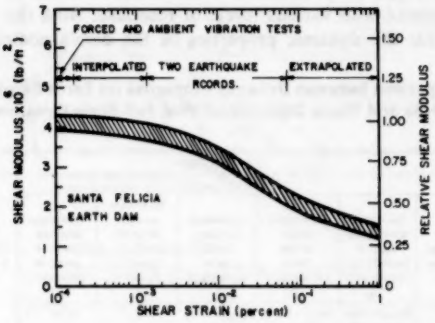

FIG. 3.—Estimated Shear Moduli and Corresponding Dynamic Shear Strains Proposed for any Earth Dam Composed Predominantly of Rolled-Fill, Essentially Cohesionless Material, with or without Relatively Thin Core

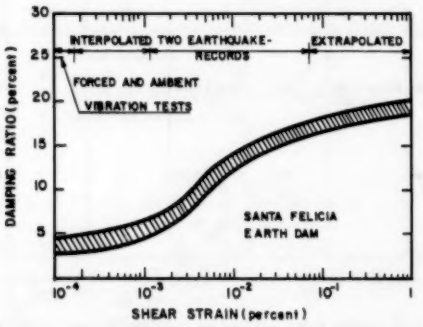

FIG. 4.—Estimated Damping Factors and Corresponding Dynamic Shear Strains Proposed for any Earth Dam Composed Predominantly of Rolled-Fill, Essentially Cohesionless Material, with or without Relatively Thin Core

frequencies in the L direction resulting from the forced vibration tests and those resulting from various ambient vibration measurements, as indicated by Table 3. As was considered previously in the companion paper (2), there are many closely-spaced frequencies in the L direction, and some of the L resonant frequencies are very close (even identical) to some of the U-D resonant frequencies which may suggest a strong coupling between the U-D and L vibrations.

The first L mode was apparently excited more strongly during the small (1976) earthquake (where $f = 1.27$ Hz) than during the large (1971) earthquake (where $f = 1.35$ Hz); the ratio is about 6% which corresponds to a decrease in overall stiffness by a factor of 1.12. The frequency increased to 1.425 Hz when determined from the forced vibration tests (a 12% increase over the 1976 earthquake) and to an average value of 1.446 Hz when determined from the ambient tests (a 14% increase over the 1976 earthquake). These increases of the first L frequency correspond to decreases in overall stiffness by factors of 1.25 and 1.30 for the forced and ambient tests, respectively. This behavior is similar to that observed for the U-D direction.

The situation for the V component is even more complicated as is seen from Table 4, where while the comparison between the results of the two earthquakes is quite consistent, the comparison between the two earthquake results and

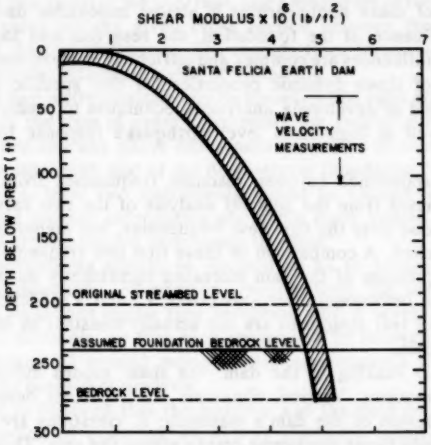

FIG. 5.—Suggested Relationship between Shear Modulus and Dam's Depth

those of the ambient vibration measurements is not consistent at all. The results of the ambient tests showed many, closely spaced resonant frequencies while the results of the two earthquakes showed well-separated frequencies.

Finally, there is also substantial indication of modal coupling and interference between the three orthogonal directions; there were many frequencies with identical values measured in the three directions.

Conclusions, Evaluation and Recommendations

It appears from all the data available on the dam's responses, including the foregoing consideration that:

1. Full-scale tests at levels of excitation much lower than those experienced during the earthquakes produced substantial changes in the dynamic properties

of the dam. The behavior is typical of yielding dynamic systems involving soil, which is known to be extremely nonlinear, but has rarely been examined at full scale.

2. Dynamic properties of the dam's constituent materials, such as shear moduli and damping factors, estimated from low-strain full-scale tests and determined from the relatively larger strains induced by the two earthquakes are consistent with established shear moduli-induced strain and damping-induced strain curves, previously proposed on the basis of laboratory tests. The lower levels of excitation involved in the ambient, forced, and popper tests gave dynamic properties which covered the lower range of induced strains in these curves, while the strong ground motion during the earthquakes resulted in dynamic properties covering the intermediate and higher-induced strains.

The losses in stiffness due to high strains have been attributed, for the most part, to the nonlinear behavior of the dam materials. An exact determination of the causes of these nonlinearities is almost impossible due to insufficient data on the influence of the foundation, the reservoir and the pore pressure changes. These influences are complex and difficult to analyze accurately. Finally, the variations of these dynamic properties for this specific dam have been generalized to aid in developing analytical techniques to predict accurately the low-strain as well as high-strain level earthquake response for most modern earth dams.

3. The correspondence between resonant frequencies from full-scale tests and those estimated from the spectral analysis of the two earthquake records is reasonably good over the first few frequencies, but higher modes could not be reliably matched. A comparison of these first few frequencies revealed that the natural frequencies of the dam increased significantly during the full-scale tests in all three orthogonal directions (U-D, L, and V). Clearly, the dynamic characteristics of real structures are not actually constant as implied by linear shear-beam models.

4. During U-D shaking of the dam, the shear modes indicated significant L and V deformations. Vertical vibrations are important because they could weaken the cohesion of the dam's materials; L vibrations are also important because they could cause transverse cracks across the axis. Thus, mathematical (i.e., analytical or finite element) models are needed to represent the prototype realistically in both L and V directions. These models should take into account the geometric variation of the dynamic properties as well as the material degradation properties.

5. Existing shear-beam theories (low levels of strain), although in reasonably good agreement with predominantly shear-like modes, do not predict all the U-D motion-type modes, indicating the inadequacy of these theories for comprehensive earthquake response computations. The nonshear U-D modes are believed to be either rocking modes or indications of U-D motion associated with L or V vibrations.

6. It appears that precise field tests and more theoretical analyses over a wide range of strains are required to establish the nature of the dynamic response characteristics of earth dams. Despite the complexity of several factors influencing the response of the dam, it is believed that full-scale test studies will yield the information necessary to formulate accurate mathematical models.

7. Concurrently, it is also desirable to reassess the installation and deployment

of strong motion instrumentation on dams in order to provide more valuable, reliable and informative results for interpretation of the dynamic behavior of these structures during earthquakes. In order to get reliable information on any dam's 3-D behavior during an earthquake, more than two sets of strong-motion instruments should be deployed on and in the vicinity of the structure. Proper placement will yield information about the response of the dam, the nature of different modes of vibration, the coupling of these modes and the nature of the input ground motion.

The following are suggestions for appropriate locations of the instruments; it should be noted that these suggestions assume an ideal set of circumstances, and, thus, do not consider any economic limitations:

a. A minimum set of four three-component accelerographs should be located on the crest and the downstream slope. One instrument should be placed on the midpoint or the central region of the crest with a second on the midpoint (or lower than this point) of the U-D face, and a similar set of two accelerographs should be located on any given cross section between the crest midpoint and either of the two abutments. The records from these instruments would help to identify the different modes of vibrations.

b. A set of two instruments should be placed on the right and left abutments (crest level) of the dam in order to correlate the ground motions at the two sides and to evaluate any phase differences as well as to compare the ground motion at the sides with that of the downstream foundation.

c. A set of at least two instruments should be located in the U-D area. This set would provide information about the input ground motion and the uniformity of ground motion underneath the dam.

All of the instruments should be situated so as to record motions in the U-D, L and V directions. In addition, records from the instruments should be time tied. Continuous digital tape recording with a several second storage buffer is highly desirable, so that each record can be recovered in its entirety from the beginning of ground motion, after simultaneous triggering. Digital recording greatly eases data analysis.

8. Finally, it is believed that the analysis and the data presented here will provide information of practical, as well as academic, significance about the dynamic characteristics of earth dams and will promote further research in this area.

Acknowledgments

This research was supported by grants from the National Science Foundation and the Earthquake Engineering Research Affiliates program at the California Institute of Technology. The assistance provided by the Department of Materials Engineering at the University of Illinois at Chicago Circle and the Department of Civil Engineering at Princeton University is greatly appreciated.

Appendix.—References

1. Abdel-Ghaffar, A. M., Scott, R. F., and Craig, M. J., "Full Scale Experimental Investigation of a Modern Earth Dam," *EERL-80-01*, California Institute of Technology, Pasadena, Calif., Feb., 1980.

2. Abdel-Ghaffar, A. M., and Scott, R. F., "Vibration Tests of Full-Scale Earth Dam," *Journal of the Geotechnical Engineering Division*, ASCE, Vol. 107, No. GT3, Proc. Paper 16096, pp. 241–269.
3. Abdel-Ghaffar, A. M., and Scott, R. F., "Analysis of Earth Dam Response to Earthquakes," *Journal of the Geotechnical Engineering Division*, ASCE, Vol. 105, No. GT12, Proc. Paper 15033, Dec., 1979, pp. 1379–1404.
4. Abdel-Ghaffar, A. M., and Scott, R. F., "Shear Moduli and Damping Factors of Earth Dam," *Journal of the Geotechnical Engineering Division*, ASCE, Vol. 105, No. GT12, Proc. Paper 15034, Dec., 1979, pp. 1405–1426.
5. Ambraseys, N. N., "On the Shear Response of a Two Dimensional Wedge Subjected to an Arbitrary Disturbance," *Bulletin of the Seismological Society of America*, Vol. 50, Jan., 1960, pp. 45–56.
6. Chopra, A. K., Dibaj, M., Clough, R. W., Penzin, J., and Seed, H. B., "Earthquake Analysis of Earth Dams," *Proceedings*, Fourth World Conference on Earthquake Engineering, Jan., 1969.
7. Chwang, A. T., and Housner, G. W., "Hydrodynamic Pressures on Sloping Dams During Earthquakes. Part I. Momentum Method," *Journal of Fluid Mechanics*, Vol. 87, Part 2, 1978, pp. 335–341.
8. Keightley, W. O., "Vibrational Characteristics of an Earth Dam," *Bulletin of the Seismological Society of America*, Vol. 56, No. 6, Dec., 1966, pp. 1207–1226.
9. Martin, G. R., "The Response of Earth Dams to Earthquakes," thesis presented to the University of California, at Berkeley, Calif., in 1965, in partial fulfillment of the requirements for the degree of Doctor of Philosophy.

JOURNAL OF THE GEOTECHNICAL ENGINEERING DIVISION

PROBABILISTIC EVALUATION OF LOADS[a]

By Wilson H. Tang,[1] M. ASCE

INTRODUCTION

In a geotechnical design, engineers have been primarily concerned with the determination of soil properties and the prediction of soil performances. Although also a major input parameter in design, loads are in most instances already prescribed to the geotechnical engineers. The same is also true regarding ground-water level and other environmental factors. Geotechnical engineers have long recognized variability in soil properties as exhibited from laboratory test results and observed field performances. Significant amounts of uncertainty could exist in the loads and environmental factors. The uncertainties may arise from spatial as well as temporal fluctuation of load and environmental factors, and from idealized assumptions necessary for evaluating load effects. In view of such uncertainties in both soil and load characteristics, safety of a geotechnical design cannot be guaranteed. Although a large proportion of the uncertainties in the load and environmental factors is due to inherent natural variability, which is perhaps beyond the engineer's control, nevertheless, an understanding of their variation and statistics is essential to achieve a design that will have a sufficiently high probability of successful performance. By adopting appropriate safety factors to reflect the relative uncertainty levels of the individual loads or load combination, consistency in reliabilities could be maintained in the design.

This paper reviews the loads that affect geotechnical designs, characterizing the uncertainties present in each load component. Probabilistic models for evaluating each component load are considered. Whenever data are available, the level of variabilities and uncertainties associated with the effect of each component on the foundation will be assessed.

[a]Presented at the April 2–6, 1979 ASCE Convention and Exhibition, held at Boston, Mass. (Preprint 3600).

[1]Prof. of Civ. Engrg., Univ. of Illinois at Urbana-Champaign, 3122 Civ. Engrg. Bldg., Urbana, Ill. 61801.

Note.—Discussion open until August 1, 1981. To extend the closing date one month, a written request must be filed with the Manager of Technical and Professional Publications, ASCE. Manuscript was submitted for review for possible publication on January 1, 1980. This paper is part of the Journal of the Geotechnical Engineering Division, Proceedings of the American Society of Civil Engineers, ©ASCE, Vol. 107, No. GT3, March, 1981. ISSN 0093-6405/81/0003-0287/$01.00.

Permanent Static Load

Gravitational load caused by the weight of structural materials such as concrete, steel, or form work is commonly referred to as dead load, whose magnitude usually does not change during the life of the geotechnical system. In general, dead load could be estimated relatively accurately. Possible sources of uncertainties include: (1) Variability in material density due to inhomogeneity and tolerance of manufacturer; (2) discrepancy in dimensions from the design values; (3) uncertainty in the final choice of building materials; and (4) variability in the nonstructural components such as decorative architectural forms. A coefficient of variation (COV) of 10% has been suggested (20) for the variation of dead load in the design of a typical floor in the superstructure. The total dead load applied to the foundation is generally composed of the sum of contributions from many component dead loads. According to the law of large numbers, the variability in the total dead load will be less than the 10% value suggested for the design of the superstructure. For example, the COV of the total load Y from n floors can be shown to be (e.g., see Ref. 1).

$$\delta_Y = \delta_x \sqrt{\frac{1 + (n-1)\rho}{n}} \quad \ldots\ldots\ldots\ldots\ldots\ldots\ldots\ldots\ldots\ldots\ldots\ldots (1)$$

in which δ_x = the COV of the load from individual floor; and ρ = the correlation coefficient between any two floors. Suppose $\rho = 0.3$ and $n = 20$, then δ_Y is only 58% of the value of δ_x. In fact, in those foundations where dead load is dominant such as tall buildings, or massive structures, it is encouraging to know that the variability of the resultant dead load is expected to decrease substantially from 10%.

Gravitational loads could also come from the weight of the soil itself such as in the evaluation of overburden pressure in settlement analysis. The vertical and lateral earth pressures will be treated separately later under soil induced loads.

Regular Occupancy Load

Most loads acting on a foundation do vary with time. The simplest example is the sustained live load, caused by the weight from regular human occupancy (as opposed to occasional large gatherings which will be treated later as an extraordinary load), furniture, and equipment. The regular occupancy load is not expected to vary much throughout the duration of a given occupancy. Such load, however, could change significantly between occupancies. For practical purposes, the regular occupancy load could be assumed to stay constant during each occupancy. An example of the changes in regular occupancy load over the life of a structure is shown in Fig. 1. The times at which occupancy changes do not necessarily take place at regular intervals. The Poisson process has been suggested to model the occurrences of such occupancy changes, with parameter ν as the average rate at which occupancy changes. This in turn implies that the duration of each occupancy follows the exponential distribution. The mean number of load changes over a structure's life of T years is simply νT.

For stability problems (such as bearing capacity) and settlement in sand,

foundation performance is governed by the maximum load during the lifetime of the foundation. Therefore, the maximum regular occupancy load over the foundation's lifetime T is of interest here. The cumulative distribution function (CDF) of the maximum regular occupancy load X_{rm} can be derived from

$$F_{X_{rm}}(x) = \sum_{i=1}^{\infty} F^i_{X_r}(x) \frac{e^{-\nu T}(\nu T)^i}{i!} = \exp\{-\nu T[1 - F_{X_r}(x)]\} \quad \ldots\ldots\ldots (2)$$

in which $F_{X_r}(x)$ = the CDF of the load during each regular occupancy; i = the number of changes of occupancy; and the values of X_r between occupancies are assumed to be identically and independently distributed. If exactly n changes of occupancy are known to have occurred, the CDF of X_{rm} is given by

$$F_{X_{rm}}(x) = F^n_{X_r}(x) \quad \ldots\ldots\ldots\ldots\ldots\ldots\ldots\ldots\ldots\ldots\ldots\ldots\ldots\ldots (3)$$

The statistics of regular occupancy load X_r have been collected by Mitchel and Woodgate (18) in the United Kingdom and by Culver (6) in the United States. For example, results show that the mean value of X_r is about 11.6 psf (555.4 N/m^2) for an office floor area over 100 sq ft (9.3 m^2), whereas the standard deviation of X_r will decrease as floor area increases. For a typical

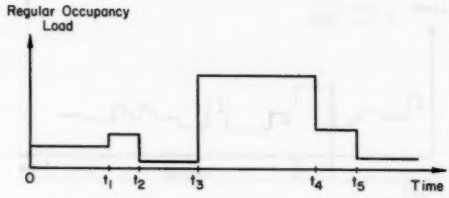

FIG. 1.—Changes of Regular Occupancy Load

floor area of 2,000 sq ft (186.1 m^2), the COV of X_r is about 0.5. The CDF of the lifetime maximum regular occupancy load could be evaluated for a given distribution of X_r and a given expected number of occupancy changes νT. Assuming X_r to be lognormally distributed, and for eight changes of occupancy, the mean and COV of X_{rm} for a floor area of 2,000 sq ft (186.1 m^2) could be shown to be about 20.5 psf (981.5 N/m^2) and 0.30, respectively.

The total regular occupancy loads from the individual floors are required for the design of foundations supporting a multistory structure. Since the maximum regular occupancy loads of each floor may not necessarily occur at the same time, it would be somewhat conservative if the maximum regular occupancy loads in each floor are combined to give the maximum total regular occupancy load for foundation design. Since the times at which changes of occupancy occur are random, the total regular occupancy load at the foundations will appear as shown in Fig. 2, where load changes occur much more frequently especially where there are many floors. The load process now is correlated since at given load change, the load at only one floor changes whereas the loads in the other floors remain as before. Wen (34) has studied the statistics of the maximum of this correlated load process over the lifetime of a structure.

For a 50-story structure with $\nu T = 7.2$ for each floor, the mean total maximum lifetime regular occupancy load is about 23 psf, compared to 20.5 psf for the mean maximum of a single floor. A correlation coefficient of 0.3 was assumed as suggested in Ref. 19 to account for the dependency of loads between successive floors in the foregoing analysis due to possible common usage.

On the other hand, if settlement due to consolidation is to be evaluated for a foundation, the loads considered would not be the lifetime maximum, which may occur only over a brief period of time. Instead, the statistics of the long-term weighted average of the regular occupancy load will be needed. The effective regular occupancy load may be given by

$$X_e = \frac{\Sigma \alpha_i X_{ri}}{\Sigma \alpha_i} \quad \ldots \ldots \ldots

Extraordinary Loads

Loads classified as extraordinary loads include forces due to snow, wind, and storm waves, earthquake and extreme occupancy loads. The general characteristics of the extraordinary load are depicted in Fig. 3. For a majority of the time, such loads do not occur at all (or normally their magnitudes are negligible such as light breezes or ordinary waves). When such loads do occur, the duration as well as the load magnitude are uncertain. In view of the short duration of load application, relative to dead load or regular occupancy loads covered previously, the contribution of such loads to consolidation settlement will be negligible. The extraordinary loads are, however, critical for problems related to stability and transient motions. Some common features of and statistical concepts relevant in design against extraordinary loads are considered in the following sections.

Lifetime Maximum Extraordinary Load.—Assuming the occurrence of an extraordinary load follows a Poisson process with mean rate of occurrence ν, and the magnitudes of the load between occurrences are statistically indepen-

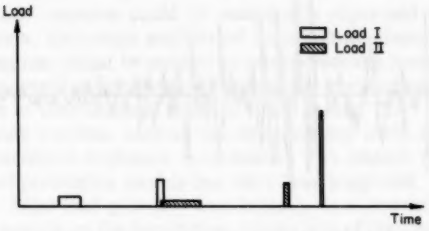

FIG. 3.—Extraordinary Loads

dent, then the CDF of the lifetime maximum of an extraordinary load can be shown to be the same expression as that in Eq. 2, in which X_r is interpreted as the maximum load magnitude X in each occurrence. Alternatively, if the statistics of an extraordinary load, such as wind speed and wave height, are available in terms of the annual maximum values, then the CDF of the lifetime maximum load is the same expression as that in Eq. 3 in which $X_Y = X_a$ is the random annual maximum load assumed to be statistically independent between years; and $n = T$ is the foundation lifetime. Once the CDF has been evaluated for a given distribution of X or X_a, the mean, variance, and COV of the lifetime maximum extraordinary load could be determined accordingly. When νT or T is large, X_{max} could be shown to approach one of the limiting distribution, such as the type I extreme value (Gumbel) distribution or the type II extreme value (Fisher-Tippet) distribution or the Weibull distribution.

Return Period of Design.—Conventionally, a 100-yr wave, or a 50-yr wind velocity or an earthquake acceleration with a return period of 500 yr may be adopted as a sufficiently high (or conservative) estimate of the maximum extraordinary load that would be applied to a foundation system. These design

return periods are generally longer than the expected service lives of such systems. The return period $\bar{T}$ is simply the average time until the design load is exceeded. It could be shown that

$$\bar{T} = \frac{1}{p} = \frac{1}{1 - F_{x_a}(x_d)} \quad \ldots\ldots\ldots\ldots\ldots\ldots\ldots\ldots\ldots\ldots\ldots\ldots\ldots\ldots\ldots\ldots (6)$$

in which p = the probability that the design load x_d is exceeded in a given year. For example, if 50 yr is the design return period of an extraordinary load, the probability that such design load will be exceeded in a year is 1/50 or 0.02. Therefore, the probability that the design load will be exceeded during the foundation system's expected lifetime, say of 30 yr, could be evaluated using a binomial distribution as $1 - (1 - 0.02)^{30}$ or 0.45. It is interesting to observe that the probability of exceedence in 50 yr (i.e., within the design return period) is 0.636, implying that the design load in this case is not necessarily exceeded at the 50th year or once every 50 yr. In fact the design load could be exceeded in any year including even the first few years of operation.

FIG. 4.—Earthquake Acceleration Time History

Dynamic Amplification Factor.—A microscopic inspection of the characteristics of an extraordinary load when it occurs may reveal fluctuations as shown in Fig. 4 (for the case of earthquake acceleration). The average period between peaks of such fluctuating load cycles could range from a fraction of second (as in earthquake excitation) to a fraction of a minute (as in ocean waves) or perhaps a longer period (as in snow accumulation). Depending on the vibrational characteristics of a structure-foundation system relative to the frequency of fluctuations of the applied loads, the dynamic system response in terms of stress and displacement could be amplified significantly from their corresponding values calculated considering only statics. Three methods commonly used to model the dynamic load effect are described as follows:

1. Pseudostatic analysis: An example of this is the seismic coefficient adopted in quasistatic analysis of embankment stability, which could be a prescribed value or determined through a dynamic visco-elastic response analysis (e.g., see Ref. 25). Wu and Kraft (35) suggested the COV of the prescribed seismic coefficient could exceed 20%. The uncertainty of the seismic coefficient determined from the latter approach is expected to be smaller, but it should incorporate

the uncertainties in parameters such as soil damping, mass density, shear wave velocity, and most of all in the visco-elastic model itself for representing the actual behavior.

2. Time History Approach: The effect of the uncertainty in the load time history input could be analyzed by repeating the dynamic analysis to various recorded time histories and perhaps simulated time histories all properly scaled to the same maximum accelerations. Moreover, using a Monte-Carlo simulation procedure, uncertainties in the parameters of the deterministic model such as the stress-strain relationship, damping characteristics, and density of the soil stratum might also be incorporated in assessing the overall variability in the dynamic stress. Tremendous amount of computer time is generally required.

3. Random Vibration Analysis: Christian (4) summarized the concept of random vibrations as well as the state of the art of its application to geotechnical engineering. Through random vibration analysis the statistics of the dynamic stress response could be derived analytically.

Nevertheless, the statistics of the dynamic stress would account for only uncertainties in the inherent variability of the time sequence of load fluctuations. Uncertainties in the system parameters would also affect the dynamic stress. Since the dynamic response could be analytically expressed in terms of the system parameters, first-order analysis of uncertainties (based on the Taylor Series approximation) might be applied to incorporate the system uncertainties in evaluating the overall uncertainties of the dynamic stress response. An example of this approach to wind loadings could be found in Ref. 22.

In the following sections, each of the extraordinary loads that would be of interest to geotechnical engineers, is examined with respect to its sources of uncertainties and probability models that have been suggested.

Wind Load.—Wind load generally acts laterally on a structure, thus creating an overturning moment on the foundation. As one side of the foundation receives downward load from the overturning moment, uplift forces will occur on the other part of the foundation. Pulling of piles and caissons could be potential modes of failure in addition to stability failures under wind action. Moreover, if the wind velocity is much larger in one direction, say from the west as compared to that from the east, then differential stress may be induced on two opposite ends of the foundation, which may lead to differential settlement or tilt if the wind environment persists over a long time period.

The annual maximum wind velocity has been suggested to follow the extreme value distribution. Thom (30) proposed that the type II extreme value distributions should be used throughout the United States. However, it has also been shown (27) that in a well-behaved wind climate, such as the continental interior which is unaffected by hurricane disturbances as in the coastal areas, type I extreme value distribution may be more appropriate. In areas where tornadoes and hurricanes are prevalent, though at infrequent intervals, the effects of these extreme winds should be superimposed on the ordinary wind effects. The distribution of the combined maximum wind velocity (ordinary wind plus hurricanes and tornadoes) has been derived (32), which could deviate significantly from the extreme value distribution.

Wind pressure is proportional to the square of the wind velocity. Considerable mathematical simplification could be achieved by adopting the type II instead

of type I distribution for the wind velocity, since the corresponding wind pressure can be derived to follow also the type II distribution. The typical COV of the maximum mean hourly wind velocity would range from 0.09–0.12. The COV of the corresponding maximum wind pressure will be approximately twice (since $p \alpha V^2$), thus ranging from 0.18–0.24, with the lower value for the suburban area and the higher value for the inner city. These statistics, however, assume only static wind load. For a structure-foundation system with large natural period of vibration, static wind load may be satisfactory; otherwise, the dynamic response of the system to wind forces should be considered. Combining the probability distribution of wind velocity and direction and the response characteristics obtained from wind tunnel tests, Davenport (7) established probability contours of specific response (stress or displacement). Nevertheless, uncertainties in the response and structural parameters were not considered in his evaluation. If the effects of the uncertainties in the gust response factor and the turbulence nature of the wind environment are incorporated, the value of the COV of wind forces could range from 0.27–0.52 for city environment and 0.25–0.48 for suburban areas (22). An independent evaluation (21) suggests that the COV of the lifetime (50 yr) maximum wind pressure would typically range from 0.37–0.41 (assuming a specific COV of 16% for the lifetime maximum wind velocity), which appears to agree well with the previous study.

Earthquake Load.—Earthquakes have been regarded as a major threat to dam safety. For slope stability consideration the maximum lateral force due to earthquake motion could be modelled quasistatically as a function of mass of the structure, the maximum ground horizontal acceleration during earthquake excitations, and the dynamic amplification factor. Several factors need to be considered in evaluating the statistics of the maximum ground acceleration; these include: (1) Identification of all the potential sources of earthquakes (such as existing faults) in the vicinity of the site; (2) the probability distribution of earthquake magnitude; (3) frequency of occurrence of earthquakes; (4) the direction of fault slip, if any; (5) the distance from each source of earthquake; and (6) attenuation characteristics of the region. Analytical models for estimating the maximum acceleration at a site have been proposed by Cornell (5), Der-Kiureghian and Ang (9), considering separately different types of earthquake sources (i.e., fault lines, aerial sources and point sources), each having the magnitude distribution and activity rate assessed based on available earthquake records. The relative frequency of earthquake magnitude in a region is assumed to follow the Richter's Law. They also used attenuation equations to relate site ground acceleration intensity to earthquake magnitude and focal distance. Cornell's model assumed that the energy released during an earthquake is concentrated at a point whereas DerKiureghian and Ang's model assumed that the slip length for a large earthquake may be several hundred kilometers, and thus, the largest contribution to the acceleration intensity at the site might be caused by the slip location closest to the site. Although the latter model appears to be more realistic, difficulty exists in defining the magnitude of an earthquake in such a case. Because of lack of data for establishing the attenuation equation for sites close to the sources, prediction of acceleration level is expected to be very crude. The maximum ground acceleration for San Francisco and San Juan, Puerto Rico have been evaluated (8); the results are reproduced in Fig. 5. The probability that a ground acceleration of 0.4 g will be exceeded in a

year is 10 times higher in a San Francisco site than in a San Juan site. Based on this annual maximum acceleration distribution, the distribution of the lifetime maximum acceleration could be derived accordingly. To convert the ground acceleration to the maximum acceleration in the structure-foundation system, the response characteristics of the system should also be considered. Portillo (20) estimated the COV in the dynamic amplification factor is typically around 0.33 for reinforced concrete structures. For soil material whose dynamic stress-strain relationships are less well understood and where soil parameters are subject to spatial variation and sampling uncertainties, the COV of this factor is expected to be somewhat higher. Nevertheless, since the level of uncertainty associated with the attenuation equation ranges from 0.5–0.85 in terms of COV (10,11,17),

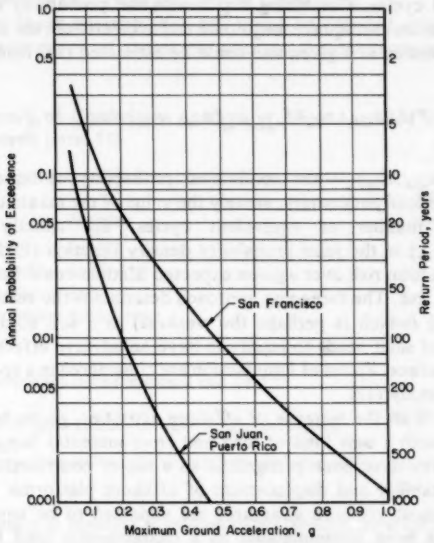

FIG. 5.—Estimated Risks for Maximum Ground Acceleration for San Francisco and San Juan, Puerto Rico (after 8)

it is apparent that the major contribution of uncertainty in the maximum acceleration would perhaps come from the seismicity factors rather than from the structural systems response.

In those soil conditions where substantial strength loss could result from pore pressure development during earthquake excitation, liquefaction analysis is required. For the evaluation of liquefaction potential, the number of significant equivalent stress cycles during earthquake excitation is also important (26). The number of equivalent cycles, N_{eq}, depends on: (1) Duration of an earthquake; (2) magnitude of an earthquake; (3) equivalent stress level expressed in terms of percentage of the peak stress; and (4) the soil strength curve at the specific

site characterizing the reduction in soil strength with increased number of constant load cycles. Based on the data in Ref. 16, the relationship between N_{eq} earthquake magnitude, equivalent stress levels, and soil strength curves has been analyzed statistically (13). Nonlinear regression analyses were performed to obtain the mean and variance of N_{eq} as a function of magnitude M. The sensitivity of the prediction equation is found to be minimum when the equivalent stress level is adopted as 75% of the peak stress. The corresponding mean value function is

$$E(N_{eq}|M-m) = 106 - 36.4\,m + 3.3\,m^2; \quad 5 \leq m \leq 8.25 \quad \ldots\ldots\ldots\ldots (7)$$

and the scatter about this prediction curve is represented by a constant standard deviation of 5.4 cycles. Combining Eq. 7 with the probability distributions of the annual maximum earthquake magnitude and acceleration, the annual probability of the liquefaction at a given site could be estimated (14) from

$$P_f = \int_{n_{eq}} \int_{a_{max}} P(L|a_{max}, n_{eq}) f_{A_{max},N_{eq}}(a_{max}, n_{eq})\, da_{max}\, dn_{eq} \quad \ldots\ldots\ldots\ldots (8)$$

in which $P(L|a_{max}, n_{eq})$ = the conditional probability of liquefaction at the site assuming the load parameters, namely the value of the maximum acceleration a_{max} and the number of equivalent cycles, are exactly known; and $f_{A_{max},N_{eq}}(a_{max}, n_{eq})$ = the joint probability density function (PDF) of A_{max} and N_{eq}. The liquefaction risk over a given expected lifetime could be then evaluated from the annual risk. The foregoing approach determines the risk of liquefaction at a single point (which is perhaps the weakest) in a soil stratum. However, a large volume of sand needs to liquify to have an adverse effect on a structure on the ground surface. Zones of liquefaction are considered in a recent probabilistic liquefaction study (12).

Wave Load.—With the increase of offshore activities, geotechnical engineers are confronted with a new kind of load and environmental factors. The forces from ocean waves have been recognized as a major contribution to the loads governing the stability and displacement of offshore platforms. Although economic lives of most offshore structures are expected to be approx 20 yr, the 100-yr wave has been recommended as a characteristic load for subsequent deterministic analysis. Realistically, the maximum wave height during a 20-yr period is a random variable. Based on a probabilistic stability analysis for a typical Condeep gravity platform located in the North Sea (15), and neglecting consolidation effect on the soil from the platform weight and previous storms, the probability of stability failure assuming a random 20-yr maximum wave height is approximately equal to the probability of stability failure assuming a deterministic 100-yr wave height. Thus, the 100-yr design wave height may perhaps be a consistently (reliability-wise) chosen characteristic load for stability analysis of gravity platforms in the North Sea.

The long-term wave height distribution has been modelled by the Weibull distribution (2) or alternatively by the Gumbel distribution (23). The general lack of sufficient field measured data and possible errors associated with the assumed distribution model will give rise to uncertainties in addition to the inherent variability. Calibrated visual wave heights and those hindcasted from

storms are often used as supplemental data. In this case, calibration and hindcasting error would need to be considered. For a given wave height and wave period, wave force can be evaluated from various empirical equations or laboratory model tests or sophisticated analytical studies. Varying levels of uncertainty are associated with each of these procedures. An example of the uncertainty analysis is performed for the stability of a gravity platform in the North Sea based on 4 yr of wave height data, is summarized in Table 1. A sensitivity analysis of the laboratory model test data reveals that the estimated uncertainties in wave height and period would result in a COV of 11% in the wave forces; whereas discrepancy between laboratory model tests and field performance could be subject to a COV of 20% based on the assumptions that the uncertainty level should be somewhat less than that observed for smaller structural members in steel jacket structures (30%–40%).

The undrained shear strength of a soil could be reduced substantially from the repeated wave action of the storm prior to the occurrence of the largest

TABLE 1.—Summary of Uncertainty Analysis of Wave Load for Gravity Platform Stability and Analysis (after 15)

Variable (1)	COV, as a percentage (2)
Wave height: inherent variability	7
Wave height: insufficient data	10
Wave height: distribution model error	5
Wave height: Total	13
Wave period	5
Wave forces: discrepancy between model and field performances	20
Wave forces: due to uncertainties in wave height and period	11
Wave forces: Total	23

wave. The reduction in strength is related to the accumulated cyclic strain which in turn depends on the height of the individual waves. The distribution of wave heights in short-term sea state (such as during a storm) has been suggested to follow a Rayleigh distribution, from which the statistics of the reduction in undrained strength could be evaluated.

In problems where the dynamic system response is critical, wave energy spectra such as Jonswap or modified Pierson-Moskowitz-Kitaigorodskii (P-M-K) have been suggested to describe the stochastic nature of waves. Using these spectra as input, random vibration analysis may be performed to obtain statistics of the dynamic response. The problem of which spectrum to use is still controversial. On the basis of 41 wave spectra from six storm records, Sartre (23) suggested that the sharper peak of the Jonswap spectrum appears to fit the data better than the P-M-K spectrum. However, data are still lacking in defining the spectrum for the severe storms, e.g., that with a 20-yr return period of more in the North Sea.

Combination of Loads

Each load component considered previously acts separately on a foundation, which occasionally could be subject to stresses resulting from combined actions of two or more load components. The critical load combinations that a foundation may encounter sometime during its lifetime are identified as follows, together with a brief review of the corresponding models for probabilistic treatment.

Dead Load + Maximum Regular Live Load.—Since dead load is assumed to act permanently, and regular live load only changes with each turnover of occupancy, it is obvious that the combined action of these two loads will achieve a maximum during the occupancy with the largest live load. Let the maximum combined load be

$$Z = X_{rm} + Y \quad \ldots \quad (9)$$

in which X_{rm} = the maximum regular occupancy load; and Y = the permanent static load. Assuming X_{rm} and Y to be statistically independent, the CDF of Z could be shown (e.g., see Ref. 1) to be

$$F_Z(z) = \int_y F_{X_{rm}}(z-y)\, F_Y(y)\, dy \quad \ldots \quad (10)$$

in which $F_{X_{rm}}$ may be determined from Eqs. 2 or 3; and $f_Y(y)$ = the PDF of Y. Alternatively, if only the mean and standard deviation of Z are required, they could be evaluated directly from Eq. 9 in terms of those of X_{rm} and Y as

$$\mu_z = \mu_{x_{rm}} + \mu_y \quad \ldots \quad (11)$$

and

$$\sigma_Z = \sqrt{\sigma^2_{X_{rm}} + \sigma^2_Y} \quad \ldots \quad (12)$$

Dead Load + Regular Live Load + 1 Extraordinary Load.—When one of the extraordinary load (e.g., wind, wave, snow, earthquake, or extraordinary live load) achieves its maximum value over the lifetime of the foundations, it is unlikely that it occurs during the occupancy with the maximum regular live load. Assuming that there is only one extraordinary and live load over the period of one occupancy could be first established as follows. Let

$$Z = X + E \quad \ldots \quad (13)$$

in which X = the regular live load during a given occupancy; and E = the maximum value of an extraordinary load over the period of the given occupancy. Similar to the previous case, the CDF and statistics of Z could be shown to be

$$F_Z(z) = \int F_E(z-x) f_X(x)\, dx \quad \ldots \quad (14)$$

$$\mu_z = \mu_x + \mu_E \quad \ldots \quad (15)$$

$$\sigma_z = \sqrt{\sigma^2_x + \sigma^2_E} \quad \ldots \quad (16)$$

The CDF and statistics of the maximum of a given extraordinary load may be evaluated according to the procedures covered in previous sections. Assuming Poisson process for the occurrence of occupancy changes, Eq. 2 can be applied to yield the CDF of the maximum combined extraordinary and live load over

the foundation's lifetime as

$$F_{Z_{max}}(z) = \exp\{-\nu T[1 - F_Z(z)]\} \quad \ldots \quad (17)$$

in which ν = the mean rate of occupancy change; and T = the lifetime of the foundations. The maximum combined load over the foundation's lifetime is then the sum of Z_{max} and the permanent static load Y. Replacing X_{rm} by Z_{max}, Eqs. 10–12 could be then used for determining the corresponding CDF and statistics.

Dead Load + Regular Live Load + 2 Extraordinary Loads.—Let R denote the maximum load value due to two independent extraordinary load sources over the foundation's lifetime. The value of R will be higher than that of E in the previous case for two reasons. First, the second extraordinary load itself could have a maximum lifetime load higher than E. Secondly, the two extraordinary loads could occur simultaneously and the combined load could exceed E. The probability of simultaneous occurrence of two extraordinary loads will increase with the frequency of occurrences of each load as well as the duration of each load. Suppose the loads follow Poisson processes with mean rates of occurrence ν_1 and ν_2, and the mean durations of each extraordinary load when it occurs are μ_{d_1} and μ_{d_2}, respectively. Wen (33) suggests an approximate expression for the CDF of R over a time period t as

$$F_R(r,t) \simeq \exp\{-\nu_1 t[1 - F_{E_1}(r)] - \nu_2 t[1 - F_{E_2}(r)]$$
$$- \nu_1 \nu_2(\mu_{d_1} + \mu_{d_2}) t[1 - F_{E_{12}}(r)]\} \quad \ldots \quad (18)$$

in which F_{E_1}, F_{E_2}, and $F_{E_{12}}$ = the CDFs of extraordinary loads E_1, E_2, and $E_1 + E_2$. The CDF of R then can replace that of E in Eqs. 14, 17, and 10 for subsequent evaluation of the CDF of the lifetime maximum combined load. The aforementioned formulation could be extended to the case of more than two extraordinary loads.

Soil Induced Loads

Another load commonly encountered by geotechnical engineers is that generated by the soil itself, such as the overburden pressure on a given soil layer in a settlement analysis. The average density over a soil stratum would be the relevant parameter here instead of the density at a specific point. Because soil properties generally exhibit spatial correlation in a given stratum, Vanmarcke (31) suggested that the variability in the average property (e.g., density) over a soil stratum is considerably smaller than its point spatial variation. The amount of reduction in the variability depends on the volume of soil under consideration and the spatial correlation characteristics of the soil density. In general, for natural deposits or compacted embankment, a much larger correlation is observed in the horizontal plane than along the vertical direction. Assuming perfect correlation among soil density in the horizontal plane and an exponential decay correlation model vertically with correlation distance b, the COV of the average density over a soil layer of thickness H can be derived as

$$\delta_{\bar{\gamma}} = \frac{b}{H}\sqrt{2\left(\frac{H}{b} - 1 + e^{-H/b}\right)}\,\delta_\gamma \quad \ldots \quad (19)$$

in which δ_γ = the COV of densities between the individual soil samples. For example, if $\delta_\gamma = 10\%$ and $b = 0.3$ m (0.98 ft), $\delta_{\bar{\gamma}}$ for a 1-m (3.28-ft) and 10-m (32.8-ft) thick soil layer could be shown to be 6.5% and 2.5%, respectively. Therefore, the variability in the average density over a large stratum of soil is expected to be very small, except for the case where the soil stratum is highly heterogeneous and insufficient representative samples are available for density determination.

Lateral earth pressure, encountered in retaining structures, are generally empirically calculated in terms of the average density $\bar{\gamma}$ and a stress coefficient such as K_o, K_A, or K_p, which is in turn a function of the friction angle ϕ. The COV of ϕ could reach 10%–20% (28). The uncertainty in the coefficient K due to the variability in ϕ could be evaluated using the first-order approximation formula. For example, with $K_A = (1 - \sin\phi)/(1 + \sin\phi)$, the mean and

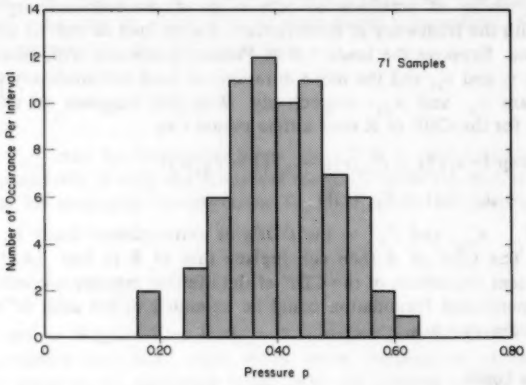

FIG. 6.—Histogram for Earth Pressure on Braced Cut (after 29)

variance of K_A could be evaluated approximately from

$$\bar{K}_A \simeq \frac{1 - \sin\bar{\phi}}{1 + \sin\bar{\phi}} \quad \ldots\ldots\ldots\ldots\ldots\ldots\ldots\ldots\ldots\ldots\ldots\ldots\ldots\ldots\ldots\ldots (20)$$

$$\text{and} \quad \text{Var}(K_A) \simeq \frac{4\cos^2\bar{\phi}}{(1 + \sin\bar{\phi})^4}\,\text{Var}(\phi) \quad \ldots\ldots\ldots\ldots\ldots\ldots\ldots\ldots\ldots\ldots\ldots\ldots (21)$$

which yields a COV of K_A of $(2\bar{\phi}/\cos\bar{\phi})\,\delta_\phi$ after simplification. As an illustration, for a design situation where the mean friction angle is 30° and a COV of 10%, the corresponding COV of the active pressure coefficient K_A is approx 12%. Additional error could also exist in the empirical model itself, assumptions adopted in the static analysis, presence of residual stresses and values of wall friction. From the histogram plotted in Fig. 6 for data on 71-strut loads in braced excavation systems in granular soil, the apparent earth pressure is estimated (29) to have a mean of 0.4 and a COV of 0.23. After removing the contributions of uncertainty

from K_A (estimated at 12%) the uncertainty in the model is estimated to be about 0.19. Nevertheless, data are still generally lacking for evaluating such model uncertainties.

When a hard layer is overlain by a consolidating stratum, drag force (commonly known as negative skin friction) could be generated on the piles or caisson due to relative downward movement of the soil adjacent to the pile surfaces. Drag force is function of soil parameters such as friction angle and cohesion coefficient. Again, spatial variability, measurement, and sampling error in these parameters and model uncertainties would give rise to variability in the drag force, which could be conveniently analyzed through first-order approximate formulas.

Pore Pressure and Seepage Force

Pore pressure is another major parameter in geotechnical analysis. Even in the simplest case where pore pressure results from hydrostatic condition defined by the ground-water level, uncertainties in pore pressure at a point in the stratum still arises due to seasonal changes, rainstorms, construction, or dewatering activities in the adjacent neighborhood. Spatial fluctuation in pore pressure could also occur in addition to temporal fluctuation. However, foundation performance is generally governed by the average pore pressure over an area. Thus, the effect of spatial fluctuation will not be as crucial as the temporal fluctuation. If piezometric measurements are available, long-term predictions could be made from the recorded seasonal cycles and short-term stochastic fluctuations (from rainstorms). Alternatively, if piezometric data are not available, which is generally the case, hydrologic models considering precipitations and infiltration rates may be used to predict ground-water levels. From the annual maximum water level, statistics of the lifetime maximum ground-water level could be evaluated using procedures suggested earlier. According to the measurements recorded by the Illinois State Water Survey, due to natural causes, the annual maximum ground water is typically 5 ft (1.53 m) above the mean ground-water level with a COV of 35%. Over a period of 20 yr, the high-water level could be expected to be more than 8 ft (2.44 m) above the mean ground-water level. On the other hand, if low ground-water level is of interest, the CDF of its lifetime minimum is given by

$$F_{X_{\min}}(x) = 1 - [1 - F_{X_a}(x)]^T \quad \ldots \ldots \ldots \ldots \ldots \ldots \ldots \ldots \ldots \ldots \quad (22)$$

in which X_a = the annual minimum ground-water level.

Movement of water through soil stratum would give rise to seepage forces which is a function of the hydraulic gradient which in turn depends on the relative permeability over the soil stratum. It is generally recognized that the error in measuring permeability could be plus or minus one order of magnitude. The ratio of horizontal and vertical permeability, that is important in the construction of flow nets, could be thus subject to large uncertainty. In addition, due to inhomogeneous deposits of sand and clay, and erratic location of sand lenses, further uncertainties are associated with the prediction of seepage force at any part of a soil stratum.

In the case of slopes, based on Refs. 3 and 24, the COV of the pore pressure was estimated (36) to vary between 0.05 and 0.1. With various assumptions

on the relative permeability of rock and boulder clay and the ground water flow conditions, they also estimated that the COV of the pore pressure along the sliding surface for a slope at Selset to be 6%, in addition to the uncertainty due to seasonal fluctuation in the ground water level.

Conclusion

The major loads affecting geotechnical performance have been reviewed. In view of the underlying uncertainties, these loads and conditions should be treated probabilistically. With properly formulated probabilistic models and supplemented with adequate statistical data, the probability of encountering a certain magnitude of load or load combination over a foundation's lifetime could be evaluated. Such information is necessary in rational planning of geotechnical system and in the establishment of load values for design purposes.

Acknowledgment

The research reported here was supported in part by the National Science Foundation (NSF) under grant No. PFR 78-19680. Any opinions, findings, conclusions or recommendations expressed herein are those of the writer and do not necessarily reflect the view of the NSF.

Appendix I.—References

1. Ang, A. H-S., and Tang, W. H., *Probability Concepts in Engineering Planning and Design*, Vol. I—"Basic Principles," John Wiley and Sons, New York, N.Y., 1975.
2. Battjes, J. A., "Long Term Wave Height Distribution at Seven Stations Around the British Isles," *NIO Report A44*, National Institute of Oceanography, Wormley, Godalming, Surrey, England, 1970.
3. Bishop, A. W., "The Use of the Slip Circle in the Stability Analysis of Slopes," Geotechnique, Vol. 5, No. 1, 1955.
4. Christian, J. T., "Probabilistic Soil Dynamics: State-of-the-Art," *Journal of the Geotechnical Engineering Division*, ASCE, Vol. 106, No. GT4, Proc. Paper 15339, Apr., 1980, pp. 385–397.
5. Cornell, C. A., "Engineering Seismic Risk Analysis," *Bulletin of Seismological Society of America*, Vol. 58, No. 5, Oct., 1968, pp. 1583–1606.
6. Culver, C., "Survey Results for Five Loads and Live Loads in Office Buildings," *NBS Building Science Senic 85*, National Bureau of Standards, Washington, D.C., May, 1976.
7. Davenport, A. G., "The Prediction of Risk Under Wind Loading," *Proceedings*, 2nd International Conference on Structural Safety and Reliability, Kupfer, et. al., ed., Werner-Verlay, Dusseldorf, Germany, 1977, pp. 511–538.
8. DerKiureghian, A., and Ang, A. H-S., "A Line Source Model for Seismic Risk Analysis," *Structural Research Series No. 419*, University of Illinois, Urbana, Ill., Oct., 1975.
9. DerKiureghian, A., and Ang, A. H-S., "Fault-Rupture Model for Seismic Risk Analysis," *Bulletin of Seismological Society of America*, Vol. 67, No. 4, Aug., 1977, pp. 1173–1194.
10. Donovan, N. C., "Earthquake Hazards for Buildings," Building Practices for Disaster Mitigation, R. Wright, S. Kramer, C. Culver, ed., *Buildings Science Series 46*, U.S. Department of Commerce, National Bureau of Standards, Feb., 1973.
11. Donovan, N. C., "A Statistical Evaluation of Strong Motion Data Including the February 9, 1971 San Fernando Earthquake," *Proceedings*, Fifth World Conference on Earthquake Engineering, 1973.

12. Fardis, M. N., "Probabilistic Liquefaction of Sands During Earthquakes," thesis presented to the Massachusetts Institute of Technology, at Cambridge, Mass., in 1979, in partial fulfillment of the requirements for the degree of Doctor of Philosophy.
13. Haldar, A., "Probabilistic Evaluation of Liquefaction of Sand Under Earthquake Motions," thesis presented to the University of Illinois, at Urbana, Ill., in 1976, in partial fulfillment of the requirements for the degree of Doctor of Philosophy.
14. Haldar, A., and Tang, W. H., "A Probabilistic Evaluation of Liquefaction Potential," *Journal of the Geotechnical Engineering Division*, ASCE, Vol. 105, No. GT2, Proc. Paper 14374, Feb., 1979, pp. 145–163.
15. Hoeg, K., and Tang, W. H., "Probabilistic Considerations in the Foundation Engineering for Offshore Structures," *Proceedings*, Second International Conference on Structural Safety and Reliability, Kupfer, et. al., ed., Werner-Verlay, Dusseldorf, Germany, 1977, pp. 267–296.
16. Lee, K. L., and Chen, K., "Number of Equivalent Significant Cycles in Strong Motion Earthquakes," *Proceedings*, International Conference on Microzonation, Nov., 1972.
17. McGuire, R. K., "Seismic Structural Response Risk Analysis, Incorporating Peak Response Repressions on Earthquake Magnitudes and Distance," *Research Report R74-51*, Massachusetts Institute of Technology, Cambridge, Mass., 1974.
18. Mitchell, G. R., and Woodgate, R. W., "Floor Loadings in Office Buildings—The Results of a Survey," *Current Paper 3/71*, Building Research Station, Garston, Watford, England, 1971.
19. Peir, J. C., and Cornell, C. A., "Spatial and Temporal Variability of Live Loads," *Journal of the Structural Division*, ASCE, Vol. 99, No. ST5, Proc. Paper 9747, May, 1973, pp. 903–922.
20. Portillo, G. M., and Ang, A. H-S., "Evaluation of Safety of Reinforced Concrete Buildings to Earthquakes," *Structural Research Series No. 433*, University of Illinois, Urbana, Ill., 1976.
21. Ravindra, M. K., Cornell, C. A., and Galambros, T. V., "Wind and Snow Load Factors for Use in LRFD," *Journal of the Structural Division*, ASCE, Vol. 104, No. ST9, Proc. Paper 14006, Sept., 1978, pp. 1443–1457.
22. Rojiani, K. B., "Evaluation of Reliability of Steel Buildings to Wind Loadings," thesis presented to the University of Illinois, at Urbana, Ill., in 1978, in partial fulfillment of the requirements for the degree of Doctor of Philosophy.
23. Saetre, H. J., "On High Wave Conditions in the Northern North Sea," *Oceanology International 75*, Conference Papers, Brighton, 1975, pp. 280–289.
24. Scott, J. D., "Slope Failures in Over-Consolidated Fissured Clays in Southwestern Iowa," thesis presented to the University of Illinois, in Urbana, Ill., in 1964, in partial fulfillment of the requirements for the degree of Doctor of Philosophy.
25. Seed, H. B., and Martin, G. R., "The Seismic Coefficient in Earth Dam Design," *Journal of Soil Mechanics and Foundation Division*, ASCE, Vol. 92, No. SM3, Proc. Paper 4824, May, 1966, pp. 25–28.
26. Seed, H. B. and Idrise, I. M., "Analysis of Soil Liquefaction: Niigata Earthquake," *Journal of the Soil Mechanics and Foundation Division*, ASCE, Vol. 93, No. SM3, Proc. Paper 5233, May, 1967, pp. 83–108.
27. Simiu, E., and Filliben, J. J., "Probabilistic Models of Extreme Wind Speeds: Uncertainties and Limitations," *Proceedings of the Fourth International Conference on Wind Effects on Buildings and Structures*, 1975.
28. Singh, A., "How Reliable is the Factor of Safety in Foundation Engineering," *Proceedings*, First International Conference on Application of Statistics and Probability to Soil and Structural Engineering, Sept., 1971.
29. Tang, W. H., Yuceman, M. S., and Ang, A. H-S., "Reliability Analysis and Design of Braced Excavation Systems," *Proceedings*, First International Conference on Applications of Statistics and Probability to Soil and Structural Engineering, Sept., 1971, pp. 187–202.
30. Thom, H. C. S., "New Distributions of Extreme Winds in the United States," *Journal of Structural Division*, ASCE, Vol. 94, No. ST6, Proc. Paper 6038, July, 1968, pp. 1787–1801.
31. Vanmarcke, E. H., "Probability Modelling of Soil Profiles," *Journal of the Geotechnical*

Division, ASCE, Vol. 103, No. GT11, Proc. Paper 13364, Nov., 1977, pp. 1227–1246.
32. Wen, Y. K. and Ang. A. H-S., "Tornado Risk and Wind Effect on Structures," *Proceedings of the 4th International Conference on Wind Effect on Buildings and Structures*, Sept., 1975, pp. 63–73.
33. Wen, Y. K., "Statistical Combination of Extreme Loads," *Journal of the Structural Division*, ASCE, Vol. 103, No. ST5, Proc. Paper 12930, May, 1977, pp. 1079–1093.
34. Wen, Y. K., "On Statistics of Extreme of Live Loads on Buildings," *Journal of the Structural Division*, ASCE, Vol. 105, No. ST10, Proc. Paper 14886, Oct., 1979, pp. 1893–1900.
35. Wu, T. H., and Kraft, L. M., "Seismic Safety of Earth Dams," *Journal of the Soil Mechanics and Foundation Division*, ASCE, Vol. 96, No. SM6, Proc. Paper 7686, Nov., 1970, pp. 1987–2006.
36. Yuceman, M. S., and Tang, W. H., "Long Term Stability of Soil Slopes—A Reliability Approach," *Proceedings*, Second International Conference on Applications of Statistics and Probability to Soil and Structural Engineering, Sept., 1975, pp. 215–230.

Appendix II.—Notation

The following symbols are used in this paper:

A_{max} = maximum earthquake acceleration;
b = correlation distance;
E, E_1, E_2 = maximum extraordinary load;
E_{12} = $E_1 + E_2$;
$F_X(x)$ = cumulative distribution function;
H = thickness of soil layer;
K_A, K_o, K_p = horizontal stress coefficients;
n = number of floors or occupancy changes;
$P(\ )$ = probability of ( );
p = probability of exceedence, wind pressure;
R = maximum of two extraordinary loads combined;
T = expected service life;
$\bar{T}$ = return period of design;
V = wind velocity;
X_e = effective regular occupancy load;
X_r = regular occupancy load;
x_d = design load;
Z = combined load;
α = weighting factor for consolidation settlement;
β = reduction coefficient;
δ = coefficient of variation;
γ = density of soil;
μ = mean value;
ν = mean rate of occurrence;
ρ = correlation coefficient;
σ = standard deviation; and
$\bar{\Phi}$ = mean friction angle of soil.

JOURNAL OF THE GEOTECHNICAL ENGINEERING DIVISION

DESIGN CONSIDERATIONS FOR COLLAPSIBLE SOILS[a]

By Samuel P. Clemence,[1] M. ASCE and Albert O. Finbarr,[2] A. M. ASCE

INTRODUCTION

Metastable or collapsible soils are defined as any unsaturated soil that goes through a radical rearrangement of particles and great loss of volume upon wetting with or without additional loading (2). The existence of these soils throughout the world and difficulties with building on them have long been recognized. The reason for the lack of information on many of these soil deposits is that they are located in predominantly arid regions with limited economic development. Recent advances in irrigation have made it possible to open up many of these regions to farming and industrial development. These developments include industrial and urban complexes, and provide opportunities for the use of water in large quantities. The consequent problems resulting from excessive settlements have given impetus to the study of these soils. The most comprehensive state-of-the-art papers on collapsing soils are by Northey (18), Sultan (24), and Dudley (9). Bara (2), in 1976, has also presented a brief summary of present theories and treatment of collapsible soils. Since 1970, the major research has been devoted to determining the mechanism of collapse. Other studies have been devoted to predictive methods, treatment methods, and case histories (3,13,21). The most recent study is a comprehensive review of geotechnical investigations of loess in North America by Lutenegger et al. (16).

[a]Presented at the April 14–18, 1980, ASCE Annual Convention and Exposition, held at Portland, Oreg.

[1]Assoc. Prof. of Civ. Engrg., Syracuse Univ., Syracuse, N.Y. 13210.

[2]Pres., Building and Civ. Engrg. Contractors Makurdi, Nigeria; formerly Grad. student, Syracuse, Univ., Syracuse, N.Y. 13210.

Note.—Discussion open until August 1, 1981. To extend the closing date one month, a written request must be filed with the Manager of Technical and Professional Publications, ASCE. Manuscript was submitted for review for possible publication on September 15, 1980. This paper is part of the Journal of the Geotechnical Engineering Division, Proceedings of the American Society of Civil Engineers, ©ASCE, Vol. 107, No. GT3, March, 1981. ISSN 0093-6405/81/0003-0305/$01.00.

Types of Collapsible Soils

The most extensive deposits of collapsible soils are Aeolian or wind-deposited sands and silts (loess). In addition, alluvial flood plains, fans, mud flows, colluvial deposits, residual soils, and volcanic tuffs may produce collapsible soils. In most cases, the deposits are characterized by loose structures of bulky-shaped grains often in the form of silt to fine sand size (see Fig. 1).

Aeolian Deposits.—These deposits consist of materials transported by wind which form dunes, loess, loessial-type deposits, aeolic beaches, and large volcanic dust deposits. They consist of cohesionless or slightly cohesive soils and may have a low relative density. The natural structure of these soils may contain a clay cement binder such as the loessial soils. These deposits are characteristic of arid regions where the water table is at great depth below the ground surface. Upon saturation, the clay cement binder loses its strength. Under these conditions, the material suffers structural collapse. The fine aeolian sediments are sometimes found protected from weathering in nature by a surface crust of impermeable

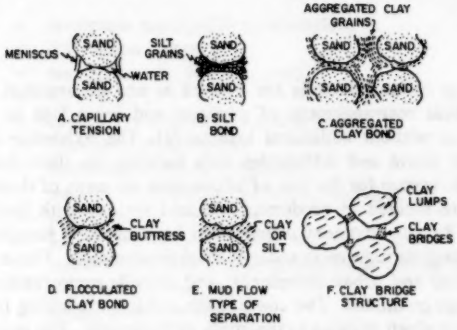

FIG. 1.—Typical Collapsible Soil Structures (3)

clay. This crust protects the entrance of large quantities of water, thus preserving the natural structure. For this reason, even in climates of medium rainfall, fine aeolian deposits are modified either not at all or only partially.

Large areas of the earth's surface, particularly in the midwestern and western United States, and parts of Asia and southern Africa, are covered with loess that is susceptible to a large decrease in bulk volume when saturated. Loess, a yellow to reddish-brown soil covers approx 17% of the United States, about 17% of Europe (including the low countries), parts of France, Germany, and Eastern Europe, 15% of Russia and Siberia, and large areas of China. Loess is found in New Zealand and the plains region of Argentina and Uruguay, principally between latitudes 30° and 40°. Loess appears to be formed by wind-borne deposits traveling over glacial outwash causing precipitation of the soil particles.

Water-Laid Deposits.—Water-laid deposits consist primarily of loose water-deposited sediments which form alluvial fans, flows, and flowslides. In the San Joaquin Valley of California, e.g., cases have been observed of subsidences

up to 15 ft in water-laid deposits. These materials were originally deposited by flash floods or mud flows derived from small watersheds subject to cloudbursts at infrequent intervals. These deposits dry out and never again become saturated until the arrival of another flow. Flows consist of poorly consolidated materials that contain considerable clay. The amount of clay in a flow has an important bearing on the soils' behavior. Bull (6) has shown that the maximum subsidence occurs when the clay amounts to about 12% of the solids. Below 5% there is little subsidence, and above 30%, the clay swells. In between, there are cases in which soils with larger pore spaces settled more than those at the same void ratio, but with smaller pores.

Residual Soil.—Residual soils are the product of weathering, i.e., the disintegration and mechanical alteration of the components of parent rocks. The particles of residual materials may vary in size from large fragments to gravel, sand, silt, colloids, and in some cases, organic matter. The collapsible grain structure has developed as a result of leaching of soluble and colloidal material. This leaching out of the soluble and fine material results in a high void ratio and unstable structure. Low densities may be found in the upper part of the subsoil due to eluviation. Generally, residual soil profiles are encountered in thicknesses ranging from a few inches to several feet, depending on the climate and physiographical environment of the region. Residual decomposed granites in South Africa and northern Rhodesia, e.g., have been found to have a total collapse amounting to about a 7%–10% increase in density (5).

Other soil types that exhibit collapse upon wetting are those derived from volcanic tuff (17), gypsum (25), loose sands cemented by soluble salts, dispersive clays, and sodium-rich montmorillonite clays (23).

Wetting of Soil Structure

Russian studies (11) have shown that there are four main types of wetting that can trigger the collapse of soils:

1. Local, shallow wetting of a random nature caused by water sources from pipelines or to uncontrolled drainage of surface water from construction. Water from local wetting does not usually penetrate to great depths and there is normally no rise in the ground-water level. In this case, settlement occurs mainly in the upper layer of soil below the wetted zone.
2. Intense, deep, local wetting of soil caused by discharge of industrial effluents or irrigation. If the flow rate is sufficient to cause a continuous rise in the ground-water level, then the entire zone of collapsible soil may be saturated in a short time span (several months to a year). In this case, the settlement is extremely uneven and dangerous. It may include the whole thickness of the soil layer and collapse may occur either under the load from existing structures or under the weight of the soil itself.
3. Slow and relatively uniform rise of the ground-water level under the influence of water sources outside the collapsible soil area. The settlement is normally uniform and gradual.
4. Gradual slow increase of the moisture content of a thick layer of soil, resulting from condensation of steam and accumulation of moisture caused by changes in the evaporation conditions (e.g., when the ground is covered by

concrete or asphalt). The weakening of the internal cohesion of the soil is then partial. Correspondingly, the settlement is incomplete, and slowly increases with the wetness of the soil. Collapse may be triggered by water alone, or by saturation and loading acting together.

Causes of Phenomenon

According to Barden et al. (3), appreciable collapse of a soil requires the following three conditions: (1) An open, potentially unstable, partly saturated structure; (2) a high enough value of an applied or existing stress component to develop a metastable condition; and (3) a strong soil bonding or cementing agent to stabilize intergranular contacts, with a reduction which, upon wetting, will produce collapse.

All cases so far studied have shown that these soils have a honeycomb structure of bulky-shaped grains with the grains held in place by some bonding material or force. When the support is removed, the grains are able to slide over onto one another, moving into vacant spaces.

In cases where the soil consists of sand with a fine silt binder, the temporary strength is due to capillary tension. As the soil dries below the shrinkage limit, capillary action places the water under tension. This increases the apparent strength of the soil. However, addition of water reduces the strength, and if the soil is porous, a rapid decrease in volume may occur. According to Aitchison and Donald (1), for uniform spherical grains in an open or cubical packing, the maximum added pressure due to the capillary effect occurs at a moisture content of about 32%. For the densest packing of uniform spherical grains, the maximum tension occurs at 10% moisture. Investigations conducted with various collapsible soils indicate that the peak effective stress values occur at moisture contents less than saturation and above 10% water content.

Knight (15) has shown that sands and silts loaded in the unsaturated state may collapse upon wetting. This collapse follows a unique virgin compression line. It has been suggested by Blight (4) that the uniqueness of the virgin saturated compression line holds for swelling soils, although Burland (7) has expressed the view that the soils with high clay content, the effect of stress history on soil structure will become significant. Holtz and Hilf (12) explained the collapse on the basis that saturation releases confining stresses, and the sample fails in shear, thus undergoing additional settlement. Holtz and Hilf (12) also obtained compression curves showing that collapse occurs in soils compacted to high densities when dry of optimum moisture content.

The majority of collapsing soils involve the action of clay particles in the bonds between the bulky sand grains. A number of structural arrangements of the clay particles are possible depending on the history of the soil (see Fig. 1). Clays that are formed by authigenesis possibly form a parallel plate onionskin effect around the quartz particles. Gradual evaporation of the pore water can cause the clay plates to retreat with the water into the menisci at interparticle contacts. Knight (15), using an electron microscope, found that under such conditions the clay grains cluster around the junctions in a random flocculated arrangement, giving a buttress type of support to the bulky grains. The nature of the clay bonding is complex and it is not yet clear how much is due to electrochemical effects and how much to capillary effects. However,

it has been observed that in most cases, the lower the water content, the greater the bond strength.

Cementing agents such as iron oxide, calcium carbonate, or the welding of the grain contacts, provide strength for many collapsible soils. This cementing action is often the main agent in loessial soils. The rate at which a cementing agent loses its effectiveness depends on the degree of contamination of the incoming water and the rate of the solution of the cementing agent involved.

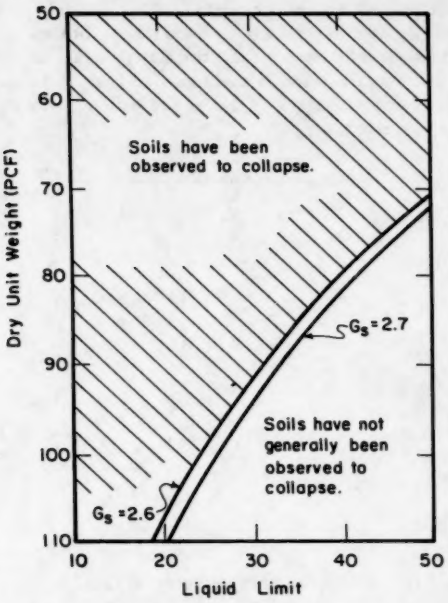

FIG. 2.—Collapsible and Noncollapsible Loess (12)

An increase in load could add to this effect, as an increase in pressure on the soils will increase their rate of solution, which could produce a delayed increase in consolidation. However, whatever the physical basis of the bond strength, all collapsible soils are weakened by the addition of water. Collapse in strength is more immediate in the case where the grains are held together by capillary suction, slow in the case of chemical cementing, and much slower in the case of clay buttresses.

Recognition of Problem in Field and Laboratory

A geotechnical engineer needs to be able to identify readily the soils that could collapse and to determine the amount of collapse that may occur. Soil deposits most likely to collapse are: (1) Loose fills; (2) altered wind-blown

sands; (3) hillwash of loose consistency; and (4) decomposed granite or other acid igneous rocks.

Gibbs (10) has proposed the use of the natural dry density and liquid limit as criteria for predicting collapse. His method is based on the premise that a soil, which has sufficient void spaces to hold its liquid limit moisture at saturation, is susceptible to collapse upon wetting (see Fig. 2). Soil densities that plot above the line shown in Fig. 2 are in a loose condition, and when fully saturated will have a moisture content greater than the liquid limit.

A very simple test which can be performed in the field is the "sausage" test. A hand-size sample of the soil to be tested is broken into two pieces, and each is trimmed until they are approximately equal in volume. One of them is then wetted and molded in the hands to form a damp ball. The two volumes are then compared again. If the wetted ball is obviously smaller, then collapse may be suspected.

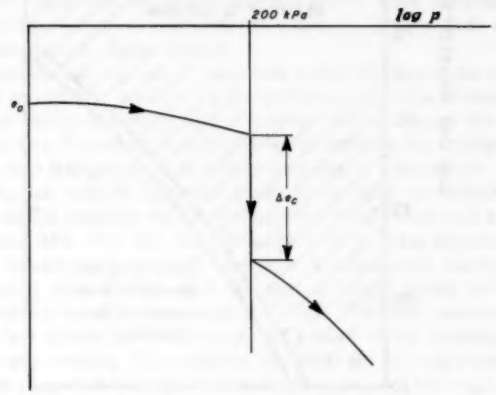

FIG. 3.—Typical Collapse Potential Test Result

A more satisfactory test can be done with a consolidation test, as suggested by Knight (15). A sample of the soil is cut to fit in the consolidometer ring, and loads are applied progressively until about 200 kPa is reached. At the end of this loading, the specimen is flooded with water and left for a day, and the consolidation test is then carried on to its maximum loading limit. The resulting curve is shown in Fig. 3. The collapse potential is then defined as:

$$CP = \frac{\Delta e_c}{1 + e_o} \quad \ldots\ldots\ldots\

in which ΔHc = change in height upon wetting; and Ho = initial height. This collapse potential is only a guide to the collapse which may be encountered. Jennings and Knight (13) have suggested some values for collapse potential which are shown in Table 1.

Calculation of Collapse Settlement

A method to predict the collapse settlement of a soil for design purposes has been proposed by Jennings and Knight (13), using the results of a double consolidation test. The use of this test will give not only a qualitative determination

TABLE 1.—Collapse Potential Values

CP, as a percentage (1)	Severity of problem (2)
0–1	No problem
1–5	Moderate trouble
5–10	Trouble
10–20	Severe trouble
20	Very severe trouble

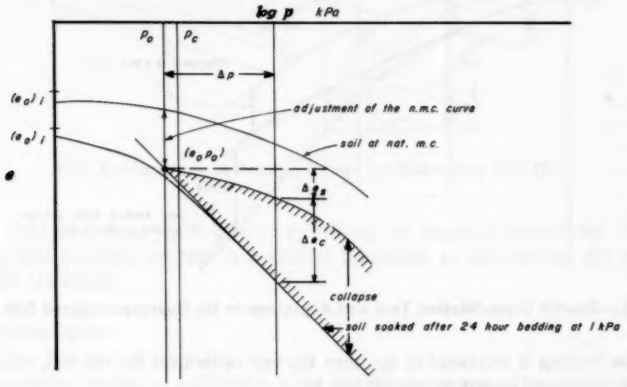

FIG. 4.—Double Consolidation Test and Adjustments for Normally Consolidated Soil (13)

of the possibilities of collapse, but also quantitative information to allow estimates to be made of the magnitude of the collapse.

Two undisturbed similar samples, preferably block samples cut by hand (those taken using a thin-walled tube are usually disturbed), are tested. Both samples are carefully trimmed into consolidometer rings, and placed in a consolidometer under a light 1 kPa seating load for 24 h. At the end of the 24 h, one sample is inundated by flooding with water, while the other sample is kept at its natural water content. Both samples are then left for a further 24 h. If the soaked sample swells, it is possible that either a rebound effect is being experienced

or the soil may be of the heaving type. Generally, most collapsing soils of a sandy type will show little or no change during this 24-h soaking period. The test is then carried out in the ordinary manner, doubling the applied loads each 24 h, and the results are plotted. From the plot it can be observed that the initial void ratios of the two samples after the first 24 h of loading are not identical, and that the two curves do not start from the same point (see Fig. 4). The total overburden pressure, P_o, at the depth of the sample, is calculated and plotted on the e versus log p curves obtained from the two tests. The precompression pressure, P_c, is found from the soaked curve and compared with P_o.

Normally Consolidated Case.—For the case in which P_c/P_o is equal to 0.8–1.5 (essentially normally consolidated), compression is considered to take place on the virgin curve and the natural moisture content curve is adjusted to the e_o, P_o point by drawing a curve parallel to the natural moisture consolidation curve, as shown in Fig. 4.

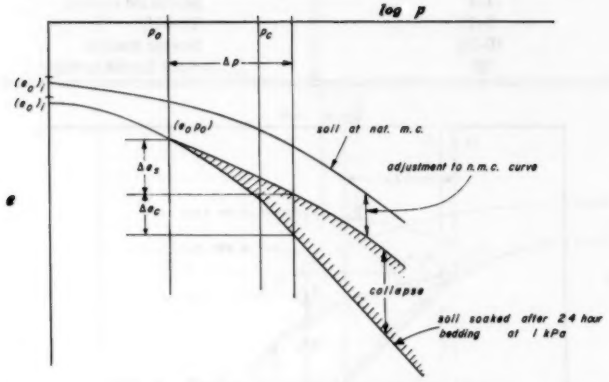

FIG. 5.—Double Consolidation Test and Adjustments for Overconsolidated Soil (13)

If the loading is increased to Δp, then the unit settlement for the soil, without change of natural moisture content will be

$$\frac{\Delta e_s}{1 + e_o} \quad \ldots \ldots \ldots

Overconsolidated Case.—In the case of an overconsolidated soil ($P_c/P_o < 1.5$), the adjustment to the curve largely follows the ordinary settlement computation practices. The only difference between the two cases lies in the determination of the e_o, P_o point, as shown in Fig. 5.

Jennings and Knight (14) conducted several field studies and found that the agreement between observed and predicted collapse settlements was good. There are several but infrequent cases in which tests have been conducted with samples having an equal or nearly equal $(e_o)_i$. This can be attributed to disturbance during sampling. Since there is a variety of mechanisms supporting collapsible soils, and a number of predictive techniques, a field test should be performed whenever possible to check the laboratory analysis and the efficiency of the wetting technique used. The major drawback of field tests however, is that they are expensive and time consuming. Recent studies by Riggs (19), and Riggs and Schmidt (20), have indicated that allowable design pressures can be determined

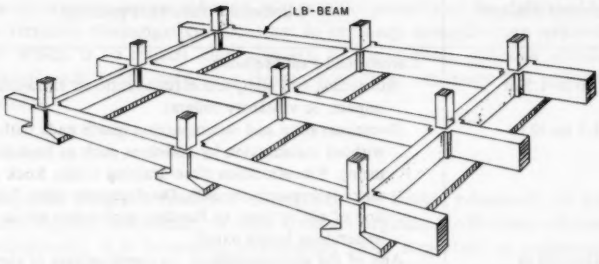

FIG. 6.—Continuous Footing Design for Collapsible Soil (26)

from field plate load tests, laboratory testing, or standard penetration tests. The initial moisture content is a critical parameter in determining the most suitable technique.

Foundation Design

Foundation design in collapsible soils is difficult at best. The results from laboratory or field tests can be used to predict the amount of settlement that can be expected. In many cases, deep foundations (piles, caissons, etc.) may be required to transmit foundation loads to suitable bearing strata below the "collapsible" soil deposit. In cases where it is feasible to support the structure on shallow foundations on or above collapsing soil, the use of continuous strip footings may provide a more economical and safer foundation than isolated footings. Differential settlement between columns can be minimized, and a more equal distribution of stresses may be achieved with the use of strip footings. A practical procedure for the design of a strip foundation, suggested by Zeevaert (26), is shown in Fig. 6. The foundation system is comprised of reaction beams formed by footing beams and load balancing beams in the longitudinal direction; the load balancing beams are reinforced to make the system sufficiently stiff.

The performance of continuous footings, as well as other shallow foundation schemes may be improved, i.e., the vertical displacements may be reduced, and more load carrying capacity gained with the use of compensated footings (26). If the footing area becomes greater than 50% of the entire area of the building, then a mat foundation should be considered for the entire foundation.

Current Treatment Methods

On some sites, it may be feasible to apply a pretreatment technique in order to either stabilize or cause collapse of the soil deposit prior to construction of a specific structure or facility. The amount of treatment and type depends

TABLE 2.—Methods of Treating Collapsible Foundation Soils

Depth of subsoil treatment desired (1)	Foundation treatment method (2)
	Current and Past Methods:
0 m–1.5 m	Moistening and compaction (conventional extra-heavy, impact, or vibratory rollers).
1.5 m–10 m	Overexcavation and recompaction (earth pads with or without stabilization by additives such as lime or cement); Vibroflotation (free-draining soils); Rock columns (vibroreplacement); Displacement piles; Injection of silt or lime; or Ponding or flooding (if no impervious layers exist).
Over 10 m	Any of the aforementioned, or combinations of the aforementioned, where applicable; Ponding and infiltration wells; or Ponding and infiltration wells with the use of explosives.
	Possible Future Methods:
	Heat treatment to solidify the soils in place; Ultrasonics to produce vibrations that will destroy the bonding mechanisms of the metstable soil; Chemical additives to strengthen the bonding mechanism of the metstable soil structure (possibly electrochemical methods of application); or Use of grout-like additives to fill the pore spaces before solidification.

on the depth of collapsible soil and the support requirements for the proposed facility. A great variety of treatment methods have been used in the past. Table 2 is a summary by Bara (2) of various treatment methods used. Further technological advances are necessary before heat treatment, ultrasonics, or chemical additives (other than lime or cement), are feasible.

The Russians have conducted extensive studies with chemical stabilization techniques (21,22). The methods currently employed are: (1) Gaseous silicatization of sandy and loessial soils; (2) strengthening of carbonate cements by polymers; and (3) chemical strengthening of alluvial soils by clay-silicate solutions (21). The gaseous silicatization treatment involves a mixture of soil, carbon dioxide, and a sodium silicate solution. Field tests on noncarbonate-type sandy soils

pretreated with carbon dioxide have shown strength increases of 20%–25%.

Recent investigations by Sokolovich (22) have shown that stabilization of loessial soils by treatment with ammonia is possible. In this method, gaseous ammonia is injected via boreholes into loessial soil prone to slump-type settlements. The ammonia is absorbed by water films of the loessial soil and reacts with its absorbing complex. As the result of an exchange reaction with the absorbed calcium, highly-dispersed calcium hydroxide is formed. During adsorption saturation of 1 m^3 of loess, 5 kg–8 kg of gaseous ammonia is adsorbed, leading to the precipitation of 10 kg–17 kg of highly-dispersed calcium hydroxide. Reaction of the precipitated calcium hydroxide with the silica and colloidal silicic acid of the soil leads to formation of a calcareous-siliceous binder which stabilizes the soil.

In the case of gaseous stabilization of loessial soils, the lime precipitated by the exchange reaction is located on the surface of the colloidal absorbing complex. In this case, only the skeleton of the loessial soil is stabilized, and its natural structure is strengthened, whereas the porosity of the stabilized loessial soil is virtually unchanged. In contrast to ordinary strengthening methods, the aim of which is to impart high strength to the ground, gaseous stabilization of loessial soils leads only to a decrease in their tendency for collapse-type settlements.

Conclusions

Collapsible soils are scattered throughout the world, principally in arid and semi-arid regions. Since many of these areas are beginning to develop economically and industrially, it is becoming increasingly more important to understand and predict the behavior of these soils. Structures or facilities (canals, embankments, etc.) of any nature constructed on these soils should receive careful attention.

General methods of recognizing collapsible soils and predicting their performance are summarized herein, along with a number of pretreatment techniques that may be applicable to sites underlain by collapsible soils.

In many instances, collapsible soils are undetected during initial soils investigations. An increased awareness of the existence of these soils and more full-scale research are needed to evaluate the present predictive techniques and treatment methods.

Acknowledgments

A number of individuals assisted in preparation of this paper through encouragement and helpful reviews. The writers are most grateful to J. G. LaBastie, former Chairman of the Shallow Foundations Committee, Joseph J. Rixner, Harvey Wahls, and Alan B. Gifford.

Appendix.—References

1. Aitchison, G. D., and Donald, I. B., "Effective Stresses in Unsaturated Soils," *Proceedings*, Second Australia-New Zealand Soils Mechanics Conference, 1956, pp. 192–199.
2. Bara, J. P., "Collapsible Soils," presented at the September 1976, ASCE Annual Convention and Exposition, held at Philadelphia, Pa.

3. Barden, L., McGown, A., and Collins, K., "The Collapse Mechanism in Partly Saturated Soil," *Engineering Geology*, Amsterdam, The Netherlands, 1973, pp. 49–60.
4. Blight, G. E., "Effective Stress Evaluation for Unsaturated Soils," *Journal of the Soil Mechanics and Foundations Division*, ASCE, Vol. 93, No. SM2, Proc. Paper 5146, Mar., 1976, pp. 125–148.
5. Brink, A. B. A., and Kantey, B. A., "Collapsible Grain Structure in Residual Granite Soils in South Africa," *Proceedings*, Fifth International Conference on Soils Mechanics and Foundation Engineering, 1961, pp. 611–614.
6. Bull, W. B., "Alluvial Fans and Near-Surface Subsidence in Western Fresno County, California," *Professional Paper, 437-A*, United States Geological Survey, Washington, D.C., 1964, p. 72.
7. Burland, J. B., "Effective Stress in Partially Saturated Soils," thesis presented to the University of Witwaterstrand, at Johannesburg, South Africa, in 1961, in partial fulfillment of the requirements for the degree of Doctor of Philosophy.
8. Dudley, John H., "Review of Collapsing Soils of Luanda and Luso Regions," *Fifth Regional Conference for Africa on Soil Mechanics and Foundation Engineering*, 1971.
9. Dudley, John H., "Review of Collapsing Soils," *Journal of the Soil Mechanics and Foundations Division*, ASCE, Vol. 96, No. SM3, Proc. Paper 7278, May, 1970, pp. 925–947.
10. Gibbs, H. J., and Bara, J. P., "Predicting Surface Subsidence from Basic Soil Tests," *Special Technical Publication No. 322*, American Society for Testing and Materials, 1962, pp. 231–247.
11. Goldshtein, M. N., "Principles of Building Design on Soils Prone to Slump-Type Settlement Owing to Wetting," *Osnovaniya, Fundamenty i Mekhanika Gruntov*, No. 6, Nov.–Dec., 1969, pp. 25–27.
12. Holtz, W. G., and Hilf, J. W., "Settlement of Soil Foundations Due to Saturation," *Proceedings*, Fifth International Conference on Soil Mechanics and Foundation Engineering, Vol. 1, 1961, pp. 673–679.
13. Jennings, J. E., and Knight, K., "A Guide to Construction on or with Materials Exhibiting Additional Settlement Due to 'Collapse' of Grain Structure," *Sixth Regional Conference for Africa on Soil Mechanics and Foundation Engineering*, Sept., 1975, pp. 99–105.
14. Jennings, J. E., and Knight, K., "The Additional Settlement of Foundations due to Collapse of Sandy Soils on Wetting," *Proceedings*, Fourth International Conference on Soil Mechanics and Foundation Engineering, Vol. 1, Aug., 1957, pp. 316–319.
15. Knight, K., "The Origin and Occurrence of Collapsing Soils," *Proceedings*, Third Regional Conference for Africa on Soil Mechanics and Foundation Engineering, Vol. 1, 1963, pp. 127–130.
16. Luetenegger, R., Hallberg, G., and Handy, R., "Review of Geotechnical Investigations of Loess in North America," International Union for Quarternary Research, Brussels, Belgium, 1979.
17. Morland, L. W., and Hastings, C. R., "A Void-Collapse Model for Dry Porous Tuffs," *Engineering Geology*, Amsterdam, The Netherlands, Vol. 7, No. 2, 1973, pp. 81–97.
18. Northey, R. D., "Engineering Properties of Loess and Other Collapsible Soils," *Seventh International Conference on Soil Mechanics and Foundation Engineering*, 1969, pp. 445–452.
19. Riggs, C. O., "Shallow Foundations on Dense Silty Loessial Soils," thesis presented to the University of Missouri-Rolla, at Rolla, Mo., in 1978, in partial fulfillment of the requirements for the degree of Doctor of Philosophy.
20. Riggs., C. O., and Schmidt, N. O., "Foundation Design for Loessial Collapsible Soils," presented at the April 14–18, 1980, ASCE Annual Convention and Exposition, held at Portland, Oreg.
21. Sokolovich, V. E., "New Developments in the Chemical Strengthening of Ground," *Osnovaniya, Fundamenty i Mekhanika Gruntov*, No. 2, Mar.–Apr., 1971, pp. 23–25.
22. Sokolovich, V. E., and Gubkin, V. A., "Gaseous Silicatization of Loessial Ground," *Osnovaniya, Fundamenty i Mekhanika Gruntov*, No. 5, Sept.–Oct., 1970, pp. 26–28.
23. Sowers, G. F., "Shallow Foundations," *Foundation Engineering*, G. A. Leonards, ed., McGraw-Hill Book Co., Inc., New York, N.Y., 1962.
24. Sultan, H. A., "Collapsing Soils, State-of-the-Art," *Seventh International Conference on Soil Mechanics and Foundation Engineering*, No. 5, 1969.

25. Toulemont, M., "Geological Observations of the Dissolution of Gypsum in the Paris Area," *Proceedings,* First International Congress, International Association of Engineering Geology, Vol. 1, 1970, pp. 62–73.
26. Zeevaert, L., *Foundation Engineering for Difficult Subsoil Conditions,* Van Nostrand Reinhold Publishing Co., New York, N.Y., 1972.

JOURNAL OF THE GEOTECHNICAL ENGINEERING DIVISION

GEOTECHNICAL CONSIDERATIONS FOR CONSTRUCTION IN SAUDI ARABIA

By Issa Oweis,[1] M. ASCE and John Bowman[2]

INTRODUCTION

The rapid and continuing development of Saudi Arabia has attracted the attention of many engineering firms and contractors competing for a share of the Saudi construction program. A prior knowledge of ground conditions is necessary not only for a proper basic design but also to assure that the construction is compatible with environmental geology. This paper describes ground conditions and their implication in design and construction in the Kingdom of Saudi Arabia. Many of the concepts presented are applicable in many other areas of the Near East as well.

To assess ground conditions in Saudi Arabia, a general knowledge of topography, climate, and bedrock geology is essential. These factors control the development of surface soils and rocks and, therefore, control ground conditions.

Saudi Arabia, approximately 830,000 sq miles in area, occupies most of the Arabian Peninsula (see Fig. 1). The terrain is quite irregular. The principal physical divisions are the relatively flat western coastal area, the western mountain zone (Asir and Hejaz), the central plateau which declines northward in elevation to the Plains of Jouf, and the relatively flat terrain of the Eastern Province bordering on the Persian (Arabian) Gulf. Several depressions, believed to be the result of tectonic movement, are superimposed. Examples are the Rub al Khali (Empty Quarter) Desert, the Dibdibba Basin, and Wadi as Sirhan Basin. Other basins such as the Tabuk Basin that extends to the Jordanian border are believed to be the result of erosion.

[1]Vice Pres., Converse Ward Davis Dixon, 91 Roseland Ave., P.O. Box 91, Caldwell, N.J. 07006.

[2]Chf., Foundation, Material and Survey Branch, United States Army Corps of Engrs., Middle East Div.

Note.—Discussion open until August 1, 1981. To extend the closing date one month, a written request must be filed with the Manager of Technical and Professional Publications, ASCE. Manuscript was submitted for review for possible publication on June 3, 1980. This paper is part of the Journal of the Geotechnical Engineering Division, Proceedings of the American Society of Civil Engineers, ©ASCE, Vol. 107, No. GT3, March, 1981. ISSN 0093-6405/81/0003-0319/$01.00.

CLIMATE

The development of surface sediments is influenced by the arid and semi-arid hot climate in the Kingdom. In addition, this climate has significant effect on materials used in superstructures. Chemical reactions affecting durability of

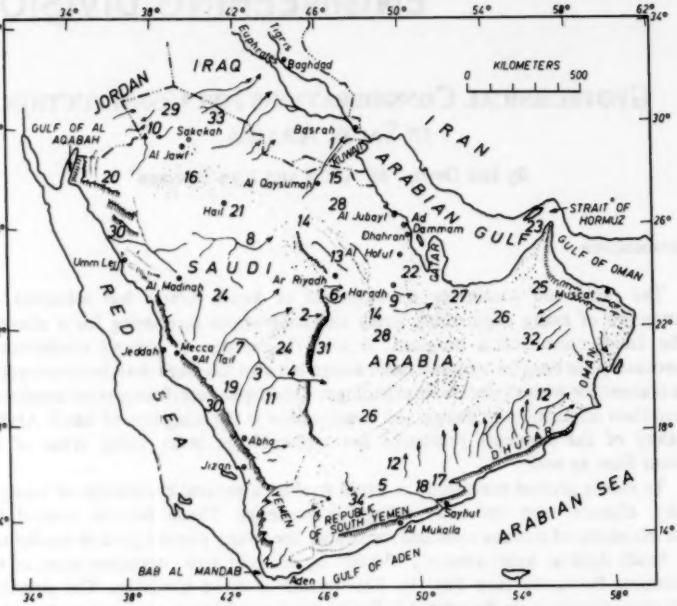

NUMBERS INDICATE LOCATIONS OF WADIS AND LANDFORMS.

WADIS: 1. WADI AL BATIN, 2. WADI BIRK, 3. WADI BISHAH, 4. WADI AD DAWASIR, 5. WADI HADHRAMAWT, 6. WADI NISAH, 7. WADI RANYAH, 8. WADI AR RIMAH, 9. WADI AS SAH'BA, 10. WADI AS SIRHAN, 11. WADI TATHLITH.

LANDFORMS: 12. ADEN HINTERLAND, 13. AL 'ARAMAH ESCARPMENT, 14. AD DAHNA, 15. AD DIBDIBAH, 16. GREAT NEFUD, 17. HADHRAMAWT PLATEAU, 18. HADHRAMAWT VALLEY, 19. AL HIJAZ PLATEAU, 20. HISMA PLATEAU, 21. JABAL SHAMMAR, 22. AL JAFURAH, 23. MUSANDAM PENINSULA, 24. NAJD PEDIPLAIN, 25. OMAN MOUNTAINS, 26. AR RUB' AL KHALI, 27. SABKHAT MATTI, 28. AS SUMMAN PLATEAU, 29. SYRIAN PLATEAU, 30. TIHAMAH, 31. TUWAYQ ESCARPMENT, 32. UMM AS SAMIM, 33. AL WIDYAN, 34. YEMEN HIGHLANDS.

FIG. 1.—Map of Arabian Peninsula Showing Principal Geomorphic Features [Courtesy, Springer-Verlag (2)]

concrete are accelerated by higher temperatures, and extreme temperature fluctuation causes expansion and contraction in concrete elements and bituminous paving. Some of the effect of the hot climate on concrete construction (compared to a temperate climate) is shown in Fig. 2.

The Arabian Peninsula is bisected by the Tropic of Cancer. In summer months, daytime temperatures frequently exceed 40° C (extremes above 50° C have been recorded). Daily variations in temperatures of 15° C are not uncommon. Winter temperatures are about 20° C on the average and in some elevated regions, like Qasim, temperatures may drop to below zero. Precipitation is quite low (some areas receive little or no rainfall for several years) and evaporation rates are very high, exceeding precipitation by a factor as high as 30. While the rainfall is quite low (see Fig. 3), it occurs with a high intensity creating flash floods. With little or no soil or vegetation cover in hilly areas, high runoffs occur, resulting in flooding and the development of watercourses (wadis). The flash floods can cause significant damage to property and construction sites. Recognition of the flood potential is particularly significant in assessing the need for protection of highway embankments. Some of these wadis change course over the years, and thus a proper assessment of the need for highway

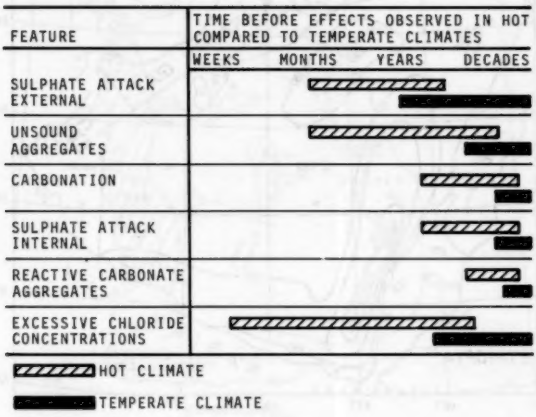

FIG. 2.—Some Aspects of Concrete Deterioration Related to Certain Environmental Factors and Time (1)

protection in the long term is required. Many small culverts are usually preferred over small numbers of widely spaced large culverts. It should be noted that estimates of flow (for a site drainage or highway culvert) from standard hydraulic handbooks may lead to gross underestimates if the "flash flood" condition is not recognized. The major wadi flood areas are shown in Fig. 4.

The development of salt flats (sabkhas) or salt bearing soils in Saudi Arabia is mostly attributable to climate. These saline soils are evaporites that form in desert basins or wadi lakes, or form in other areas by fluctuating groundwater. Along the coast, sabkhas develop above the level of normal high tide either due to intense evaporation of salty water drawn to the surface by capillary action, or due to evaporation of tidal water that periodically inundates the surface. Evaporite salts are also present in local bedrock and therefore shallow groundwater or water drawn to the surface by capillary action is usually salty. The evaporites

are aggressive and mostly made up of the soluble salts (halite and anhydrite) and the less soluble gypsum. Saline soils could cause corrosion of steel and deterioration of foundation concrete. Structural collapse of salt cemented soil can occur upon prolonged exposure of the soil to water.

Climatic effect is also evidenced by the loss of support of pavements in coastal areas. Evaporation is prevented or retarded by impervious asphalt surfaces, and capillary action increases moisture content beneath the pavement. This destroys capillary tension and saturates the subgrade. For subgrades sensitive

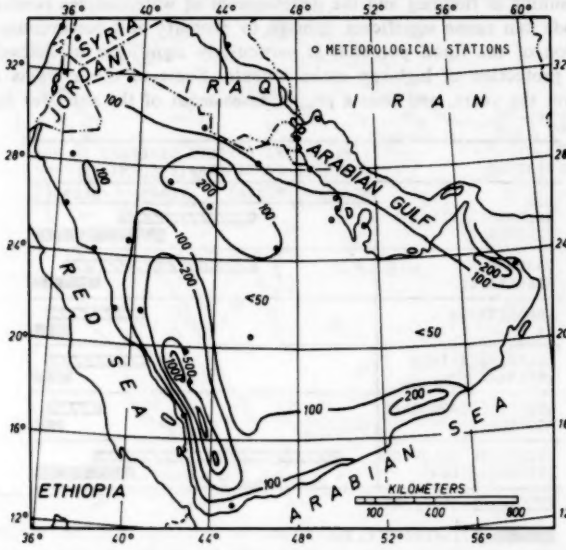

FIG. 3.—Isohyetes of Average Yearly Precipitation, in millimeters [Courtesy, Springer-Verlag (2)]

to saturation, pavement instability would occur. For this reason, most designers use "soaked" California Bearing Ratio (CBR) for pavement design.

Geology

Approximately one-third of Saudi Arabia is underlain by a Precambrian Basement Complex of igneous and metamorphic rocks (Arabian Shield) (see Fig. 5). The remaining area (nearly 600,000 sq miles) is underlain by sedimentary rocks of various ages (Cambrian to Quaternary) deposited over the basement rocks with thicknesses of several hundreds of meters and gentle dips (to north, south, and east) of 1°–2°. Many of the sedimentary formations are pervious and contain water and oil. The source of groundwater is primarily the runoff from elevated areas of the Arabian Shield where rocks are impervious and

where groundwater is confined to wadi alluvium.

The western coastal plain along the Red Sea is low in elevation, in many areas covered by the salt bearing deposits, and is flooded as a result of rainstorms. In some locations, salt bearing soils are absent and in their place are terraces of coralline limestone overlooking the Red Sea and, further inland, localized deposits of argillaceous silts and gypsum outcrops can be found. The coastal plain is usually protected or isolated by offshore bars and limestone reef chains which often form lagoons. Elevated limestone reefs often outcrop, and raised beaches, sand dunes, and occasionally gypsiferous sands and gravels are encountered.

FIG. 4.—Main Drainage Systems of Saudi Arabia (3)

West of the coastal plains, offshore coral banks and reefal limestones can be found either outcropping or covered with mostly carbonate sands.

The coastal plains of the Red Sea rise gently into an eastern plain (Piedmont), consisting of granular soils (gravels, boulders, cobbles, sands, and silts), overlying Tertiary (limestones, shales, siltstones, and sandstones) or crystalline rocks. In some cases, especially near the fringes of the coastal plain, the granular soils were deposited during floods originating from the mountains to the east, and thus overlie soft coastal plain deposits. Salt beds, e.g., halite in Jizan, can be found in the Tertiary rocks. This Piedmont zone extends to the mountainous Arabian Shield. Gravels and boulders are usually found in the high zone of the slope, and finer soils prevail with increased distance down the gentle slope.

The Precambrian rocks of the Arabian Shield are mainly of the igneous and

metamorphic type, e.g., in Khamis Mushayt are found granites and gneisses and in Taif are found granites, schists, amphibolites, and gneisses. The rocks form a dome-shaped topography and often are overlain by younger volcanics (mainly basalts) or thin (less than 10 m) strata of alluvial sands and gravels, or both. In addition, late Precambrian nonmetamorphosed red arkoses and conglomerates can be recognized in isolated basins or folds over much of the southwestern part of the Arabian Shield.

Uplift of the shield is believed to have occurred in the late Precambrian Age. The eroded Precambrian basement is covered by successions of mostly sandstones, overlain by shales, with the lower sandstones extending northward into the marine Cambrian rocks of Jordan. Erosion has continued since the Precambrian time producing present-day alluvial fans and wadi deposits.

Sedimentary rocks (mostly limestone, but also sandstones and shales) of various ages overlie the basement rocks east of the Arabian Shield and extend to the

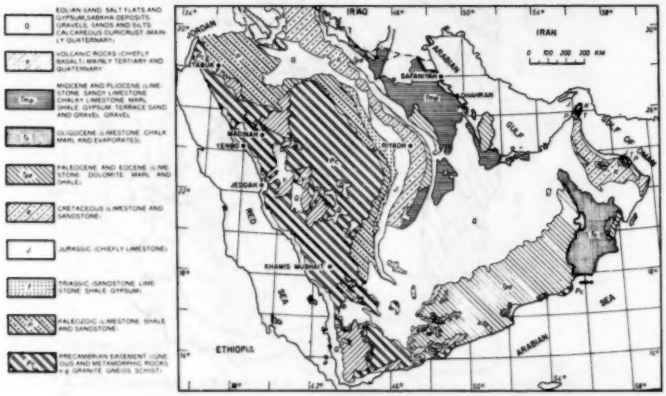
EOLIAN SAND, SALT FLATS AND GYPSUM, SABKHA DEPOSITS, GRAVELS, SANDS AND SILTS (CALCAREOUS DURICRUST MAINLY QUATERNARY)
VOLCANIC ROCKS (CHIEFLY BASALT) MAINLY TERTIARY AND QUATERNARY
MIOCENE AND PLIOCENE (LIMESTONE, SANDY LIMESTONE, CHALKY LIMESTONE, MARL, SHALE, GYPSUM, TERRACE SAND AND GRAVEL, GRAVEL)
OLIGOCENE (LIMESTONE, CHALK, MARL AND EVAPORITES)
PALEOCENE AND EOCENE (LIMESTONE, DOLOMITE, MARL AND SHALE)
CRETACEOUS (LIMESTONE AND SANDSTONE)
JURASSIC (CHIEFLY LIMESTONE)
TRIASSIC (SANDSTONE, LIMESTONE, SHALE, GYPSUM)
PALEOZOIC (LIMESTONE, SHALE AND SANDSTONE)
PRECAMBRIAN BASEMENT (IGNEOUS AND METAMORPHIC ROCKS e.g. GRANITE, GNEISS, SCHIST)
IRAQ
JORDAN
IRAN
ARABIAN
SAUDI ARABIA
DAMMAM
GULF
GULF OF OMAN
TABUK
MEDINA
RIYADH
JEDDAH
RED SEA
KHAMIS MUSHAYT
ETHIOPIA
ARABIAN SEA
0 100 200 300 KM

FIG. 5.—Generalized Geologic Map of Arabian Peninsula (Modified) [Courtesy, Springer-Verlag (2)]

Persian (Arabian) Gulf. Overlying these sedimentary rocks is a typically thin soil cover (a few meters, resulting from either rock weathering or windblown sand) or with a thicker (several meters) cover of wadi alluvium or residual soils (mostly stiff clays) that are also the product of rock weathering.

Sedimentary rock deposits dip gently to the east (1°–2°) and extend to the Gulf. These rocks have been subjected to uplift and erosion (probably in the Tertiary Age) and the more resistent or massive rock units form west-facing escarpments such as Jabal Tuwayq near Riyadh. Sands and gravels of the Quaternary Age can be found in wadis between escarpments such as wadi Hanifa west and south of Riyadh and along escarpments near Riyadh. Deposits of Tertiary sands and gravels and lacustrian limestone can be found along erosion channels, such as wadi Sahba in Al-Kharj.

The coastal plain of the Gulf (eastern coastal plain) is covered by Quaternary

sediments consisting of salt bearing soils, inter sabkhas, areas of sand dunes, and outcrops of limestone and calcareous sandstones. The near-shore Gulf floor consists of shelly and clayey sands, corals, limestones, and sandy limestones. Often the shelly sands are cemented to a thin and relatively hard "caprock" or marine conglomerate. The layering and occurrence of surface and near-surface sands and rocks in the Gulf Plain and floor is related to Quaternary marine processes.

Geotechnical Considerations

Foundation Zones.—From a geotechnical viewpoint the Kingdom can be divided into four major zones as follows:

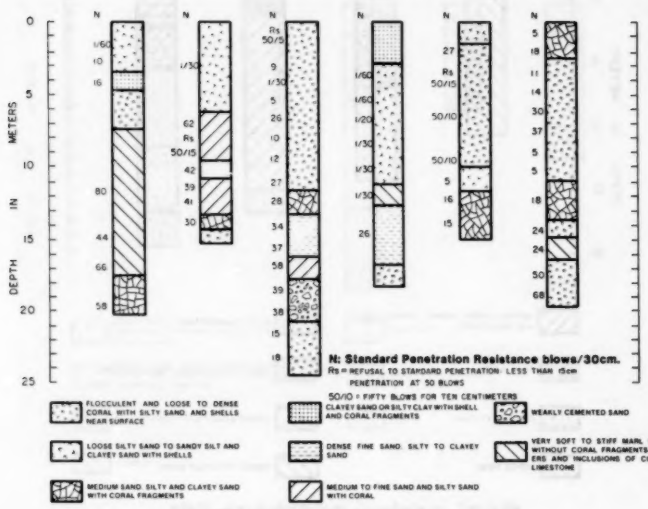

FIG. 6.—Subsurface Conditions, Zone A-1

1. Zone A—Western coastal plain consisting of Zone A-1, generally covered by soft sabkha coastal deposits, and Zone A-2, covered by alluvial deposits from coast to Arabian Shield.
2. Zone B—Arabian Shield extending north and east to the coastal plains of the Gulf.
3. Zone C—Sedimentary rocks from Shield to coastal plains of the Gulf.
4. Zone D—Eastern coastal plain.

Foundations.—Determination of the most suitable method for foundation support depends on the subsurface conditions at a particular site, considered as follows.

Zone A (Western Coastal Plain).—Soil conditions in this zone vary from generally soft and loose surface sabkha deposits in the western portion (Zone A-1) to the generally dense alluvial fans and wadi deposits extending eastward to the foothills of the Arabian Shield (Zone A-2). The sabkha deposits, varying in classification from sand to clay within the same site, can be found with variable thickness but usually not more than 10 m and typically less than 3 m thickness, and may be underlain by dense granular soils, reefal limestone, or loose sand and soft clay layers with coralline rock layers or ledges. The soft and loose coastal soils may range in thickness from a few meters to 20 m or greater, so that a typical profile could be misleading. At some sites, e.g., Yanbu, boulders and cobbles transported by wadi floods may overlie the soft and loose deposits.

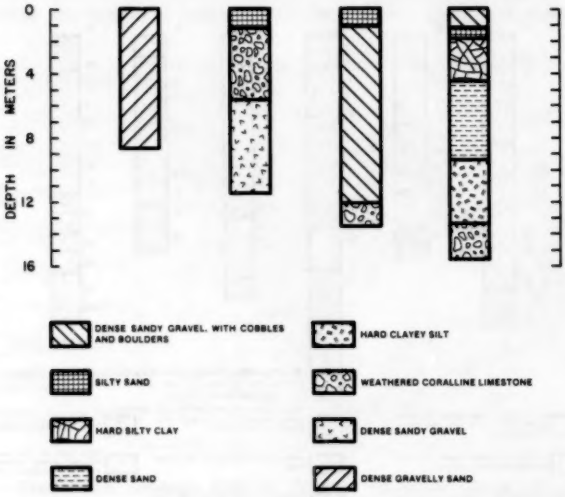

FIG. 7.—Subsurface Conditions, Zone A-2

Figure 6 depicts conditions encountered by various borings for a large site in the vicinity of Jeddah. The density of the coral formations vary erratically as well as the occurrence and stratigraphy of soil strata. In a marine environment such as Zone A-1, extrapolation of data to an adjacent unexplored location involves great uncertainties.

Methods used for foundation support in Zone A-1 vary, depending on the loads and performance requirements, e.g., preloading and conventional foundations have been used successfully in Jeddah to support 1 story–2 story structures. The time of preloading is generally less than 6 months but depends on the stratigraphy at the specific locations. As in other places, deep stabilization techniques may be used to densify the loose granular soils but a high shell content may retard the usefulness of this technique since it may not be possible to achieve the required density.

The use of piles or other deep foundations should consider the extreme variations in the rock surface, e.g., in Jeddah, and the presence of hard rock ledges or layers above loose soils. A properly conducted site investigation prior to design and construction should reduce the risk of surprise related to the extreme variability of subsurface conditions, and identify potential problems posed by high water table. Requirements, design, and construction problems in Zone A-1 vary along the coast, e.g., the width and thickness of this zone in Yanbu is less than in Jeddah. Piles driven onshore in Yanbu can be expected to be shorter and may bear on the dense granular stratum beneath the upper loose and soft stratum (and not necessarily on rock of unknown thickness and extent with large variations in pile lengths, as is sometimes the case in Jeddah).

Zone A-2 soils (generally dense sands and gravel or hard clays) present no

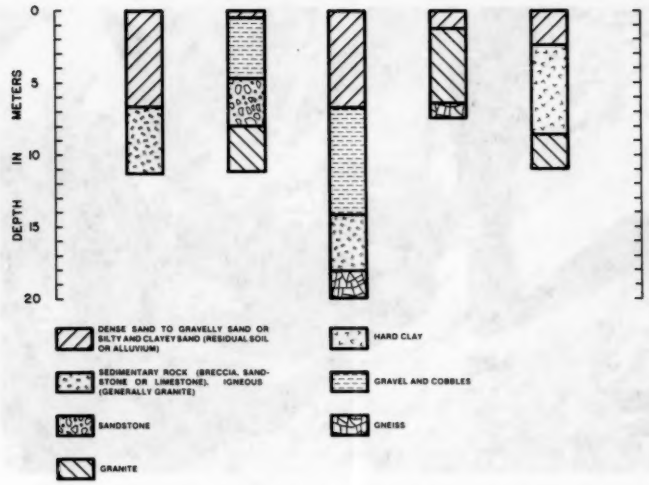

FIG. 8.—Subsurface Conditions, Zone B

unusual design and construction problems. Example stratifications are depicted in Fig. 7. Spread or strip footings on natural soil or compacted fill may be used. In some coastal locations, e.g., Jizan, soft surface soils are sometimes encountered and associated problems are compounded by the presence of soluble salts in the sedimentary formations. For these conditions, support by piles bearing in layers not affected by solution have been suggested. However, proper site and facility drainage to prevent prolonged exposure to water would be more appropriate. The same applies to soluble gypsum bearing soils in other coastal areas, e.g., Yanbu. In addition to the potential for solution, the gypsum bearing soils have a structure that is prone to collapse (resulting in significant settlements) upon prolonged exposure to water. Identification of such soils is critical to the proper selection of foundation design and construction methods. One procedure to qualitatively evaluate the potential for collapse under prolonged

exposure to moisture is the use of the plate load test on the soil under dry and saturated conditions in the field.

Zone B (Arabian Shield).—Problems related to the presence of soft soil conditions are not common in this zone. A geotechnical section (see Fig. 8) would show relatively shallow cover composed of in-place weathered soil, wadi alluvium, or windblown sands and silts over rock (mostly igneous and metamorphic) with varied degrees of weathering. In some cases rock weathering has resulted in layers of residual soil (generally dense sand and gravel but occasionally hard clay near the eastern border of the Arabian Shield). At some sites, e.g., in Taif, soil cover (dense wadi sands and gravels) as deep as 7 m can be encountered. The use of the saturated penetration test in this zone for site investigation should be supplemented by test pits, trenching, and shallow seismic

FIG. 9.—Cavity Development, Limestone of Arab Formation, Riyadh

refraction surveys. Because of expediency, hollow stem augering is often used for the borings. The classification of the materials based on cuttings is poor, especially when distinguishing residual soil from completely weathered rock. For a typical site, individual footings could bear on dense natural soil (or compacted fill), or residual soil or rock. Depending on the magnitude of design loads, some special site preparations may be required to minimize differential settlements. Evaluating rock rippability and blasting requirements are of primary significance in any site investigation in this zone. In general, rock encountered within 2 m of the surface can be expected to be rippable. However, variations can be expected. Trenching may be used effectively to evaluate rippability in conjunction with other techniques (seismic velocities, point load test, RQD, etc.). As the rock is relatively impervious, shallow groundwater conditions may be created, depending on site grades, as a result of irrigation, e.g., in Taif,

and underdrains may be necessary, depending on the design particulars.

Zone C (Sedimentary Rocks).—This zone covers the area east and north of the Arabian Shield to the coastal plains of the Gulf. Foundation requirements in the zone are influenced by: (1) The presence of cavities in limestone bedrock, e.g., in Riyadh, Dammam, Buraydah, and other locations; (2) the presence of gypsum bearing soils in basins and other poorly drained locations, e.g., Tabuk, Qaysumah, Al-Kharj, Riyadh, and other locations; (3) the presence of inland sabkhas, e.g., in wadi Sirhan, southeast of Buraydah, and other locations; and (4) variability of foundation material within the same site, e.g., rock versus clay residual soil.

Thick sequences of sedimentary rocks have been deposited in this zone since

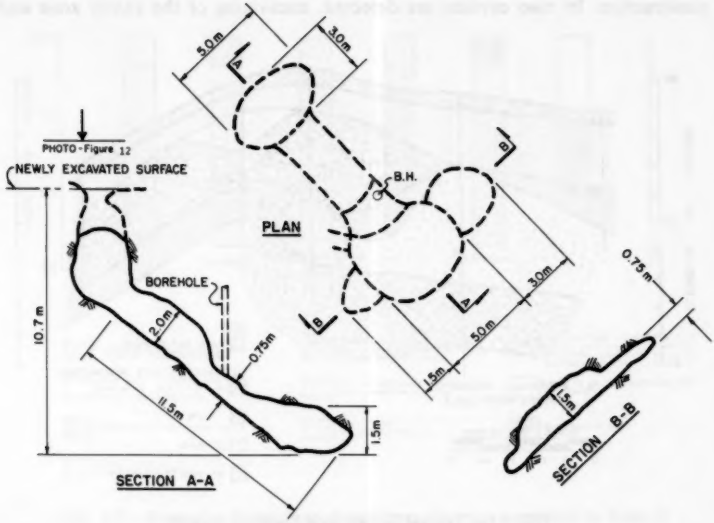

FIG. 10.—Subsurface Section of Figure 12

Precambrian time. Relatively thick layers (a few meters) of calcareous silt can be expected in between the more resistant limestone formations. Some limestones, e.g., the Arab Formation, contain anhydrite beds in which past surface dissolution has resulted in present-day dry cavities and solution channels. Cavity presence in the Arab Formation (Fig. 9) is most frequent along the north-south axis of the city of Riyadh. Figure 10 shows details of a solution channel found at a site in Riyadh. These cavities are often encountered (during construction) between locations where borings showed no cavity development (the subsurface section in Fig. 11 for a site in Riyadh typifies the variability of the limestone for a typical site).

Since the upper rock surface in Zone C is usually shallow (typically 0 m–3 m), cavity presence heavily impacts foundation design and site preparation.

Numerous cavities have been encountered within 10 m beneath the surface. Unfortunately, detailed bedrock verification techniques are expensive and may not be effective, depending on particular site conditions. Usually, reliance is placed on borings and cheaper probes using wagon drill. Other sophisticated means for bedrock verification such as microgravity and resistivity have not, to the writers' knowledge, been applied successfully in Saudi Arabia. Observations and verification (by wagon drill probes at foundation locations) during construction are quite important and sometimes imperative if foundation failure is to be avoided. Another measure useful for design of lightly loaded structures is to use properly sized and reinforced strip footings (instead of spread footings) to span undetected cavities. When spread footings are employed, it is preferable and relatively inexpensive to verify conditions below each footing during construction. In case cavities are detected, excavating of the cavity zone and

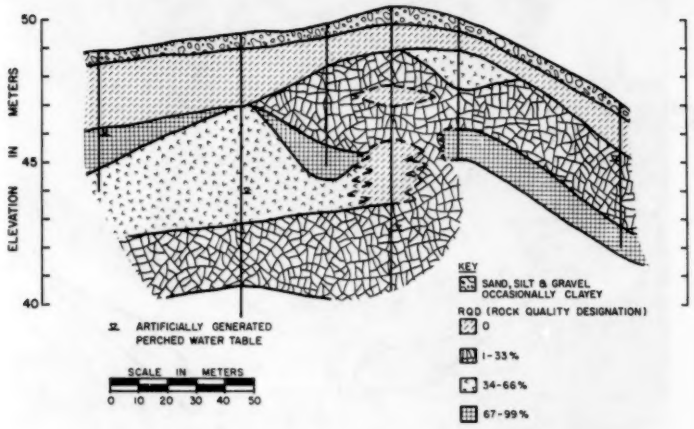

FIG. 11.—Typical Subsurface Section, Riyadh

backfilling (with soil or concrete) or grouting may be employed depending on conditions. As is the case in Zone B, evaluating rippability and need for blasting is essential and can be accomplished by site and laboratory investigation techniques, e.g., rock coring and logging, shallow seismic refraction techniques and laboratory strength tests.

The potential for cavernous limestone is not confined to Riyadh. Extensive cavity developments have also been encountered in Buraydah, Dammam, and Hofuf and some cavities have even occurred near Al Batin beneath the overlying conglomerates.

While conditions of shallow rock in Zone C are typical, relatively deep-soil profiles (alluvium or alluvium over residual soil) may be encountered. In a site situated in downtown Riyadh, the soil profile consisted of 10 m of dense gravelly sand underlain by 10 m of stiff plastic clay over marly cavernous

limestone. Figure 12 exemplifies some soil profiles in various Zone C sites.

Some sedimentary formations, e.g., the Russ Formation in the eastern region, contain thick layers of marls. Attempts are usually made to auger through the highly indurated layers (or boulders) and if this fails, coring is then attempted. The marl is classified as ML or SM or CL according to the Unified Classification System. Allowable bearing values on marl are variable. Allowable bearing values used for footings on the Rus Formation have varied from 3 tons/sq ft to as high as 9 tons/sq ft. In a typical profile, layers of rock or rock fragments are embedded in a dense soil matrix. The marl is often used as compacted fill to support spread footings. When this is done, proper site and facility drainage is essential since the marl is known to lose strength and settle upon prolonged exposure to moisture.

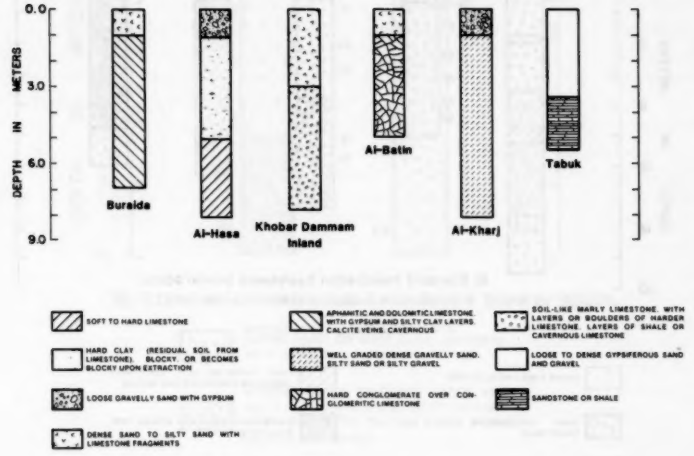
DEPTH IN METERS
0.0
3.0
6.0
9.0
Buraida
Al-Hasa
Khobar Dammam Inland
Al-Batin
Al-Kharj
Tabuk
SOFT TO HARD LIMESTONE
APHANITIC AND DOLOMITIC LIMESTONE WITH GYPSUM AND SILTY CLAY LAYERS. CALCITE VEINS. CAVERNOUS
SOIL-LIKE MARLY LIMESTONE WITH LAYERS OR BOULDERS OF HARDER LIMESTONE. LAYERS OF SHALE OR CAVERNOUS LIMESTONE
HARD CLAY (RESIDUAL SOIL FROM LIMESTONE) BLOCKY OR BECOMES BLOCKY UPON EXTRACTION
WELL GRADED DENSE GRAVELLY SAND, SILTY SAND OR SILTY GRAVEL
LOOSE TO DENSE GYPSIFEROUS SAND AND GRAVEL
LOOSE GRAVELLY SAND WITH GYPSUM
HARD CONGLOMERATE OVER CONGLOMERITIC LIMESTONE
SANDSTONE OR SHALE
DENSE SAND TO SILTY SAND WITH LIMESTONE FRAGMENTS

FIG. 12.—Example, Subsurface Conditions, Various Locations in Zone C

Gypsum bearing soil can be encountered in poorly drained areas anywhere in Zone C. Support of footings on gypsum bearing soils can be made safe by extending footing depth to zones where the percentage of gypsum can be considered acceptable, and providing stringent control of water access, e.g., grading the site for water to drain away from the footing, concrete paving, enclosing water carrying pipes in impermeable galleries, etc. The most economic solution would depend on specific site conditions. It should be mentioned that gypsum bearing soils may occur in localized areas and for a large site, they may be missed by borings. Therefore, proper verification during construction is essential. The percentage of gypsum in soils used for compacted fill should be controlled depending on the grading plans and the moisture environment. As explained earlier, plate load tests may be used to evaluate the potential for collapse of the soil structure.

The problems associated with inland sabkhas are not much different from those of coastal sabkhas. The depth of inland sabkha zones varies and the current highway practice in the Kingdom is either to avoid these areas or to displace the weak material by fill. Typically, bridges are pile supported. The filling scheme is not entirely satisfactory as significant roadway settlements have been reported. The method could be improved by excavating to hard bottom first and reestablishing grade with controlled compacted fill.

Superimposed on Zone C are extensive areas of sand dunes and areas of alluvial deposits. The alluvial wadi deposits (fine gravels and sands), e.g., in Al-Kharj, may be several meters thick overlying bedrock and usually provide good foundation support.

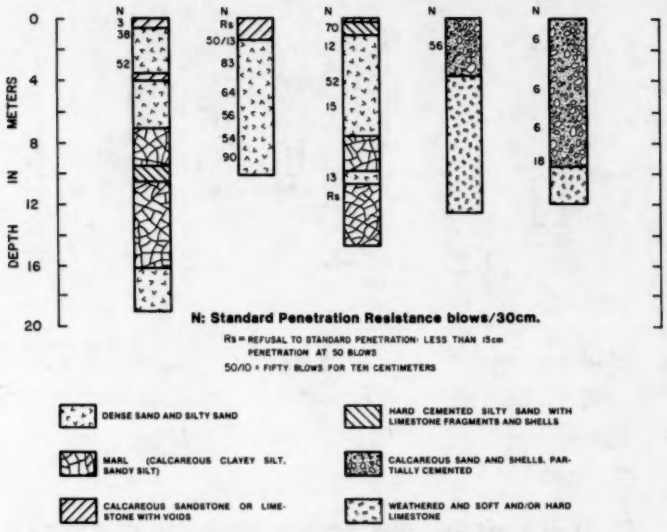

FIG. 13.—Subsurface Conditions, Off-Shore, Jubail

Sand dune areas may be loose, especially near the surface. Mobile dunes present maintenance problems for roads. In addition to design techniques (aligning route considering prevailing wind direction and location of sand source, little or no crown, etc.), techniques such as cutting of dunes, fencing, planting, paving, or oil spraying and impregnation may be considered for dune stabilization. None of these techniques are problem free and as most are relatively expensive, continuous maintenance may be cheaper and more effective.

Zone D (Eastern Coastal Zone).—Most of the eastern coastal plain is categorized by the presence of salt bearing soils or sand dunes. Typically, subsurface conditions are defined by an upper zone (usually less than 3 m thick) of soft and loose deposits in low-lying areas near the shore and generally medium dense to dense sands below. Layers of stiff to hard clays, ledges or lenses

of soft to hard rock can be encountered in thicknesses up to several meters. Artesian groundwater conditions also may be encountered with piezometric level several meters above ground surface. Some soil profiles below the mudline in the offshore portion of Jubail are exemplified in Fig. 13. Figure 14 depicts conditions along or near the shore. Surface limestone caprock is often encountered along the shore with thicknesses up to 2 m, which could present problems during dredging. Soil conditions below the mudline can vary from loose to very dense depending on location.

Selection of suitable methods for foundation support in Zone D again depends on location. Generally, considerations described for Zone A apply to Zone D.

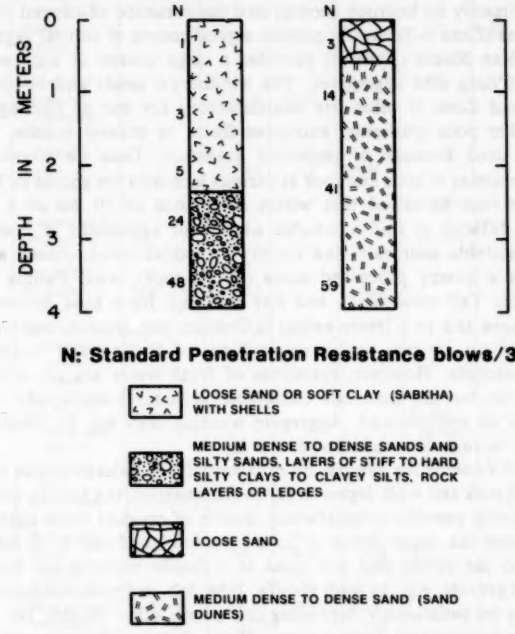

FIG. 14.—Typical Near Shore Deposits, Zone D

However, the thickness of loose soils and the required depth of stabilization in Zone D is generally less than in Zone A. Thus, excavating the soft or loose soils and replacing by fill probably would be more cost effective in Zone D. Shallow foundations bearing on natural soil or compacted fill are feasible in the medium dense to dense sand areas. The same methods of support may be feasible for supporting light to medium heavy structures on properly filled and preloaded loose sabkha areas. Pile foundations may have to be used for heavy structures depending on the sensitivity of structures to settlements. Soil improvement techniques, e.g., vibroflotation, terraprobe, and dynamic compac-

tion, may be considered if shelly layers are not prevalent. The applicability of these techniques should be assessed by construction of carefully controlled and monitored test sections.

As indicated previously, loose soils may contain large volumes of shells and these could preclude the effectiveness of the stabilization method selected. The underlying denser soils may also contain large concentrations of shell that may affect both pile installation and support. A properly conducted site investigation is therefore prudent. The presence of rock ledges and lenses that are not continuous should be considered in planning underground structures, dredging, and design of pile foundations.

Construction Materials.—The availability and quality of construction materials are dictated primarily by bedrock geology and the presence of alluvial deposits. The alluvial fans (Zone A-2) usually provide a good source of natural aggregates, while the Arabian Shield (Zone B) provides a large source of rock which is suitable for crushing into aggregates. The windblown sands and beach sands in Zone A-1 and Zone D often are unsatisfactory for use as fine aggregate because of either poor gradation, excessive fines, or excessive salts. Quarry sand is often used because of improved gradation. Data on physical and engineering properties of soils and rock at various locations are shown in Table 1.

In general, it can be stated that within a distance of 30 km of a site, it should not be difficult to find a suitable source for aggregates in Zone A or Zone B, e.g., suitable sources in the vicinity of Jeddah can be found at Jabal At Tawilah for a quarry processed stone (basalt rock), wadi Fatima (which extends from the Taif mountains), and Ras at Belejh for a sand borrow area. In the Yanbu area and to a lesser extent in Jeddah, construction materials are abundant and there appears to be no problem of finding and transporting construction materials. However, resources of fresh water are nil or limited, and salts that render the materials unsuitable in natural aggregates without processing may be encountered. Aggregate washing may not be feasible and processing may have to be conducted in the dry.

In Zone C and Zone D, the availability of construction material is also dictated by the quality of rock and wadi deposits. In several quarries, the Jubaila limestone formation in Riyadh provides a satisfactory source of crushed stone aggregates. At many locations the upper meter or so is case hardened and is of relatively better quality to the extent that it is used as a facade material for buildings. Wadi sands and gravels, e.g., in wadi Hanifa, Jubaylah, Sulbukh, Al-Ammariyah and others, may be satisfactory depending on, among other factors, the degree of their alkali reactivity and fines content. Most of the sandstones and shales in Tabuk do not usually meet specifications for concrete aggregates and reliance is made on wadi deposits in the area, e.g., wadi Al Uthayli and wadi Al Altheeli. In some locations, aggregates have to be obtained from distant off-site sources as exemplified by the town of Taima, where the aggregates used are obtained from wadi Al Qa about 100 km south of the town.

Unfavorable bedrock geology is the key to the lack of good quality aggregates near Jubail. The quarries near Dhahran (95 km south) provide suitable sources of aggregates from limestone rocks of the Al Khobar member of the Dammam Formation. Proper quality control should be exercised to avoid contaminated or weak aggregates. Another potential aggregate source is the limestone of the Hofuf Formation, some 110 km west of the Jubail/Dhahran axis. Some outcrops

TABLE 1.—Physical and Engineering Properties: Various Sites

Location (1)	Material (2)	Specific gravity (3)	Absorption (4)	Los Angeles abrasion (5)	Soundness (6)	Maximum density, in pounds per cubic foot (7)	Optimum moisture content, in percent (8)	CBR	
								100% maximum density (9)	95% maximum density (10)
Jubail	Sand (SP)	2.64–2.71	0.86–1.8	14–40	7.1–23.4	112–115	9.6–13	23–75	14–50
Dhahran	Limestone aggregates	2.59–2.71							
	Clayey sandy marl					121	13	46	6
	Eolian sand					121	7.1	55	25
Hofuf	Limestone aggregates		3.9–5.6	31–44					
Al-Batin	Calcitic dolomite		0.24–3.9		3.1–70.7				
	Sandy limestone		0.1–4.5		3.4–91				
	Silty and clayey sands					123–130	8–14.3	44–105	10–44
Riyadh	Silty and clayey sand (SM-SC)					125–134	7–11	35–96	5–45
	Wadi sand (SP-SW)	2.45–2.5	1.69–2.3		13–20				
	Crushed limestone (Jubaila formation)	2.35–2.55	1.8–5	31–51	17–75				
Al-Kharj	Sand (SP-SW)					116	7–8	26–40	20
Tabuk	Silty and clayey sand (SM-SC)					80–100 (in situ density)		0.7–5[a]	0.7–5[a]
	Wadi sand (SW)	2.7–2.9				126–142	5–7	40–105	
	Clayey sand (SC)	2.73				118	15.2	65	
	Wadi gravel			14–22	4–5				
Taif	Diorite quarry aggregate	2.8	0.9	30–40	9–20				
	Wadi gravel	2.9–3	1–1.5	33–40	3.5–8				
	Wadi sand	2.6–2.8	1–1.8		2–16				
	Crushed granite	2.7–3	0.8–1.8	47	6				
	Crushed schist	2.9	1.1	42	3.7				
Khamis Mushayt	Surface soil (silty and clayey sand, sand)					120–130	7–9	40–90	10–20
Jeddah (Zone A2)	Silty and clayey sand	2.7				110–130	6–11	38–100	20–50
	Crushed basalt	2.7	0.2	17–22	1.4				

[a] In situ soaked CBR; moisture content 13%–20%.

near Jubail (within 30 km) may be suitable for rock fill.

With regard to water supply for construction purposes, supplies are mostly brackish water with total dissolved solids concentration above 1,500 ppm. For large construction, on-site water treatment may be required depending on the availability of potable water supply. In some cases, natural waters are of adequate quality to be used in construction without treatment. However, potential sources

TABLE 2.—Some Results of Soil and Water Analyses

Location (1)	Classification (2)	Moisture content, in percent (3)	Dry density, in grams per cubic centimeter (4)	pH (5)	Sulphate content, in parts per million (6)	Chloride content, in parts per million (7)	Field resistivity (dry) (8)	Laboratory resistivity (wet) (9)
Jeddah area	Sand (SP)	1.6	1.95	7.7	9,000	15,000	7 ohm-m	2.7 ohm-m
	Tap water			8.2	132	255		750 ohm-cm
Yanbu area	Sand (SP-SM)	6.5	1.94	8.1	15,000	28,000	28 ohm-m	1.06 ohm-m
	Water			7.3	3,200	34,000		23 ohm-cm
Taif area	Sand (SP)	1.5	1.83	8.8	600	100	350 ohm-m	81 ohm-m
	Water (well)			6.73	460	753		242 ohm-cm
Khamis Mushayt area	Sand (SM)	3.9	1.71	8.2	1,500	100	120 ohm-m	26 ohm-m
	Tap water			8.2	106	56		
	Tap water			7.9	500	324		
Tabuk area	Sand (SM)	2.6	1.52	7.7	160,000	2,000	500 ohm-m	1.7 ohm-m
		4.5	1.73	8.0	9,000	3,000	400 ohm-m	0.73 ohm-m
	Water (irrigation canal)			7.19	90	131		1234 ohm-cm
	Water (tap)				80	120		
Riyadh area	Sandy clay (CL-SC)	8.0	1.78	7.7	6,000	50,000	7.5 ohm-m	1.06 ohm-m
	Sand and gravel (GM-SM)				15,000	40,000	1.3 ohm-m	1.02 ohm-m
				8.0	85	17		
				7.8	300	213		
	Water (tap)			7.44	265	131		905 ohm-cm
				7.7	1,520	810		
				8.0	434	44		
Al-Kharj area	Sand (SM)	12.4	1.75	8.3	900	200	750 ohm-m	17.6 ohm-m
	Water (farm well)			7.5	497	168		690 ohm-cm
Jubail area	Sand (SP)	10.3	1.74	8.5	1,200	100	10 ohm-m	12.3 ohm-m
		2.2	1.7	8.3	21,000	3,000	50 ohm-m	9.2 ohm-m
	Water (tap)			8.1	94	190		
Ras Al Mishab area	Sand (SP)	1.1	1.47	7.9	35,000	200	52 ohm-m	2.2 ohm-m
	Sand (SP-SM)	0.4	1.49	8.2	3,000	3,000	60 ohm-m	2.9 ohm-m
Al-Batin area	Sand (SW)	4.2	1.33	7.8	90,000	1,000	25 ohm-m	3.7 ohm-m
	Sandy gravel (GP)	1.6	1.66	8.5	1,200	100	450 ohm-m	128 ohm-m
	Water (deep well)			7.6	907	304		460 ohm-cm

for water and aggregates should be identified and tested prior to the design phase of a specific project. The timing for testing could be important, especially when alkali reactivity of potential aggregates with cement paste is suspected. The American Society of Testing and Materials (ASTM) Standards C295 (Petrographic Examination of Aggregates for Concrete), C289 (Test for Potential Reactivity of Aggregates—Chemical Method) and C227 (Mortar Bar Method) are useful in evaluating the potential of reactivity of aggregates. If the relatively

quick chemical test (C289) or petrographic examination indicate a potential for reactivity, then the mortar bar test (C227) should help quantify that expansion (and thus the potential for damage) due to potential reactivity. The mortar bar test duration should be at least 3 months and preferably 6 months or a year, depending on the test results obtained. The writers are not aware of concrete failure in the Kingdom directly related to alkali-silica reactivity of aggregates with cement paste. Reported problems in concrete are primarily related to high content of salts (sulphates, chlorides) in concrete constituents or surrounding environment. It is known that dolomitic limestones in the eastern region contain chalcedonic cherts having the capability of producing a reaction. However, in cases known to the writers, such cherts in commercial quarries, e.g., rimrock at Dhahran, are found in such small proportions that their effect is not harmful to concrete in existing structures. Chalcedonic cherts could also be found in dune sand. Recognizing the potential harmful effect on concrete, it is prudent to investigate concrete constituents from all unknown sources with regard to potential reactivity. The cost for doing such investigations is small. The specifications should limit the salt content in concrete since marginally high salts in aggregate coupled with marginally high salt content in water would yield too high a salt content (overall) in concrete.

Corrosivity and Chemical Attacks.—Examples of sulphate attack of concrete are common in Saudi Arabia, especially in the sabkha and shoreline areas where conditions are suitable for capillary action carrying salts to and around concrete foundations. Design and construction safeguards include the use of sulphate resistant (Type V) cement, provision of a capillary barrier beneath the foundation or, in some cases, tanking the foundations, i.e., using bitumemastic coating on all sides and the bottom. In most areas of the Kingdom (Zone B and Zone C) the use of Type V cement would most probably be sufficient. In several areas of Zone B, special precautions are not required as the salt concentrations are tolerable.

Corrosion of buried pipes and metallic structures is a real problem. Chemical tests for salt content and laboratory and field electric resistivity tests and perhaps polarity measurements are performed to evaluate the potential corrosive nature at a particular site. The lower the electrical resistivity, the higher the potential for corrosion. Soils with resistivities less than 30 ohm-meter are usually considered very corrosive and embedded metallic structures may require cathodic protection. Table 2 shows data from several sites. Corrosivity is more severe in a saturated or moist environment. Buried pipework, at most sites, would require protection by coating and wrapping techniques, or, in some cases, cathodic protection could be necessary. Soil acidity is not usually a corrosion factor for the sites listed in Table 2.

Summary

Several geologic environments prevail in Saudi Arabia. Problems in design and construction are intimately related to the environment at particular locations. Coastal areas are generally characterized by particularly soft and loose corrosive soils. Limestones in the interior are characterized by the potential for the presence of mostly dry cavities and solution channels. Igneous and metamorphic rocks of good bearing quality characterize the high mountains overlooking the west

coast. Superimposed are areas of sand dunes and salt flats which could present special foundation problems. Availability of construction materials is dictated by bedrock geology varying from relatively good availability in the western areas to poor in the eastern region. As is the case in many marine environments, offshore conditions in the Red Sea are characterized by varied subsurface conditions at relatively short distances, thus affecting the design of offshore facilities. Offshore conditions are relatively more uniform along the Persian (Arabian) Gulf.

Acknowledgments

The writers are grateful to the staff of the Foundation, Material and Survey Branch, United States Army Corps of Engineers, Middle East Division, for their assistance in providing data; to D. Murphy, who reviewed the paper and provided data; to J. Portelli, who helped in preparing the illustrations; and to J. Sorensen, who typed the manuscript. The writers are also grateful to ASCE reviewers for their helpful comments and to A. Prevost and B. Randa for providing illustrations on cavity development.

Appendix.—References

1. Fooks, P. C., and Collins, L., "Concrete Problems in the Middle East," *Concrete*, Vol. 9, No. 7, 1975.
2. *Quaternary Period in Saudi Arabia*, S. A. Saad and J. G. Zötl, eds., Springer-Verlag, New York, N.Y., 1978.
3. Dequin, H., *The Challenge of Saudi Arabia*, Eurasia Press, Singapore, 1976.

JOURNAL OF THE GEOTECHNICAL ENGINEERING DIVISION

SAFETY OF A CONSTRUCTED FACILITY: GEOTECHNICAL ASPECTS

By T. William Lambe,[1] F. ASCE, W. Allen Marr,[2] M. ASCE, and Francisco Silva,[3] M. ASCE

INTRODUCTION

Civil engineers have always given priority to the safety of the facilities they design and help construct. Indeed, the public, through its action groups and governmental regulatory agencies, demands a high degree of safety for certain constructed facilities. However, differences exist in the degree of safety employed by engineers. Structural engineers use factors of safety ranging from 1-1/2–4 and higher in designing structures of steel, concrete, and wood to allow for "unknown and unforseen factors." Geotechnical engineers also employ factors of safety for the geotechnical aspects of constructed facilities. Unfortunately, economic considerations often require that the geotechnical engineer use lower factors of safety than those used by the structural engineer despite the fact that the properties of soil, the geotechnical medium, vary more than those of steel, concrete, and wood. The geotechnical engineer usually employs factors of safety ranging from 1.1–1.5 for earth slopes (but higher safety factors for foundations).

As a consequence of these relatively low safety factors, the geotechnical engineer necessarily employs greater supervision and review of construction and surveillance of operations than do other engineers in order to help ensure the safety of their constructed facilities.

With the recent dam failures in the United States [a coal slag dam at Buffalo Creek, W. Va. (Feb. 1972); the Bouldin Dam near Montgomery, Ala. (Feb.

[1]Edmund K. Turner Prof., Dept. of Civ. Engrg., Massachusetts Inst. of Tech., Cambridge, Mass. 02139.

[2]Research Assoc., Dept. of Civ. Engrg., Massachusetts Inst. of Tech., Cambridge, Mass. 02139.

[3]Geotechnical Consultant, Lexington, Mass.

Note.—Discussion open until August 1, 1981. To extend the closing date one month, a written request must be filed with the Manager of Technical and Professional Publications, ASCE. Manuscript was submitted for review for possible publication on February 5, 1980. This paper is part of the Journal of the Geotechnical Engineering Division, Proceedings of the American Society of Civil Engineers, ©ASCE, Vol. 107, No. GT3, March, 1981. ISSN 0093-6405/81/0003-0339/$01.00.

1975); the Teton Dam in Idaho (June 1976); and the Kelly Barnes Lake Dam at Toccoa Falls, Ga. (Nov. 1977)], and the resulting loss of life and property, national attention has focused sharply on dam safety. In August 1972, Congress passed Public Law 92-367 concerning dam safety; in a December 2, 1977 statement, the President initiated the Federal Dam Safety Program. We can expect further regulations on dam safety from both state and Federal agencies. Responding to the increased concern for safety of geotechnical facilities such as dams, offshore structures, and foundations for nuclear power stations, engineers have devised and executed systems of "quality control" to help reduce risks.

The details and the effectiveness of an appropriate safety program for a constructed facility depend on various factors, including; (1) Consequences of failure; (2) stage of life of the facility; (3) desired degree of safety; and (4) nature of the facility and the site. An engineer can tailor the comprehensive safety program presented herein to suit a particular situation.

This document presents an approach to "safety of a constructed facility" by outlining, analyzing, and illustrating various components of a comprehensive "safety program." Aided by Massachusetts Institute of Technology (MIT) associates, we have, over a period of 25 yrs, developed this safety program and applied parts of it to approximately 20 facilities, primarily dams and natural slopes. We continue to develop the program as we gain experience with its use.

Comprehensive Program

Approach.—When dealing with important, complex geotechnical facilities, experience clearly shows that the geotechnical profession cannot feasibly create a facility which completely fulfills all performance criteria for the entire life of the facility. Rather, the only logical approach is to "engineer a facility for its design life," i.e., create a reasonable design, construct the facility according to the design, and then execute an appropriate ongoing safety program.

Factors Dictating Approach.—For two decades, we have investigated the geotechnical engineer's capability to predict the performance of a geotechnical facility. Students of MIT, practicing engineers, and leaders in the geotechnical profession have made predictions for a variety of situations prior to the occurrence of the event. The predictors did not know of the actual outcome at the time of their predictions. By comparing *predicted performance* with *measured performance*, we obtained an approximate measure of the profession's capability to predict performance. Our evaluations suggest that the geotechnical engineer can predict with the following reliability:

1. Deformation—Predicted vertical deformation = ±50% of the measured deformation. Predicted horizontal deformation = ±150% of measured deformation.
2. Stress—Predicted change of pore pressure = ±25% of measured change of pore pressure. Predicted lateral stress = ±50% of measured lateral stress.
3. Stability—Predicted factor of safety = ±25% of measured factor of safety.
4. Flow—Predicted flow = ± one order of magnitude of measured flow.

Candidate Facilities.—Experience shows the desirability of a long-term safety

program for the following types of facilities: (1) Natural slopes, especially cut slopes; (2) excavations; (3) fluid retention systems; and (4) offshore and waterfront facilities. Natural slopes, particularly those involving a reduction of stresses from cutting, can become less safe over a period of time. The drop in stability results from a rise in pore water pressure and, for certain types of soil, a loss in shear strength. Professor Skempton's work in England and our own experience in Puerto Rico and Venezuela show natural slopes that failed years after formation.

Dams, like natural slopes, can weaken with time. Filling a reservoir tends to increase the pore water pressures in the dam, thereby lowering its strength. In addition, the removal of soil fines by flowing water may worsen with time.

Structures designed for earthquakes or sea storms will normally experience their most severe loading months or years after construction. Engineers should use measurements of performance during the early life of the facility to check on its safety prior to arrival of the maximum loading. This procedure, a feature of the program described herein, may prevent a failure similar to that which occurred at Sines, Portugal where a large breakwater failed under storm conditions less severe than the design storm.

Components of Program.—The Geotechnical Safety Program has the following purposes:

1. To determine the degree of safety of a constructed facility (geotechnical aspects).
2. To help maintain a predetermined degree of safety of a constructed facility.
3. To furnish the technical base to permit alteration of the facility to obtain a different, usually higher, degree of safety.

Our comprehensive geotechnical safety program has nine components:

1. Performance Criteria:
   a. Determine the consequences of failure.
   b. Select an acceptable level of risk.
   c. Establish criteria of performance.
   d. Ensure that the criteria meet appropriate legal requirements and accepted standards of practice.
2. Design Assessment:
   a. Check the design conditions, such as loads.
   b. Identify the critical mechanisms of performance.
   c. Identify typical and critical sections.
   d. Review the field and laboratory data used by the designer. Inspect the site and run selected tests on the soil(s) that greatly affect the design.
   e. Examine the prediction methods employed by the designer. Check to see whether the designer's methods rest on mechanisms approximating the expected actual ones.
   f. Check the designer's predictions of performance and compare them with the performance criteria.
   g. Prepare a Design Summary which states clearly and references the loads used by the designer as well as his prediction methods and parameters, and portrays the predicted performance.

h. Use the designer's methods and parameters to predict performance for conditions expected during the early life of the facility.

i. Identify major uncertainties and critical aspects of performance.

3. Field Measurement System:

a. Select appropriate field instruments and place them so they can measure critical aspects of performance.

b. Install instruments which can reveal mechanisms and values of key parameters. The engineer should observe the installation of instruments to ensure that they are placed at the correct locations and that they read correctly.

c. Periodically check and maintain the field instruments.

4. Construction Assessment:

a. Make periodic inspections of the facility during its construction. Compare the actual construction with the design and document the significant features of construction, particularly those features which vary from the original design.

b. Assess the significance on predicted performance of such departures from the design.

c. Make frequent site visits where difficult site conditions prevail. For highly complex situations, have a representative present on the site during critical stages of construction.

5. Surveillance:

a. Make periodic visual inspections of the project, searching for any evidence of malfunction.

b. Measure important aspects of performance.

c. Obtain information—data on mechanisms and parameters.

d. Portray (versus time) field measurements, significant events, and predicted values.

6. Performance Evaluations:

a. Periodically compare predicted performance, measured performance, and performance criteria. Attempt to explain any differences shown by the comparison.

b. Compare predicted and measured mechanisms and parameters.

7. Safety Assessment:

a. Determine and indicate (in terms of safety factor or probability of failure) the degree of safety of the facility.

b. State and evaluate any change in degree of safety during the period since the last safety assessment.

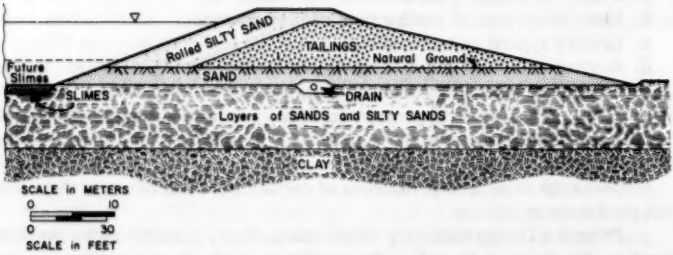

FIG. 1.—Critical Section of Dam

c. State whether or not the existing degree of safety meets performance criteria.

8. Remedial Measures:
   a. Design and assist in executing remedial measures to bring the degree of safety to a satisfactory level if the safety assessment reveals an inadequate level of safety.
   b. Evaluate the effectiveness of remedial measures.
9. Contingency Plan:
   a. Develop a plan to limit the consequences of a failure.

The preceding nine components constitute the comprehensive safety program. The following portion of this paper illustrates "Design Assessment," "Performance Evaluation," and "Safety Assessment." These illustrations come from actual projects.

Design Assessment

The preceding section listed the components of a design assessment. The thoroughness of and approach to the design assessment depends on the nature and importance of any given project. The engineer making the design assessment should maintain independence from the organization designing the facility. The following six steps give a general framework for the design assessment:

1. Review the design documents and drawings.
2. Examine the site.
3. Consider the design with the designer and the owner.
4. Perform selected check or supporting tests and analyses, or both.
5. Summarize the design assessment.
6. Analyze the assessment with the designer and the owner.

Fig. 1 shows a critical section of a design for a dam built to initially store

TABLE 1.—Design Parameters

Soil (1)	Designer's Value (2)	Assesser's Value (3)
(*a*) Permeability, in meters per second $\times 10^{-6}$		
White sand	10	25
Black silty sand	0.1	1
Silty sand (hardpan)	0.5	1
Brown sand	1	25
Marly sand	10,000	300
Silt	0.1	50
Clay	0.001	0.001
(*b*) Strength, in degrees		
White sand	37	37
Black silty sand	38	32
Silty sand (hardpan)	38	32

TABLE 2.—Summary of Typical Design Assessment

	PERFORMANCE ASPECT	OWNER'S CRITERIA	DESIGNER'S PREDICTION	BASIS FOR PREDICTION	ASSESSOR'S EVALUATION	ASSESSOR'S RECOMMENDATIONS
FORCE DEFORMATION	CRACKING	width ≤ 0.5 inch length ≤ 6 ft. depth ≤ 6 inches	$w_c \geq$ 0.5 inch $l_c \geq$ 6 feet $d \geq$ 6 inches	Observed cracking of adjacent, existing dam		Initiate steps to reduce likelihood and consequence of cracks
	SETTLEMENT	total settlement ≤ 2 ft.	$P_{max} \leq$ 1.5 feet	Settlement of embankment from self-weight		Local regrading may be required to maintain surface drainage
	embankment / foundation	differential settlement ≤ ℓ/200	$\Delta\rho/\ell \leq$ 1/2000	Difference in total settlement due to varying height of embankment	$\Delta\rho/\ell$ may exceed criterion where dam crosses from mined to unmined foundation and at connections to existing dam	Observe these locations during construction Repair any cracks
STABILITY	SHEAR SLIDE	factor of safety ≥ 1.5	F.S. ≥ 1.8	Stability analyses for deep circles	F.S. may decrease to 1.5 with ϕ from assessor's lab test	
			F.S. = 1.1	Stability analyses for shallow circles	Local sloughs possible. Repair immediately to avoid progressive failure	Criterion not met. Must observe and prepare remedial plan.
					Stability of mass on east side between dam toe and mine cut not considered.	Have designer evaluate
	LOW EFFECTIVE STRESS	artesian head ≤ 0	$a_{max} \simeq$ 3 ft.	Flow nets	Control of artesian heads depends on assumptions that • R.L. < 125 ft. until slimes reach elev. 120 • slimes effectively seal bottom of reservoir	R.L. cannot exceed +125 until slimes reach +120 Piezometers required at locations with predicted artesian heads.
	black sand & hardpan				FEDAR analyses show "a" could exceed 5 ft. below black sand.	May require remedial work during operation to reduce artesian head Install drain through black sand and hardpan to reduce artesian head
SEEPAGE	SEEPAGE QUANTITY in gpm/1000 lin. ft.	collected flow ≤ 70 flow into ground ≤ 200	$Q_c \simeq$ 0 $Q_g \simeq$ 0	Estimated Vertical seepage thru slimes and foundation	From FEDAR $Q_t = Q_c$ = 650	Criterion on total flow exceeded. Requires further consideration.
		flow off property ≤ 20 total flow ≤ 275	Q_o = 400 Q_t = 400	$Q_o = Q_t - Q_g - Q_c$ From flow net with R.L. = 135 and slimes		
	SOIL TRANSPORT	critical gradient / gradient ≥ 5	ratio = 1.1 on downstream slope ratio = 2.1 at toe	Stability analyses for shallow circles Corps of Engineers method	Designer's calculation not consistent with definition of criteria From designer's nets $i_{max} \sim$ 1.0 From FEDAR analyses i_{max} = 3.5 F.S. = 10/3.5 = 3 Seepage breakout predicted to occur.	Criterion on maximum gradient exceeded. Requires further consideration
	SEEPAGE QUALITY X** in ppm	Meet Federal and State requirements	Off-property flow will meet requirements		Seepage of mine water thru dam improves mine water quality	
MISCELLANEOUS	STORM CAPACITY	Freeboard ≥ 5 ft. Spillway capacity for 12 in. rainfall in 24 hr.	Freeboard > 5 ft. Spillway capacity > 12 in. rainfall in 24 hr.	Dam crest 5 ft. > max. R.L. Rainfall over reservoir and capacity of spillway i		
	ANIMAL HOLES	Hole length ≤ 2 feet Hole diameter ≤ 3 in.	Not a problem	Previous experience with earth dams in this area		
	VEGETATION	Height ≤ 6 inches	Height > 6 inches unless mowed	Previous experience in this area	High thick vegetation hinders geotechnical inspection	Requires maintenance by owner

1 GPM = 0.063 #/sec 1 FOOT = 0.305 meters

water, and later clay slimes. The foundation consists of layers of clay, silty sands, and sands. The embankment consists of hydraulically-placed mine tailings with a drain and an upstream face of mixed and rolled silty sands.

Tables 1 and 2 summarize a design assessment for this facility. Table 1 compares parameters for permeability and strength used by the designer with values selected by the assessor. Different results from lab tests and different interpretations of the field conditions explain the disparity in values. Table 2 presents a detailed comparison of performance criteria and predicted performance, along with an evaluation of the design. The first column indicates critical aspects of performance for the facility and the second column lists numerical criteria for performance as adopted in considerations among the owner, designer, and assessor (one desirable product of a design assessment may be a clear statement and understanding of design criteria for the facility). The third and fourth columns summarize the designer's predictions of performance and the basis for these predictions. The fifth column gives the assessor's evaluation of the designer's prediction methods, parameters, and mechanisms, and the last column lists departures of predicted performance from the owner's design criteria and indicates required future actions.

This design assessment resulted in investigations which ultimately led to modifications in the design. Performing the assessment helps to clarify the intended function, predicted performance, and any anticipated problems for the owner and designer, as well as for the assessor.

Performance Evaluation

Figs. 2 and 3 show two aspects of a performance evaluation for a recently constructed dam. Figure 2 portrays stress conditions downstream of the dam for a headwater elevation 15 ft (5 m) below the design reservoir level. As this figure indicates, effective stresses fell below the values specified in the performance criteria.

Figure 3 shows the flow net for a partially full reservoir using pore pressures measured prior to the execution of remedial measures. While the net indicates that flow through the dam met the criterion, predicted flow for full reservoir level exceeded the criterion.

The performance evaluation summarized in Fig. 4 led to the design and execution

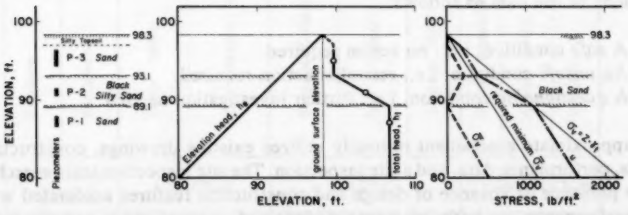

FIG. 2.—Performance Evaluation for Effective Stresses (1 ft = 0.305 mm, 1,000 lb/sq ft = 4.88 tons/m² = 47.85 kN/m²)

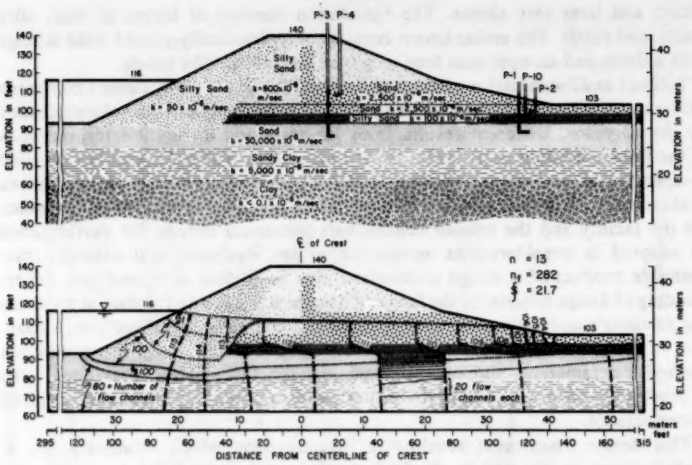

FIG. 3.—Performance Evaluation for Flow through Dam

of remedial measures which corrected nearly all of the deficiencies. Continuing periodic evaluations check deficiencies not yet fully corrected.

Approximate Safety Assessment For Dam

The engineer often must perform an approximate safety assessment due to circumstances such as:

1. Limited financial resources.
2. Limited time.
3. A need to define the scope for a complete safety program.
4. The project existing at an intermediate stage of completion.

An approximate safety assessment for a dam attempts to classify the existing conditions of the dam as follows:

1. A *safe* condition, i.e., no action required.
2. An *unsafe* condition, i.e., remedial action required.
3. A *questionable* condition, i.e., further investigation needed.

An approximate assessment normally utilizes existing drawings, construction records, performance data, and a site inspection. The site inspection team searches for the presence or absence of design and construction features associated with good performance, or both, plus any evidence of unsatisfactory performance. An approximate assessment of dam safety normally does not include additional soil borings, lab tests, or field measurements.

	PERFORMANCE ASPECT	DESIGN PREDICTIONS	MEASURED PERFORMANCE Before remedial measured	PERFORMANCE CRITERIA
FORCE-DEFORMATION	Cracking	Not discussed	No cracks observed	Crack width $\leq$ 1/2 inch Crack depth $\leq$ 6 inches Crack length $\leq$ 6 feet
	Settlement	Not predicted	Not measured	Settlement $\leq$ 2 feet Angular distortion $\leq$ 1/200
STABILITY	Shear Slide	Safety Factor $\geq$ 1.6 @ Fluid Level = 136 ft.	Fluid Level: Safety Factor 116 ft.: 1.83 135 ft.: 1.23	Safety Factor > 1.5
	Low Effective Stress	No artesian heads	Artesian Heads at Stations 20-60, 75-95 66-71, 100-115	No artesian heads
FLOW	Seepage Quantity	Total flow $\leq$ 50 gpm per 1000 ft. of dam	Fluid Level: Total Flow 116 ft.: 210 gpm/1000 ft. 135 ft.: 560 gpm/1000 ft.	Total flow $\leq$ 275 gpm per 1000 ft. of dam
	Soil Transport	Gradient $\leq$ 1.2	Fluid Level: Maximum Gradient 116 ft.: 0.8 135 ft.: 1.8	Actual gradient $\leq$ 1/5 Critical gradient i_c = 1.0
	Seepage Quality	Not predicted	Seepage conforms to state and federal regulations	Seepage must conform to state and federal regulations
MISCELLANEOUS	Storm Capability	Spillways can lower reservoir 1 ft./day; 5 feet of freeboard	Spillway capacity not measured freeboard $\geq$ 5 ft.	Spillways can lower reservoir 1 ft./day; freeboard $\geq$ 5 ft.
	Animal Holes	Not discussed	No large animal holes reported	Hole length $\leq$ 2 feet Hole diameter $\leq$ 3 inches
	Vegetation	Not discussed	Most vegetation $\leq$ 6 inches	Vegetation height $\leq$ 6 inches

NOTE: 1 gpm. = 0.063 ℓ/sec 1 foot = 0.305 meters

FIG. 4.—Summary of Typical Performance Evaluation

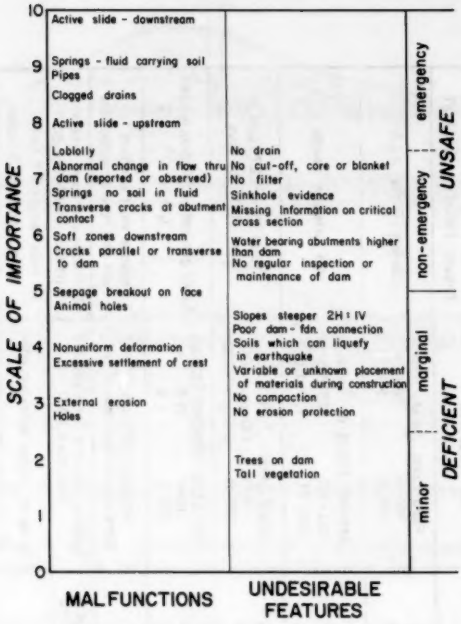

FIG. 5.—Undesirable Features and Malfunctions in Dam

Fundamentals and experience permit one to list features associated with good and poor performance of dams. We assign a scale to these features to indicate the relative importance of the various undesirable features and malfunctions. Fig. 5 gives a list which uses both a numerical scale and a descriptive scale. Key descriptive words frequently require concise definition to avoid confusion in the safety assessment. Definitions of terms used in Fig. 5 include:

1. Property—Characteristic quality, action, state, or condition.
2. Behavior—Manner in which something acts, responds.
3. Performance—Execution of function.
4. Safe—Freedom from danger, hazard, or accident.
5. Stable—Firmly established; fixed.
6. Risk—Exposure to loss.
7. Inspect—View closely; scrutinize.
8. Measure—Ascertain extent, dimensions, quantity.
9. Monitor—Watch, observe, check.
10. Surveillance—Close watch, constant guard, control, management.
11. Assess—Analyze critically and judge definitively the nature, significance, status, or merit.
12. Determine—Fix conclusively, decide, discover.

13. Evaluate—Express numerically; examine and judge worth or condition of.
14. Interpret—Explain the meaning of.

A figure depicting as accurately as possible the cross section at the station with maximum head difference and a plan of the dam and reservoir constitutes a useful means of systematically assembling and assessing information on the dam. A lack of critical information in this figure constitutes an undesirable feature which one must consider in the safety assessment.

Safety Assessment Using Risk Analysis

Execution of a complete safety assessment requires sufficient information concerning loads, parameters, and field conditions to select, represent, and analyze a critical section of a facility. Such a clearly-defined situation rarely occurs, and the engineer must therefore accommodate incomplete knowledge and limited data by making "conservative" choices.

Engineers in fields such as aircraft design, nuclear power plant design, and fire hazard reduction have developed safety programs which utilize concepts from probability theory to assess safety where mechanisms, analyses, and parameters remain uncertain. Geotechnical engineers have developed an interest in these techniques, particularly in the design of foundations for nuclear power plants to withstand extreme earthquake loads.

Risk analysis fits conceptually into our safety program because it helps us to assess numerically the degree of safety of a facility, to compare the safety of alternate designs, and to evaluate the benefits of remedial work. A numerical assessment of safety promises results superior to the normal deterministic finding of "safe," "unsafe," or "questionable."

A risk analysis attempts to identify all undesirable or abnormal events and assess the probability and consequences of each occurring. One can exclude consideration of events of low consequence.

To help organize a risk analysis one can arrange events in an event tree or a fault tree. Figures 6 and 7 present a partial combined fault-event tree for a waste storage dam. The owner plans to raise the dam crest, thereby increasing reservoir storage capacity. Conversations with the owner and an initial safety assessment of the dam revealed that the most serious event consists of a loss of contaminated fluid stored within the waste storage facility. Loss of fluid would result in major negative consequences—principally, the flow of contaminated water off property and the shutdown of the processing plant until containment of fluid was achieved and the water supply replenished.

The following five mechanisms result in loss of fluid:

1. Flow occurs along a path of high permeability resulting in flow through the dam in excess of the capability of the perimeter collection ditch.
2. Excessive rainfall nullifies freeboard and overtops the dam.
3. A sinkhole develops beneath the dam or reservoir.
4. A shear slide occurs through the crest of the dam.
5. A pipe develops through the dam by internal erosion.

The occurrence of any of these events depends on the combination of various

conditions depicted in the fault-event tree in Fig. 6. One can use various techniques to determine the probability that each mechanism will lead to loss of containment, e.g., determining the probability of loss of containment by a large shear slide in the downstream section involves estimating uncertainties in geometry, pore

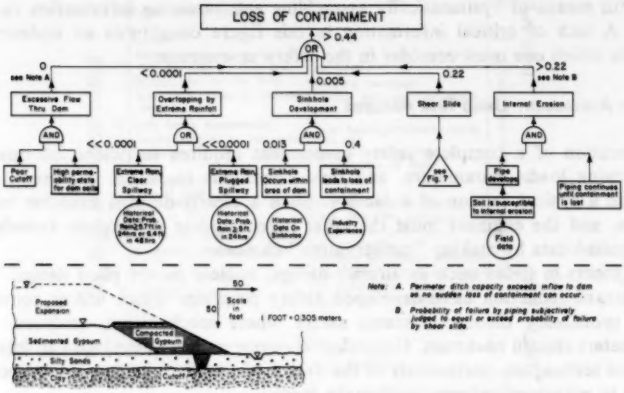

FIG. 6.—Fault Tree for Risk Assessment

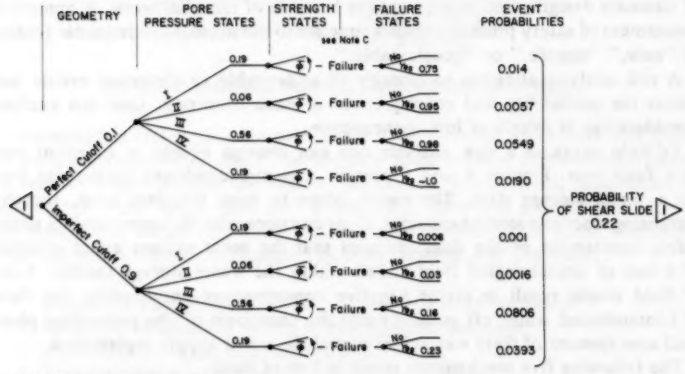

NOTE C: Mathematical operation involving mean and variance in friction angles, model uncertainty and probability distribution function for factor of safety.

FIG. 7.—Event Tree for Risk Assessment

pressure, strength, and analytical method. Figure 7 shows the steps involved in obtaining these failure probabilities using an event tree. Steps in the probability assessment follow:

1. From the geometry of the facility, determine that the main uncertainty

resides in the effectiveness of the core trench to cut off seepage.

2. Establish probability distributions for permeabilities and strength using laboratory data, field data, and the experience of the analyst.

3. Obtain pore pressures from flow nets drawn for ranges of permeability of soils.

4. Compute the minimum factors of safety against a shear slide for a range of friction angles for each set of pore pressures. We used the simplified Bishop method of slices with circular arc failure surfaces which lead to loss of containment.

5. Compute the mean and standard deviation of factor of safety for each set of pore pressures using the probability distributions of friction angles from Step 2 and an estimated analytical uncertainty of ±6% error in the calculated factor of safety.

6. Calculate the probability of failure using the results from Step 5 for each set of pore pressures, i.e., F.S. ≤ 1 with some probability distribution for F.S., for which in this case we tried both normal and lognormal distributions, with little difference in results.

7. Combine results for each set of pore pressures and geometry into one probability of failure using probabilities from Steps 1, 2, and 6.

Figure 7 gives the probabilities for each of the aforementioned steps, e.g., from piezometric data, we estimate that an *imperfect cutoff* exists with a probability of 0.9. The probability that flow net IV (which we based on sedimented gypsum being more than three times as permeable as compacted gypsum, and sand being less than 1/3 as permeable as the sedimented gypsum) represents flow in the dam equals 0.19. This calculation results from the probability distributions established in Step 2. A probability of 0.23 exists that friction angles combined with pore pressures from flow net IV give a factor of safety less than or equal to one. Consequently, the probability of a shear slide due to the combination of low friction angles, pore pressures from flow net IV, and an imperfect cutoff equals $0.23 \times 0.19 \times 0.9$, or 0.039. Combining all paths to failure in Fig. 7 gives a probability of failure by a large slide and loss of containment of 0.22.

Internal erosion, or piping of the silty sand foundation stratum underlying the reservoir, causes great concern. Substantial pipes developed in the existing dam, but loss of containment did not occur.

The fact that pipes have already developed in the sand foundation of the existing dam with some pipes inducing small slumps leads us to suspect that the probability of failure by piping of the enlarged facility must equal or exceed the probability of a shear slide. Consequently, the fault tree shows a probability of loss of containment by piping of greater than 0.22.

In summary, the probability of loss of containment in the expanded facility equals more than 0.44 during its 10-yr design life. Essentially all of the risk stems from failure by internal erosion and a shear slide. With this information, the owner readily identifies the main contributors to the risk and assesses the need for an alternate design.

As parts of this analysis suggest, we do not know the actual probabilities as precisely as the number of significant figures Fig. 6 and 7 indicate. The figures include the artificial precision to allow clear illustration of how the probabilities combine.

Summary and Conclusions

This paper describes a comprehensive program to help ensure that a geotechnical facility meets performance criteria, particularly safety criteria. The program's systematic approach rests on the fundamentals of geotechnical engineering—specifically, the effective stress principle, the stress path method, Darcy's Law, and stress-strain principles.

Successful application of the program yields:

1. A portrayal and evaluation of actual performance.
2. An assessment of prediction capability.
3. A reservoir of evaluated performance, including data on the effectiveness of remedial work.

This approach integrates activities known and applied by geotechnical engineers. These activities include: (1) Field investigations; (2) laboratory tests; (3) analyses; (4) field measurements; and (5) site inspections. The program employs "average elements," a feature of the stress path method (first and second writers, 1979). No program can guarantee "zero risk" of failure. The engineer must still search for "minor geological details" that may cause a facility to malfunction. Further, the geotechnical engineer must still deal with phenomena such as piping, dam cracking, and soil disturbance, which the profession only partially understands.

Believing in the approach of "engineering certain constructed facilities for their entire lives," we have developed—or actually evolved—the program described in this paper. We have found this approach highly effective and worthy of the effort required to implement it.

Acknowledgments

This program, both in concept and execution, benefitted from contributions by many people. R. V. Whitman and G. B. Baecher assisted in the risk assessment work. T. L. Neff made many site investigations and helped portray and interpret field data.

The Borden Company and LAGOVEN, S.A. encouraged and assisted in the development and application of the program described in this paper. They permitted us to publish work performed for them.

Engineers, especially B. Moore from the St. Louis District of the Corps of Engineers and J. Boehmer from Rijkswaterstaat in the Netherlands, helped on the assessment of dam safety.

We acknowledge with appreciation the assistance we received.

JOURNAL OF THE GEOTECHNICAL ENGINEERING DIVISION

TECHNICAL NOTES

Note.—Discussion open until August 1, 1981. To extend the closing date one month, a written request must be filed with the Manager of Technical and Professional Publications, ASCE. This paper is part of the Journal of the Geotechnical Engineering Division, Proceedings of the American Society of Civil Engineers, ©ASCE, Vol. 107, No. GT3, March, 1981.

Technical Notes

To provide a place within ASCE for publication of technical ideas that have not advanced, as yet, to the point where they warrant publication as a Proceedings paper in a *Journal*, the publication of Technical Notes was authorized by the Board of Direction on October 16–18, 1967, under the following guidelines:

1. An original manuscript and two copies are to be submitted to the Manager of Technical and Professional Publications, ASCE, 345 East 47th Street, New York, N.Y., 10017, along with a request by the author that it be considered as a Technical Note.
2. The two copies will be sent to an appropriate Technical Division or Council for review.
3. If the Division or Council approves the contribution for publication, it shall be returned to Society Headquarters with appropriate comments.
4. The technical publications staff will prepare the material for use in the earliest possible issue of the *Journal*, after proper coordination with the author.
5. Each Technical Note is not to exceed 4 pages in the *Journal*. As an approximation, each full manuscript page of text, tables, or figures is the equivalent of one-half a *Journal* page.
6. The Technical Notes will be grouped in a special section of each *Journal*.
7. Information retrieval abstracts and key words will be unnecessary for Technical Notes.
8. The final date on which a Discussion should reach the Society is given as a footnote with each Technical Note.
9. Technical Notes will not be included in *Transactions*.
10. Technical Notes will be included in ASCE's annual and cumulative subject and author indexes.

The manuscripts for Technical Notes must meet the following requirements:

1. Titles must have a length not exceeding 50 characters and spaces.
2. The author's full name, Society membership grade, and a footnote reference stating present employment must appear on the first page of the manuscript. Authors need not be Society members.
3. The manuscript is to be submitted as an original copy (with two duplicates) that is typed double-spaced on one side of 8-1/2-in. (220-mm) by 11-in. (280-mm) white bond paper.
4. All mathematics must be typewritten and special symbols must be properly identified. The letter symbols used must be defined where they first appear, in figures or text, and arranged alphabetically in an Appendix.—Notation.
5. Standard definitions and symbols must be used. Reference must be made to the lists published by the American National Standards Institute and to the *Authors' Guide to the Publications of ASCE*.
6. Tables must be typed double-spaced (an original ribbon copy and two duplicate copies) on one side of 8-1/2-in. (220-mm) by 11-in. (280-mm) paper. An explanation of each table must appear in the text.
7. Figures must be drawn in black ink on one side of 8-1/2-in. (220-mm) by 11-in. (280-mm) paper. Because figures will be reproduced with a width of between 3 in. (76 mm) to 4-1/2 in. (110 mm), the lettering must be large enough to be legible at this width. Photographs must be submitted as glossy prints. Explanations and descriptions must be made within the text for each figure.
8. References cited in text must be typed at the end of the Technical Note in alphabetical order in an Appendix.—References.
9. Dual units, i.e., U.S. Customary followed by SI (International System) units in parentheses, should be used throughout the paper.

MICROGRAVITY SURVEYS FOR EVALUATION OF ELEVATION CHANGES DUE TO RESERVOIR IMPOUNDMENT

By Dwain K. Butler[1]

INTRODUCTION

One of the primary observable effects of the impoundment of large reservoirs is the deflection of the earth's surface, presumably due to the imposed load. For small reservoirs, elevation changes may be immeasurably small, while for large reservoirs, elevation changes are easily observed. Also associated with reservoir filling (as well as with subsequent seasonal changes in reservoir level) are changes in ground-water levels in permeable formations in the vicinity of the reservoir. The objectives of this note are to: (1) Assess the potential of microgravity surveys for the evaluation of elevation changes due to reservoir impoundment; (2) determine what "size" reservoirs are likely to produce elevation changes large enough for detection by microgravity surveys; and (3) assess the role of coupled microgravity and surface leveling or ground-water-level monitoring surveys in areas with permeable bedrock. Microgravity survey nets are currently in operation at Libby Dam and Reservoir (Montana) and the Palmdale uplift area, as well as other tectonically active areas in California, (personal communication with John D. Fett, 1979).

MICROGRAVIMETERS AND DETECTABLE ELEVATION CHANGES

The normal free-air gravity gradient is approx 0.3086 mgal/m (1 gal = 0.01 m/s^2). An elevation change of 10 mm at a given gravity survey point, with no associated mass loss or gain in the subsurface, would produce a change in the vertical component of the gravitational attraction of about 0.003 mgal or 3 μgal. Studies have shown that, with careful *repeat* gravity measurements at stations of a survey net with a LaCoste-Romberg Model-D gravimeter, it is possible to obtain solutions to the survey net with a precision and accuracy in the estimate of relative gravity values of 1 μgal–2 μgal (11,12,13) with a high confidence level. The LaCoste-Romberg Model-D gravimeter has a reading

[1]Research Geophysicist, Earthquake Engrg. and Geophysics Div., Geotechnical Lab., United States Army Engineer Waterways Experiment Station, Corps of Engrs., P.O. Box 631, Vicksburg, Miss. 39180.

Note.—Discussion open until August 1, 1981. To extend the closing date one month, a written request must be filed with the Manager of Technical and Professional Publications, ASCE. Manuscript was submitted for review for possible publication on July 30, 1980. This paper is part of the Journal of the Geotechnical Engineering Division, Proceedings of the American Society of Civil Engineers, ©ASCE, Vol. 107, No. GT3, March, 1981. ISSN 0093-6405/81/0003-0355/$01.00.

sensitivity of about 1 μgal. Thus, using a true "microgal" instrument, such as the Model-D, with care, elevation changes or differences of 10 mm can be detected by repeat surveys of the same gravity survey net at different times. The precision and accuracy achieved in "routine" microgravity site surveys with the Model-D to determine relative gravity variations is 3 μgal–6 μgal (2,3,11,12); thus even in this context, elevation changes or differences of 20 mm can be detected by repeat surveys. Observed and predicted (calculated) crustal deflections associated with various reservoirs will now be surveyed in order to estimate the minimum "size" reservoir for which microgravity surveys should be considered.

Crustal Deflection Observations and Calculations

Downward crustal deflections have been observed following the impounding of many reservoirs. Elevation changes of 200 mm have been measured at Lake Mead, Ariz., agreeing very closely with elastic deflection calculations (16). At

TABLE 1.—Summary of Calculated Maximum Vertical Deflections

Reservoir (1)	Total surface load, in kilograms (2)	Calculated maximum vertical deflections, in millimeters (3)
Kariba (Rhodesia)	1.5×10^{14}	250
Mead (United States)	4×10^{13}	200
Gordon (Tasmania)	1.5×10^{13}	70
Hsinfengkiang (China)	1.2×10^{13}	100
Libby (United States)	7.2×10^{12}	—
Oroville (United States)	4.4×10^{12}	55
Hendrik Verwoerd (South Africa)	3.2×10^{12}	32

Lake Kariba, Rhodesia, the third largest man-made lake in the world, deflections along a carefully repeated level traverse were as great as 130 mm next to the reservoir, and agreed almost exactly with elastic deflection calculations (4,5). The calculations for Lake Kariba predicted a maximum deflection directly beneath the reservoir of about 250 mm. Similar calculations have been made for four other smaller reservoirs (1,7,9,10), and Table 1 summarizes the calculated maximum vertical deflections and total surface loads represented by the six reservoirs; the total surface load represented by Libby Reservoir is included for reference.

Using the data in Table 1, the relation of total surface load and maximum calculated elastic deflection, or observed deflection, or both, is shown in Fig. 1. The dashed line indicates the trend of the data. The data for the six reservoirs suggest a consistent relation between *total surface load* and deflection. The reservoirs have different areal extent, varying water depth distributions, and, of course, for the field observations, all of the complexities of differing geologies are present. This seems to imply that the *total load* is the key parameter in

determining deflection. Results of measurements of elevation change near Oroville Reservoir are smaller than corresponding values from the calculation (see Fig. 1). However, the elevation change data for Oroville are complicated by the occurrence of the 1975 Oroville earthquake (1,14).

Associated Gravity Changes

Due to Elevation Change Alone.—Considering the free-air gravity changes due to the elevation changes, neglecting any other effect at this point, the maximum

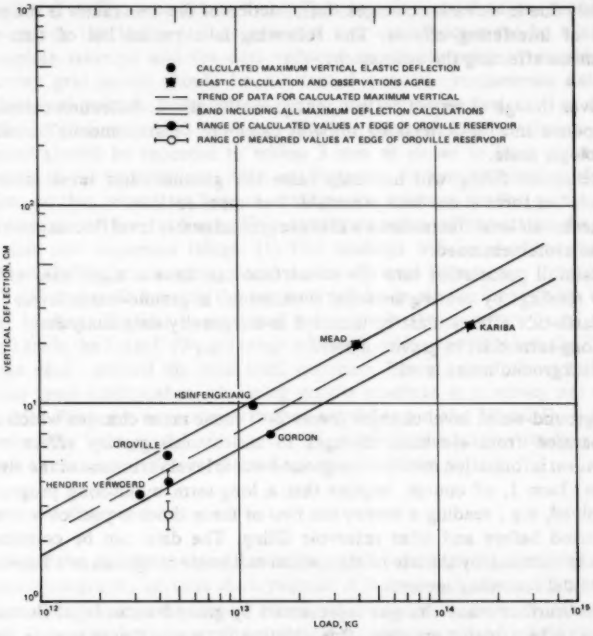

FIG. 1.—Vertical Deflections, Observed and Calculated, as Function of Total Surface Load for Six Reservoirs

to be expected from reservoir impoundment would be about 75 μgal for an "elastic-type" crustal deflection. However, cases in which an earthquake occurs in the vicinity of a microgravity survey net may exhibit locally greater elevation and gravity change (8). The 75-μgal figure is an upper limit from a practical point of view since the corresponding deflection would probably be directly under the reservoir. For the case of Lake Kariba, 200 mm represents the maximum calculated deflection which would have been accessible to measurement, or about 60 μgal gravity change, which is well within the detectability limits of the Model-D gravity meter and with careful survey procedures could be detected

with standard gravity instruments, such as the Worden or LaCoste-Romberg Model-G. On the lower end of the spectrum, a gravity change as small as 3 μgal is detectable with a reasonable degree of confidence with an instrument having microgal precision and accuracy. A 3-μgal gravity change implies a 10-mm elevation change (assuming no other interfering effects). From Fig. 1, this implies that microgravity will be of *possible* usefulness in detecting vertical deflections of the crust only for reservoirs representing loads of the order of 10^{12} kg (1.1×10^9 tons or 8.1×10^6 acre-ft) or greater.

Interfering Time Effects.—The assessment thus far has made the rather idealistic assumptions that there are no interfering effects, i.e., that gravity differences are solely due to elevation changes. Introduction of the time factor is the primary source of interfering effects. The following is a partial list of time-related phenomena affecting the assessment.

1. Even though observed deflections agree with elastic deflection calculations, the response time for deflections probably cannot be "instantaneous" considering the geologic scale.
2. Reservoir filling will not only raise the ground-water level around the reservoir but force water into permeable basement rock.
3. Reservoir level fluctuations will cause ground-water level fluctuations similar to those aforementioned.
4. Rainfall percolation into the subsurface can have a significant effect on gravity readings by causing seasonal fluctuations in ground-water level.
5. Earth-tide effects must be included in the gravity data analysis.
6. Long-term drift in gravity meter.
7. Background noise level.

The ground-water level changes (items 2–4) cause mass changes which cannot be separated from elevation changes in the overall gravity effect without *independent* information on *either* the ground-water level variations or the elevation changes. Item 1, of course, implies that a long-term monitoring program will be involved, e.g., reading a survey net two or three times a year over a several year period before and after reservoir filling. The data can be corrected for earth-tide variation by the use of theoretical earth-tide programs or a base station gravity tidal recording meter.

The subsurface mass changes represented by ground-water level fluctuations are seen to be a major problem. One solution is to coordinate precise leveling surveys with the gravimetry. While this would not determine elevation changes directly with gravimetry, it would allow the separation of elevation effects from mass change effects in the gravity data (15), which would be of considerable importance in assessing the overall effects of reservoir impoundment (such as the possible role played by water movement and pore pressure changes in triggering earthquakes). It would be necessary in this regard to begin the gravity survey several years before impoundment in order to have knowledge of the effects on gravity readings caused by normal, seasonal ground-water fluctuations. Another possibility is to locate the gravity stations on outcrops of "impermeable" bedrock if possible; this would at least minimize the effects. A third possibility is to correlate the gravity surveys with independent information on ground-water level fluctuations, provided by piezometers and other instruments. Knowledge

of ground-water level at the time of each survey would allow the separation of gravity changes due to elevation changes from those due to ground-water level changes. In general, previous work has indicated 10-μgal–30-μgal changes in some areas due to seasonal ground-water level fluctuations (11) and changes in the 30-μgal–40-μgal range have been noted in repeat surveys over an area before and after heavy rains (presumably due to very shallow ground-water concentrations) (unpublished data by Butler).

Survey Procedure.—The survey procedure itself is of crucial importance (3). The same meter should be used over the complete traverse and each traverse completed in the minimum time possible. One procedure for randomizing reading and long-term drift errors (items 6 and 7) is to use more than one instrument for the survey (6); however it is essential that each instrument be used over the complete traverse and the data reduced separately prior to combination. The survey grid points should be substantial concrete monuments extending below seasonal volume change (frost heave, thermal expansion, etc.) or at least about 0.5 m below ground surface. Gravity meter elevation relative to the monument should be repeated to within 3 mm or closer to keep errors from this source to ±1 μgal or less. Also, readings can be synchronized to the tidal variation, so that repeat readings at stations are taken at similar points on the tidal curve as earlier readings. This synchronization of repeat readings will accomplish two important things: (1) The readings will be at about the same position on the meter measuring screw to avoid errors from screw irregularities; and (2) soil and rock beneath the stations will be in similar states with respect to tidal loading. Typical background noise levels (from cultural and natural sources) are in the 5-μgal–10-μgal range, although during earthquakes, the "noise" level can easily exceed the total tidal variation. For a period of several hours following large earthquakes, obtaining gravity readings in a survey net will be impossible. With the capacitive readout capability on the Model-D, it is easy to monitor the background noise level. If required, the station reading can be obtained as the mean of several readings over a 10-min period.

Comments and Conclusions

In spite of the stringent survey demands and time-dependent interfering effects, repeated microgravity surveys show promise of being a valuable tool for studying elevation changes, or mass change effects associated with reservoir impounding, or both. A reservoir representing a total post-impoundment load of the order of 10^{12} kg (1.1×10^9 tons or 8.1×10^6 acre-ft) or greater is a candidate for microgravimetric studies for determining elevation changes. Elevation changes associated with impoundment of Libby Reservoir are probably between what should easily be detectable by microgravimetry and what can be detected only by very careful surveys using microgravimetric techniques.

Of great importance, from the standpoint of understanding crustal deflection and possible earthquake-inducing mechansims, is the need for a study of the response times of crustal deflection to load application and the time lag between reservoir filling and the arrival of pore pressure changes as a function of depth and distance from the reservoir. Considering the nature of the geologic system involved, it is difficult to imagine that the vertical deformations could occur "instantaneously" as the reservoir load is applied, even though the final

deformations agree very closely with purely elastic deformation calculations. Repeat microgravity surveys coupled with precise level surveys can play an important role in this study.

It is interesting to note, as a conclusion to this assessment, that the length of the traverse line is not a limiting factor in assessing the accuracy of a microgravity survey. The accuracy of a microgravity survey does not degrade directly as a function of survey line length. Also, microgravity surveys do not depend on line of sight-connected survey stations. However, for even the *most precise and accurate* level survey, the accuracy degrades at least as fast as $\alpha_n L^{1/2}$ in which L = the survey line length in kilometers; and α_n depends on the order of the survey with a range of 0.5 mm–6 mm (11,14). A possible example of this level survey degradation is given in Ref. 14. Thus, for long survey lines, and in rugged terrain where level surveys become more difficult, microgravimetry should be considered for elevation change surveys.

Acknowledgments

The subject of this note was suggested by Richard Carlson. The support provided by the United States Army Corps of Engineers during the writer's study at Texas A&M is gratefully acknowledged.

Appendix.—References

1. Beck, J. L., "Weight-Induced Stresses and the Recent Seismicity at Lake Oroville, California," *Bulletin of the Seismology Society of America*, Vol. 66, 1976, pp. 1121–1131.
2. Butler, D. K., "Assessment of Microgravimetric Techniques for Site Investigations," 49th International Meeting, Society of Exploration Geophysicists, New Orleans, La., 1979.
3. Butler, D. K., "Microgravimetric Techniques for Geotechnical Applications," *Miscellaneous Paper GS-80-13*, United States Army Engineer Waterways Experiment Station, Vicksburg, Miss., Sept., 1980.
4. Gough, D. I., and Gough, W. I., "Stress and Deflection in the Lithosphere near Lake Kariba, 1," *Geophysics Journal of the Royal Astronomical Society*, Vol. 21, 1970.
5. Gough, D. I., and Gough, W. I., "Load-Induced Earthquakes at Lake Kariba," *Geophysics Journal of the Royal Astronomical Society*, Vol. 21, 1970.
6. Grammel, R. B., Tarman, D. W., Clover, R. C., Leggewie, R. M., Aronstam, P. S., Kroll, R. C., and Eppink, J., "Precision Gravity Studies at Cerra Prieto—The Second Year," *LBL-9551*, Lawrence Berkeley Laboratory, Berkeley, Calif., Feb., 1980.
7. Green, R. W. E., "Seismic Activity Observed at the Hendrik Verwoerd Dam," *International Colloquim on Seismic Effects of Reservoir Impounding*, The Royal Society, London, England, Mar., 1973.
8. Guha, S. K., Gosavi, P. D., Agarwal, B. N. P., Padale, J. G., and Manvadi, S. C., "Case Histories of Some Artificial Crustal Disturbance," *Engineering Geology*, Amsterdam, The Netherlands, Vol. 8, 1974, pp. 59–77.
9. Gupta, H. K., and Rastogi, B. K., *Dams and Earthquakes*, Elsevier Scientific Publishing Company, New York, N. Y., 1976.
10. Lee, T. "A Method for Computing the Deformation of the Crust Caused by the Filling of Large Lakes," *Bulletin of the Seismological Society of America*, Vol. 62, 1972, pp. 1597–1610.
11. Lambert, A., and Beaumont, C., "Nano Variations in Gravity Due to Seasonal Groundwater Movements, Implications for the Gravitational Deflection of Tectonic Movements," *Journal of Geophysical Research*, Vol. 82, 1977, pp. 297–306.

12. McConnell, R. K., Hearty, D. B., and Winter, P. J., "An Evaluation of the LaCoste-Romberg Model-D Microgravimeter," presented at the 1974, Seventh Meeting of the International Gravity Commission, held at Paris, France.
13. Neumann, R., "Gravity Measurement Prospecting Applied to the Location of the Underground Cavities," *Compangnie Generale de Geophysique*, Massy, France, 1973.
14. Savage, J. C., Lisowski, M., Prescott, W. H., and Church, J. P., "Geodetic Measurements of Deformation Associated with the Oroville, California, Earthquake," *Journal of Geophysical Research*, Vol. 82, 1977, pp. 1667–1671.
15. Singh, S. K., Mena, M., and Monges, J., "Secular Variations of Gravity in Mexico?" *Geophysical Research Letters*, Vol. 6, 1979, pp. 469–472.
16. Westergaard, H. M., and Adkins, A. W., "Deformation of the Earth's Surface Due to Weight of Boulder Reservoir," *Technical Memorandum No. 422*, United States Bureau of Reclamation, 1934.

JOURNAL OF THE
GEOTECHNICAL
ENGINEERING DIVISION

DISCUSSION

Note.—This paper is part of the Journal of the Geotechnical Engineering Division, Proceedings of the American Society of Civil Engineers, ©ASCE, Vol. 107, No. GT3, March, 1981. ISSN 0093-6405/81/0003-0365/$01.00.

Discussions

Discussions may be submitted on any Proceedings paper or technical note published in any *Journal* or on any paper presented at any Specialty Conference or other meeting, the *Proceedings* of which have been published by ASCE. Discussion of a paper/technical note is open to anyone who has significant comments or questions regarding the content of the paper/technical note. Discussions are accepted for a period of 4 months following the date of publication of a paper/technical note and they should be sent to the Manager of Technical and Professional Publications, ASCE, 345 East 47th Street, New York, N.Y. 10017. The discussion period may be extended by a written request from a discusser.

The original and three copies of the Discussion should be submitted on 8-1/2-in. (220-mm) by 11-in. (280-mm) white bond paper, typed double-spaced with wide margins. The length of a Discussion is restricted to two *Journal* pages (about four typewritten double-spaced pages of manuscript including figures and tables); the editors will delete matter extraneous to the subject under discussion. If a Discussion is over two pages long it will be returned for shortening. All Discussions will be reviewed by the editors and the Division's or Council's Publications Committees. In some cases, Discussions will be returned to discussers for rewriting, or they may be encouraged to submit a paper or technical note rather than a Discussion.

Standards for Discussions are the same as those for Proceedings Papers. A Discussion is subject to rejection if it contains matter readily found elsewhere, advocates special interests, is carelessly prepared, controverts established fact, is purely speculative, introduces personalities, or is foreign to the purposes of the Society. All Discussions should be written in the third person, and the discusser should use the term "the writer" when referring to himself. The author of the original paper/technical note is referred to as "the author."

Discussions have a specific format. The title of the original paper/technical note appears at the top of the first page with a superscript that corresponds to a footnote indicating the month, year, author(s), and number of the original paper/technical note. The discusser's full name should be indicated below the title (see Discussions herein as an example) together with his ASCE membership grade (if applicable).

The discusser's title, company affiliation, and business address should appear on the first page of the manuscript, along with the *Proceedings* paper number of the original paper/technical note, the date and name of the *Journal* in which it appeared, and the original author's name.

Note that the discusser's identification footnote should follow consecutively from the original paper/technical note. If the paper/technical note under discussion contained footnote numbers 1 and 2, the first Discussion would begin with footnote 3, and subsequent Discussions would continue in sequence.

Figures supplied by the discusser should be designated by letters, starting with A. This also applies separately to tables and references. In referring to a figure, table, or reference that appeared in the original paper/technical note use the same number used in the original.

It is suggested that potential discussers request a copy of the *ASCE Authors' Guide to the Publications of ASCE* for more detailed information on preparation and submission of manuscripts.

Strength and Deformability of Highly Fractured Rock[a]

Discussion by J. Laginha Serafim,[3] F. ASCE

The paper by Raphael and Goodman is an excellent contribution to the knowledge of fundamental properties of rock masses with frequent joints and cracks, viz. deformability and shear strength.

The idea of building up specimens of a very jointed rock mass from fitting cores which were then tested in a triaxial machine gave the possibility of finding "envelopes" of Mohr's circles for such a material. From these, both the peak and a post-peak strength were determined. The writer has insisted in various occasions that triaxial tests on cylinders of materials with oriented weaknesses cannot be interpreted correctly by Mohr's theory (including an unpublished presentation at the 1962 Rock Mechanics Meeting, held at Salzburg, Austria); neither are such tests valid if the surfaces of minimum strength cut through the end steel plates. In fact, for layered, aniso-tropic or oriented fissured solids, the surfaces of rupture will go through the surfaces of minimum strength and not along the direction indicated by the tangent of the supposed envelope and the Mohr's circle. On the other side, when the planes of rupture have to cut through the steel loading plates, the modulus of elasticity and maximum strength will be affected by them (18), unless some special precautions are taken (use of brush loading plates, etc.). The post-peak strength indicated by the tests typified by Fig. 3 and summarised in Fig. 4 of the original paper possibly has not allowed to estimate the residual strength. This because of the previous reason and possibly because the authors were not sure that the final sliding occurred along joints. Slip took place, as they admit, in new fracture surfaces. They certainly were careful in designating this minimum strength the "post-peak strength" and not the *residual strength of the rock mass,* which corresponds to the final frictional strength along the joints. For this reason it is rather surprising that the authors have not conducted friction tests in joints. Nor have they classified the degree of roughness of the joint surfaces exposed by the cores, from which a reasonable value of the peak shear strength could also possibly be estimated.

In a recent paper by Singh (19), the residual strength in a fracture developed during the triaxial tests of an intact rock specimen was also determined by successive increases of the loads after the initial rupture.

Borehole jack tests (using the Goodman jack) were made for determining the deformability of the rock mass. The writer believes that the problem of a very close adjustment of the jack surface to the boreholes surfaces was

[a]November, 1979, by Jerome M. Raphael and Richard E. Goodman (Proc. Paper 14988).

[3]Prof. of Civ. Engrg., Coimbra Univ., Portugal; also President COBA-International Consultants, Av Marquês de Tomar 9-6, 1000 Lisboa 1, Portugal.

considered by the authors, but it was not mentioned in the paper, although an imperfect adjustment can bring about erroneous results.

This study was certainly a good opportunity to compare the deformability of the rock mass obtained by various methods. Unfortunately, large jack tests were not performed at the site to compare results with the other determinations carried out.

It would certainly be of great interest also to make a classification on the rock mass, for instance, according to Bieniawski's (17) geomechanics classification system, RMR, and introduce new points and curves in his diagrams. Neither the RQD, nor the percentage of core recovery, nor the complete statistics of number of joints per unit length of the hole and the opening of the joints were indicated, which would make this a very good opportunity to add points to the correlation between the RMR and the in situ modulus of elasticity. Maybe the authors can still make the determinations and, in this case, they will give an additional value to their important paper. It must be mentioned that the possibility of transforming results of dilatometer or borehole jack tests into results of in situ large flat jacks is an important aspect of the correlations obtained in rock classification systems.

Appendix.—References

17. Bieniawski, Z. T., "The Geomechanics Classification in Rock Engineering Applications," *Proceedings of the 4th International Congress on Rock Mechanics*, Vol. II, 1979, pp. 41–48.
18. Serafim, J. L., and Guerreiro, M. Q., "Tests and Observed Behaviour of Rock Foundations of Dams," *Proceedings of the 3rd International Congress on Rock Mechanics*, Vol. II-B, 1974, pp. 928–942.
19. Singh, D. P., "A Study of Frictional Properties of Rock," *Proceedings of the 4th International Congress on Rock Mechanics*, Vol. I, 1979, pp. 301–305.

Closure by Jerome M. Raphael,[4] F. ASCE and Richard E. Goodman,[5] M. ASCE

The authors wish to thank J. L. Serafim for his complimentary and constructive discussion. The question of multi-stage testing on rupture surfaces in triaxial compression experiments is indeed complicated because the failure planes may tend to intersect the end caps. In the experiments in question, so many possible failure surfaces exist that it is reasonable to assume that a failure surface orientation can be found close to the orientation of least strength in a position within the specimen that does not necessitate intersection with the end caps. This would not be true in a general multistage test but is assumed to be true in this specific case in which so many incipient fracture directions coexist within each specimen.

Large block tests were not conducted at the site because money was not available and the results were needed quickly. Direct shear tests on joints were

[4]Prof. of Civ. Engrg., Univ. of California at Berkeley, Berkeley, Calif. 94720.
[5]Prof. of Geological Engrg., Div. of Engrg. Dept., Univ. of California at Berkeley, Berkeley, Calif. 94720.

not run because samples of individual joints of satisfactory quality for such tests were not obtained.

From estimates of the rock mass properties, the Bieniawski Rock Mass Rating (20) is determined to be from 30–35, qualifying the rock mass as "Poor Rock," a result we already appreciated before starting the tests. The corresponding rock mass deformability cannot be obtained from Bieniawski's equation: E (in Gigapascals) equal to twice the rock mass rating minus 100. The reason is simply that this linear fit to Bieniawski's data points intersects zero modulus at a rock mass rating of 50 while the applicable rock mass rating is less than 50. If a curved fit to Bieniawski's data points is provided, as shown in Goodman (21), the point with RMR equal to 33 and E equal to 6 GPa, which corresponds to the results in our paper, will be seen to plot close to the extrapolated curve. Much more testing in the low RMR region will be required before such correlations can be established for engineering practice.

Appendix.—References

20. Bieniawski, Z. T., "Determining Rock Mass Deformability—Experience from Case Histories," *International Journal of Rock Mechanics and Mining Sciences*, Vol. 15, No. 5, 1978, pp. 237–248.
21. Goodman, R. E., *Introduction to Rock Mechanics*, John Wiley & Sons, New York, 1980, Fig. 6.11, p. 189.

Cyclic Shear Resistance of Noncohesive Soils[a]

Discussion by Yoshiharu Moriwaki,[2] A. M. ASCE and Maurice S. Power,[3] M. ASCE

The author has presented a useful way of evaluating the pore water pressures generated under undrained cyclic loading conditions. The assessment of cyclically-induced pore water pressures is becoming increasingly important because of recent emphasis on pore water pressure generation/dissipation and post-earthquake behavior associated with earth structures (12). The writers have also used a similar approach in a recent project to evaluate the results of excellent undrained cyclic triaxial tests on modeled Oroville gravel by Banerjee, et al. (9). A summary of the results and some comments on the importance of boundary conditions are presented here.

---

[a]January, 1980, by Edward G. Prater (Proc. Paper 15100).
[2]Geotechnical Consultant, Civ. Systems Inc., 2450 Washington Ave., San Leandro, Calif. 94577.
[3]Assoc., Woodward-Clyde Consultants, San Francisco, Calif.

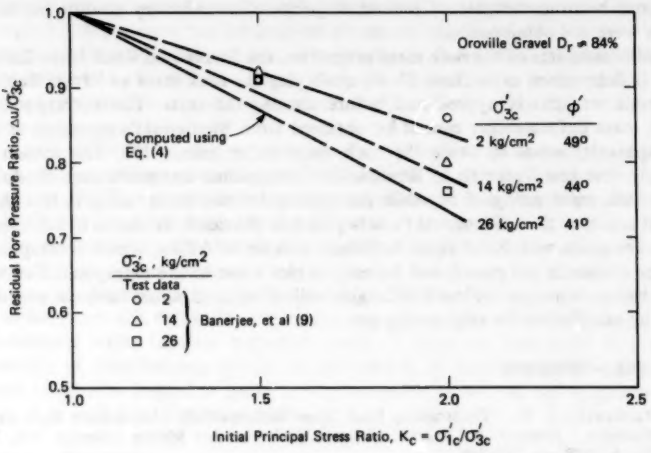

FIG. 4.—Measured and Predicted Residual Pore Water Pressure in Triaxial Specimens

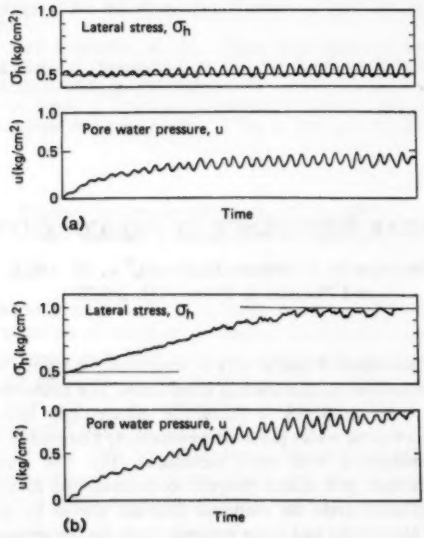

σ'_{vc} = 1.0 kg/cm², σ'_{hc} = 0.5 kg/cm², D_r = 55%

FIG. 5.—Cyclic Torsion Tests Results: (*a*) Without Lateral Confinement; (*b*) With Lateral Confinement (Ref. 10)

An equation similar to Eqs. 1, 2, and 3, but suited for the results of cyclic triaxial tests is:

$$\frac{(\Delta u_r)_{max}}{\sigma'_{3c}} = \frac{K_c + 1}{2} - \frac{K_c - 1}{2 \sin \phi'} \quad \ldots\ldots\ldots\ldots\ldots\ldots\ldots\ldots\ldots\ldots\ldots\ldots (4)$$

The values of residual pore water pressure reported by Banerjee, et al. (9), are shown in Fig. 4; also shown in Fig. 4 are the curves computed using Eq. 4 combined with ϕ' values reported by Marachi, et al. (11), for the same material under various initial confining pressures. It is clear from Fig. 4 that Eq. 4 (which is based on simple Mohr-Coulomb considerations) is sufficiently accurate to describe the trends in the observed effects of K_c and σ'_{3c}.

The writers feel that Eq. 4 is probably useful in assessing an approximate value of the maximum *residual* pore water pressure that can develop in an undrained cyclic *triaxial* text specimen. The emphasis on the residual pore water pressure is important because the transient pore water pressure can easily be higher than that indicated by Eq. 4 because an isotropic stress state can exist in a specimen during cyclic loading. The emphasis on the triaxial test is important because in a conventional triaxial test, the specimen boundary is kept at constant ambient σ_1 and σ_3 throughout the test.

However, in those tests or situations where the specimen or soil boundary is kept from permanent deformations, say in the lateral direction, Eq. 4 is no longer applicable since the total lateral stress may change during cyclic loading. This is shown in Fig. 5 which shows results from undrained cyclic torsional tests on hollow cylindrical specimens by Yasuda (10). Fig. 5(*a*) shows a case where the total lateral stress, σ_h, was kept constant but the lateral boundary was allowed to deform permanently during cyclic loading (similar to cyclic triaxial tests); the cyclically-induced pore water pressure is limited and probably controlled by a relationship somewhat similar to Eqs. 1–4. Fig. 5(*b*) shows a case where permanent lateral displacement was not allowed; σ_h increases and eventually becomes equal to σ_v and the pore water pressure also increases and becomes essentially equal to σ_v.

For horizontal soil deposits where the lateral boundary condition is probably closer to that of no permanent lateral displacement because of lateral symmetry, it is likely that the pore water pressure can increase to the value equal to σ'_v because the total lateral stress can change during cyclic loading. Therefore, the author's Eq. 3 is considered to be not appropriate for determining the maximum residual pore water pressure that can develop in horizontal soil deposits.

Appendix.—References

9. Banerjee, N. G., Seed, H. B., and Chan, C. K., "Cyclic Behaviour of Dense Coarse-Grained Materials in Relation to the Seismic Stability of Dams," *Earthquake Engineering Research Center Report No. UCB/EERC-79/13,* University of California, Berkeley, Calif., June, 1979.
10. Ishihara, K., "On Determination of Liquefaction Parameters," *Dynamical Methods in Soil and Rock Mechanics, Proceedings, Karlsruhe,* G. Gudehus, ed., Vol. 2 *Plastic and Long-term Effects in Soils,* 1978, pp. 189–193.
11. Marachi, D. N., Chan, C. K., Seed, H. B., and Duncan, J. M., "Strength and Deformation Characteristics of Rockfill Materials," *Report No. TE 69-5,* University of California, to State of California Department of Water Resources, Berkeley, Calif. 1969.

12. Seed, H. B., "Considerations in the Earthquake-Resistant Design of Earth and Rockfill Dams," *Nineteenth Rankine Lecture, Geotechnique*, Vol. XXIX, No. 3, 1979, pp. 215–263.

Closure by Edward G. Prater[4]

The sole discussion contribution is from Moriwaki and Power. The main point raised concerns the importance of sample boundary conditions in relation to horizontal soil deposits. For this field condition lateral restraint under strong shearing action requires that the associated inelastic strains occur in a vertical direction only. In the triaxial test, the sample is subjected to constant stress boundary conditions. The sample deforms as a cylinder without constraining any of the principal strains to maintain a zero value. Thus quite different stress paths are involved in the two cases. This is an important consideration and the writer is grateful to the discussers for introducing it. They also refer in this connection to the cyclic torsional tests on hollow cylindrical samples of Yasuda reported by Ishihara (10). The writer wishes to consider these tests in greater detail, but beforehand some more minor points in the discussion are dealt with.

Firstly, the discussers write Eq. 1 in terms of the minor principal stress and substituting for M (Eq. 2) they introduce $\sin \phi'$ directly. The basic equation is not modified so the use of the word similar is inappropriate. In Ref. 15 the writer has also expressed the relation in terms of σ'_{3c}.

The writer had also observed (p. 115) that the induced pore pressures can transiently exceed the residual value, even in the case of dense gravels. This pattern of response is sometimes described as "liquefaction-dilation" (16). The writer, however, would like to stress again the importance of considering changes in the grain matrix. As indicated in Fig. 1 if the structure collapses, the initial anisotropic stress state is lost and the effective stress path rapidly moves to the origin in accordance with a truly liquid state. In the paragraph concerned with loose horizontal soil deposits (p. 113) the aim was not to find the residual pore pressure (although unfortunately the author retained the same designation, Δu_r), but simply to point out that the failure envelope may be reached during a cycle before Δu reaches the value p'_o. Thus the discussers final remark is not directly relevant to the writer's intention. This, however, brings out the point as to when it is appropriate, generally, to use Eq. 1. The condition is obvious: if the state of total stress after the seismic disturbance is the same as before. Not only in horizontal deposits, but also in any earth structure like a dam, if the stresses are redistributed the induced pore pressure will change accordingly. The question remains to be investigated, however, as to what extent the static stresses are changed for loose and dense deposits, respectively.

It is encouraging that more data are becoming available for gravel samples, see Fig. 4. The writer would like to take this opportunity to present a more accurate description of the friction angle for the gravel tested. The strength envelope is, in fact, curved with the following empirical relation for $\gamma_d \simeq 2.28$ kg/cm^3 ($Dr \simeq 85\%$)

[4]Research Engr., Federal Inst. of Tech. Zurich, Inst. of Foundation Engrg. and Soil Mechanics, ETH-Honggerg, 8093 Zurich-Switzerland.

$$\phi' = 58.7 - 13.3 \log \left(\frac{\sigma'_{3c}}{p_{atm}} \right) \quad \ldots \ldots \ldots

value of $M = 1.25$, (line OB), i.e., $\phi' = 31°$. However, for reasons of static equilibrium, if the internal and external radial pressures are equal, the stress component σ_θ must equal σ_h, (13). This suggests that the stress conditions in the specimen are far from being uniform. In the case of the second test [Fig. 5(*b*)] radial strain is prevented and the shearing action cases the state of stress to be transformed to a hydrostatic one (point D). The initial deviator stress is eliminated so that the specimen is now sheared in the reverse direction in terms of the p'-q diagram.

There is an obvious need to more closely examine the state of stress and influence of end restraint in torsional tests on hollow cylinders. The proposed equation (Eq. 1) should also be verified for other tests, e.g., the true triaxial test.

Appendix.—References

13. Ishibashi, I., and Sherif, M. A., "Soil Liquefaction by Torsional Simple Shear Device," *Journal of the Geotechnical Engineering Division*, ASCE, Vol. 100, No. GT8, Proc. Paper 10752, Aug., 1974, pp. 871–888.
14. Ishihara, K., and Okada, S., "Yielding of Overconsolidated Sand and Liquefaction Model under Cyclic Stresses," *Soils and Foundations*, Vol. 18, No. 1, Mar., 1978, pp. 57–71.
15. Studer, J., Zingg, N., and Prater, E. G., "Investigation of the Cyclic Stress-Strain Characteristics of Gravel Material," *Proceedings of the 7th World Conference on Earthquake Engineering*, Vol. 3, Sept. 1980, pp. 355–361.
16. Townsend, F. C., and Mulilis, J. P., "Laboratory Strength of Sands under Static and Cyclic Loadings," *Research Report S-76-2, No. 6*, United States Army Engineer Waterways Experiment Station, June, 1979.
17. Vaid, Y. P., and Liam Finn, W. B., "Static Shear and Liquefaction Potential," *Journal of the Geotechnical Engineering Division*, ASCE, Vol. 105, No. GT10, Proc. Paper 14909, Oct., 1979, pp. 1233–1246.

Self-Boring Pressuremeter Study of San Francisco Bay Mud[a]

Discussion by Thomas C. Anderson[3] and Robert G. Lukas,[4] Members, ASCE

The work of Clough and Denby is to be commended for the advancement of the state of the art for techniques and use of the self-boring pressuremeter in soft clay. The writers wish to discuss the use of s_u/p ratios from the laboratory UU and vane tests and the comparisons with similar ratios derived from CU triaxial tests.

---

[a]January, 1980, by G. Wayne Clough and Gordon M. Denby (Proc. Paper 15148).
[3]Sr. Geotechnical Engr., Engrs. Testing Labs., Inc., P.O. Box 21387, Phoenix, Ariz. 85036.
[4]Principal Engr., Soil Testing Services, Inc., Northbrook, Ill.

Since the soft clay at both sites is slightly overconsolidated, it would appear to be more appropriate to relate the undrained shear strength (s_u) from the laboratory UU and vane tests to the preconsolidation pressure (p_c), instead of the present effective overburden pressure (p). This is especially applicable for comparisons of this strength ratio with the results of CU triaxial tests, since the triaxial samples were reconsolidated to stress levels well above the in-situ stress levels and, thus, were on the virgin consolidation curve prior to shearing.

In 1957, Skempton established the following empirical correlation for normally consolidated soils (20):

$$\frac{s_u}{p} = 0.11 + 0.0037\,(\text{PI}) \quad \ldots\ldots\ldots\

resulted in a closer prediction of the field s_u/p ratio than CU triaxial tests, which overestimated the strength ratio by 25% or more. Are DSS test results available for the Bay Mud at these two sites? Gardner (17) indicated an undrained strength ratio of 0.25 for a DSS test on San Francisco Bay Mud with a PI of 45%, while a strength ratio of 0.35 was determined from a triaxial compression test. This DSS test strength ratio is in close accord with the s_u/p ratios computed from Eq. 1 and also the s_u/p_c ratios for the two sites.

Based on the foregoing comments, the writers conclude that the strength ratios predicted by Eq. 1 and the DSS test are in reasonable agreement with the indicated s_u/p_c ratios for the two sites. These three undrained strength ratios are felt to be most indicative of the actual field strength ratio. As a result, the writers believe that the strength ratios determined from the CU triaxial tests considerably overestimate the field strength. Since the strength values derived from the pressuremeter tests are higher than the CU triaxial tests results, the pressuremeter results also appear to greatly overstate the in-situ strength.

Appendix.—References

15. Anderson, T. C., and Lukas, R. G., "Preconsolidation Pressure Predicted Using $s_u/\bar{p}$ Ratio," *Proceedings of ASTM STP Symposium on Shear Strength of Soils*, June, 1980.
16. Duncan, J. M., and Buchignani, A. L., "Failure of Underwater Slope in San Francisco Bay," *Journal of the Soil Mechanics and Foundation Division*, ASCE, Vol. 99, No. SM9, Proc. Paper 10019, Sept., 1973, pp. 687–703.
17. Gardner, W. S., "Soil Property Characterization in Geotechnical Engineering Practice," *Association of Drilled Shaft Contractors Magazine*, Jan., 1980, p. 28–72.
18. Ladd, C. C., "Test Embankment on Sensitive Clay," *Performance of Earth and Earth-Supported Structures*, ASCE, Vol. 1, Part 1, 1972, pp. 101–128.
19. Ladd, C. C., Rixner, J. J., and Gifford, D. C., "Performance of Embankments with Sand Drains on Sensitive Clay," *Performance of Earth and Earth-Supported Structures*, ASCE, Vol. 1, Part 1, 1972, pp. 211–242.
20. Skempton, A. W., "Discussion. The Planning and Design of the New Hong Kong Airport," *Proceedings of the Institution of Civil Engineers*, No. 7, 1957, pp. 305–307.
21. Wu, T. H., Chang, N. Y., and Ali, E. M., "Consolidation and Strength Properties of a Clay," *Journal of Geotechnical Engineering Division*, ASCE, Vol. 104, No. GT7, Proc. Paper 13891, July, 1978, pp. 889–905.

Discussion by J. C. P. Dalton[5]

The instrument described by G. W. Clough and G. M. Denby is now much improved. It is sufficiently different to warrant separate comments.

A special protective sheath for the membrane has been developed. It is a composite of stainless steel and rubber that is axially stiff to resist friction forces on insertion and withdrawal but radially, it is very compliant. From the appearance of early models of this device it is known as a Chinese Lantern. It consists of a series of narrow, thin, stainless steel strips which butt together around the periphery of the instrument. These strips are partly bonded on their inside to a thin rubber sleeve which serves only to exclude dirt from getting between the strips during the expansion phase. The sleeve seals no pressure

[5]Dir., Cambridge Inst., Little Eversden, Cambridge CB3 7HE, England.

and adds only a negligible amount to the membrane correction.

These bonded lanterns have proved very reliable and easy to use and they provide such good protection that the membrane puncturing described by Clough and Denby is no longer a problem. One membrane now normally lasts for the life of a lantern, often longer.

Concurrent with the development of the Chinese Lantern, a membrane more resistant to abrasion has been developed. It is made of a polyurethane polymer, Du Pont Adiprene L.42, by injection moulding techniques. Examples of this membrane only twice as thick as that used by Clough and Denby have proved capable of use without Chinese Lantern protection in stiff clay of 700 kN m^{-2} undrained shear strength.

The San Francisco Bay Mud is insensitive to effects due to the rate of loading. However the fact remains that many materials are rate-sensitive. A unit has been developed to carry out tests at a constant rate of strain, completely automatically. A soft-start control system is incorporated which, by limiting the rate of pressure rise to a preset maximum, permits the point at which the membrane lifts off the instrument and, thus, the in-situ stress to be accurately discovered. Ten rates of strain are provided both up and down, together with the ability to hold the strain constant at any value indefinitely. Thus not only can unloading and reloading loops be carried out, giving a reload modulus, but also the changes in stress caused by a given expansion can be monitored as they take place by observing the pressure being supplied to maintain a set expansion. Carrying out the whole test automatically also frees the operator for monitoring the progress of the test and also frees the test from the effects of the operator.

Recent work on in situ stresses behind a retaining wall has shown that the ability to measure the radial strain at each individual strain arm position is very important. Previously only the total strain registered at the three arms together was read out. The smooth curve of total strain versus total pressure can conceal distinct changes in the slope of the pressure-strain graph if the changes occur at different values at each strain arm. The modification to read individual arms will, with care used when inserting the instrument, provide useful data on anisotropy.

Finally, Clough and Denby mention that advancing of the instrument is by trial and error. Recent work by, among others, Clark (2) unpublished communication, has shown that it is possible to be a great deal more certain in the initial setting of the cutter. This, coupled with changes in the cutter geometry, have meant that it is no longer a procedure of trial and error to determine the correct cutter setting. It is also possible, even in stiff clay, to attain driving rates up to a meter of drilling in 10 min.

Closure by G. Wayne Clough[6] and Gordon M. Denby[7]

The writers appreciate the interest shown in the paper by Dalton, and Anderson and Lukas through their thorough discussions. Dalton provides a review of

[6]Prof. of Civ. Engrg., School of Engrg., Stanford Univ., Stanford, Calif. 94305.
[7]Sr. Engr., Golder Assoc., Seattle, Wash.

recent improvements which have been made to the Cambridge type self-boring pressuremeter. This is very appropriate since the device used by the writers is one of the early models. Clearly the reliability of the probe and the sensitivity of the system have been enhanced. However, even with the new modifications, potential users should be aware that problems will still occur in the case of conditions such as encountered by the authors at China Basin (Site II). Here, shell layers existed in the clay which clogged the probe, and likely disturbed the clay as shell fragments were pushed or dragged by the edges of the cutting shoe. Further, ground currents interfered with the recording system. Careful consideration needs to be given to potential problems like these before embarking on a self-boring pressuremeter test program.

Anderson and Lukas are concerned with defining an undrained "field" strength, and suggest an empirical equation for this purpose based on plasticity index and preconsolidation load. They conclude that it is more desirable to define an undrained "field" strength by their equation or undrained direct simple shear tests than by CU triaxial compression or self-boring pressuremeter tests. The writers are in agreement that it would be nice to have a simple empirical or single test type approach towards determining the field shear strength. However, this implies that there is one strength for a soil regardless of degree of anisotropy, stress path, or importance of creep effects. In fact, this is not the case, and the comparisons made by Anderson and Lukas between results from different types of tests ignore this. For example, it is well known that a CU triaxial test typically yields a higher undrained shear strength than does a direct simple shear test due to effects of anisotropy. Of course, this does not invalidate that CU test; rather, the results from this test provide one point on a strength curve, which, for design purposes, should be delineated in terms of stress path, anisotropy, and creep effects. Data obtained by the self-boring pressuremeter should be viewed in the same light. Prevost (11,12) has provided useful theoretical findings in this regard.

In their discussion, Anderson and Lukas utilize data from the writer's paper as well as that from the paper by Duncan and Buchignani (16) to develop an estimate of the field shear strength of San Francisco Bay Mud. The writers feel that the approach used in this exercise is not soundly based, for a number of reasons:

1. Data from UU triaxial tests and laboratory vane tests are used to justify the results obtained by the discussors' empirical equation without question as to whether the laboratory tests are appropriate to define a field strength.

2. Data from Bay Mud sites are compared without due consideration given that the minerology and sensitivity of Bay Mud varies from site to site and sometimes over small distances. Bay Mud is a generic term covering soils ranging from sands to high plasticity clays. Thus, some Bay Muds are subject to factors such as creep strength loss or strong peak-residual stress-strain response, which affect the field strength, while others are not.

3. There is no acknowledgement that Duncan and Buchignani (16) had to reduce their UU test results by 30% for sustained loading effects to obtain a field strength value consistent with the observed field behavior. Making this allowance leads to strength value below that obtained by the Anderson and Lukas equation.

Finally, Anderson and Lukas ask if there are published DSS test data for San Francisco Bay Mud. To the writers' knowledge, this information is not available. However, Duncan (4) has reported a series of carefully performed active and passive loading tests which yielded S_u/p ratios of 0.37 and 0.28 for the Bay Mud at Hamilton Air Force Base. Since the DSS test commonly yields a strength about halfway between that defined by active and compression loading, the DSS strength could be expected to be about 0.33. The point made by Anderson and Lukas concerning a need for DSS data however, is well placed, and the senior writer of the paper intends to undertake these tests in the near future.

In sum, the writers remain of the opinion that the self-boring pressuremeter offers promise as a means to define the properties of a soft clay soil. In particular, it should be reiterated that the device is useful because it not only can determine the shear strength of a soil, but also the stress-strain and pore pressure response and the lateral stress in the ground. Additional research is needed in order to more fully understand the effects of important key parameters such as rate of loading, insertion technique, and cutter setting.

Settlement Comparison Used in Tank-Failure Study[a]

Discussion by Robert E. Bigham,[3] M. ASCE

The authors have presented a fascinating analysis of failure of a large tank, and they make a strong case that the failure was caused principally by a deficient weld.

The writer has controlled loading of several tanks on soft foundations, and was initially suspicious of the increase in maximum settlement at about a 60.7-ft (18.5-m) load, and decided to make his own analysis of the data of Fig. 4. Bell later provided a larger chart similar to Fig. 4 showing actual data points upon request by the writer. Analysis of those data yielded the same conclusion as was reached based on the smaller chart, and this discussion refers only to the data shown on Fig. 4, as extracted by the writer. Any error in the writer's extraction of data is solely his responsibility.

The writer agrees with the authors that there was no soil bearing capacity failure at Tank T-270, either during loading or later.

The writer analyzes data from tank loading differently than as sometimes seen in the literature, and the method may be of interest to the authors and some others who load tanks.

---

[a]February, 1980, by Roy A. Bell and Jun Iwakiri (Proc Paper 15219).

[3]Engr., Spencer J. Buchanan & Assoc., Inc., Consulting Engrs., P.O. Box 672, Bryan, Texas 77801.

The writer's method is based on the theory that, so long as loads do not approach the then current ultimate bearing capacity too closely, the change in settlement within a standard time after a change in load will bear a constant proportion to the change in the load, and that the postulated constant proportion is characteristic of the combination of site and structure.

With small changes in load, this can be the principal control for loading a tank, and a chart of load versus settlement is all that is required to apply it to loads following the initial load. The initial load can be selected by a simple estimate of ultimate bearing capacity and a large, e.g., four or five, safety factor.

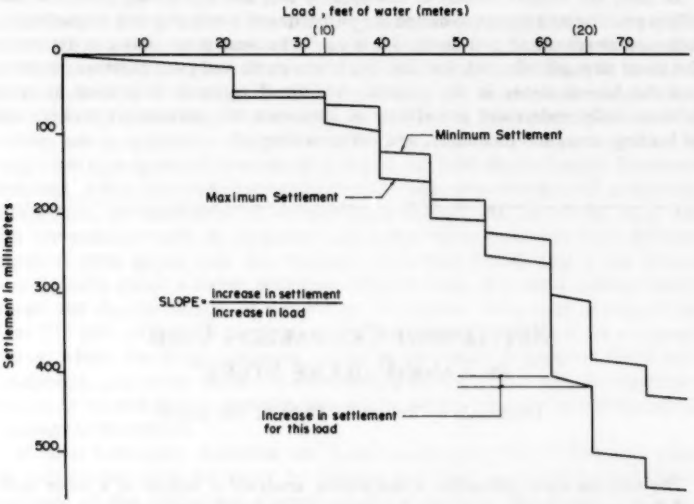

FIG. 16.—Load Settlement Chart Tank T-270

A disproportionately large (based on history at the particular site) increase in settlement following an increase in load is, according to the writer's theory, an indication that loading is approaching ultimate bearing capacity more closely than under the previous load. With small, e.g., 1-ft min, up to perhaps 2% or 3% of existing load, changes in load, this is a warning and not a bearing capacity failure. It can even be observed as a trend developing during several small changes in load. The writer increases load every working day unless warned by the chart or other evidence. When the chart gives a warning, loading is stopped, and a wait for consolidation ensues. At such a time, a chart of time versus settlement similar to Fig. 4 is useful as a index of consolidation and gives guidance on resuming loading.

Fig. 16 shows the writer's analysis of data extracted from Fig. 4. The end points are the settlement for the last day of a particular load and the settlement for the first day of the next load. The vertical lines represent continuing settlement at constant load. It can be seen that the slopes of the segments connecting

end points are all about the same, even for the last increase, and even though the 60.7-ft (18.5-m) loading changed the load from less to more than the preload. To the writer's way of thinking, this goes further to show that there was no bearing capacity failure during loading or later at Tank T-270.

This method is equally applicable to cases of large settlement, as at Tank T-270, or small settlement, or small tanks, and has been a valuable aid to the writer's judgment. It does require many (sometimes twice daily) measurements of settlement. If changes in settlement are as large as 0.01 ft (3 mm), it is possible to rig cheap reliable water levels that reduce the time required for observation to the time required to walk around the tank and make the observations a one-man job.

Closure by Roy A. Bell,[4] M. ASCE and Jun Iwakiri[5]

The discussion by Bigham presents still another empirical method of evaluating tank settlement data that could be a useful supplement to other methods of tank settlement data interpretation. The fact that it emphasizes conditions during periods of adding water load could provide an early warning signal of impending instability; but since it ignors rates of settlement during periods of constant load, other means of settlement evaluation should continue to be used in addition to Bigham's method.

Errata.—The following corrections should be made to the original paper:

Page 167, Fig. 13, the formula for Θ: Should read

$$\Theta = \arctan -\left(\frac{\Sigma z_i \cos \alpha_i}{\Sigma z_i \sin \alpha_i}\right) \text{ instead of } \Theta = \arctan \left(\frac{\Sigma z_i \cos \alpha_i}{\Sigma z_i \sin \alpha_i}\right)$$

Page 167, Fig. 14, the formula for δ': Should read $\delta' = \left[s'_j - \frac{(s'_{j-1} + s'_{j+1})}{2}\right] \times \frac{100\%}{L}$ instead of $\delta' = s'_j - \left[\frac{(s'_j - 1 + s'_j + 1)}{2}\right] \times \frac{100\%}{L}$

Page 168, Fig. 15, the formula for n: Should read $n = \frac{\pi D}{2L}$ instead of $n = \frac{D}{2L}$

The example: Should read $n = \frac{\pi\, 51.54}{2\,(20.24)} = 4.00$

$$W_{max} = \left[\frac{2(4.00)^2\, 14.6}{51.54}\right] 0.014 = 0.13 \text{ m instead of } n = \frac{51.54}{2(20.24)} = 1.273$$

$$W_{max} = \left(\frac{2(1.273)^2\, 14.6}{51.54}\right) 0.014 = 0.013 \text{ m}$$

Further corrections to Figs. 8, 13, and 14 can be obtained from the first author.

[4]Sr. Engr., Dames & Moore, 500 Sansome St., San Francisco, Calif. 94111.

[5]Mgr., Civ. Engrg. Dept., Chiyoda Engrg. and Construction Co., Ltd., Yokohama, Japan.

REPEATED LOADING ON SINGLE PILES IN SAND[a]

Discussion by N. K. Jain[3] and Gopal Ranjan[4]

The authors, through careful experimentation have aptly identified the problem of repeated loading pile response. However, the conclusions are no more than would be expected and hardly general enough for use in design. In the writers' opinions, analysis of data in nondimensional form would have been more useful.

Test piles have been pushed into a medium dense dry sand deposit using a hydraulic jack. It would be of interest to know the initial relative density of sand and the change on account of driving. A surcharge pressure of 100 KN/m^2 (14.5 psi) was applied on the sand pressure. However, the authors have not indicated any reasons for choosing this value and if any movement of pile was observed due to the application of surcharge.

On the basis of observed pile top movement, the authors have identified two distinct type of behavior with the dividing line between 0.25 Qc/O–0.30 Qc/O. The upward pile movement after first cycle for smaller loads has been attributed to reduction in elastic compression and redistribution of residual stresses. In the writers' opinion, the surcharge pressure value is likely to influence the dividing line. Therefore, smaller/large loads need be defined in relation to the applied surcharge pressure.

Closure by Sin-Fatt Chan,[5] M. ASCE and Thomas H. Hanna[6]

We thank Jain and Ranjan for their contribution. The purpose of this research work was to examine the general mechanics of long piles when subjected to slow repeated loadings. This work is not intended to be used directly for full-scale design but more to enable full-scale testing programs to be drawn up; consequently, we believe that many of the variables and factors isolated in this work are significant and worthy of study.

The piles were driven with the surcharge pressure in place and, therefore, it is very difficult to know precisely what the relative density change was due to pile insertion. The value of 100 kN/m^2 of surcharge pressure was chosen

[a]February, 1980, by Sin-Fatt Chan and Thomas H. Hanna (Proc. Paper 15222).

[3]Research Scholar, Dept. of Civ. Engrg., Univ. of Roorkee, Roorkee 247672, India.

[4]Prof., and Head, Geotechnical Engrg., Dept. of Civ. Engrg., Univ., of Roorkee, Roorkee 247672, India.

[5]Lect., Dept. of Civ. Engrg., Univ. of Malaya, Kuala Lumpur, Malaysia.

[6]Prof., Dept. of Civ. and Structural Engrg., The Univ. of Sheffield, Mappin St., Sheffield, S1 3JD, England.

as a convenient value to raise the stress level of the sand in the vicinity of the pile. Its value was dictated in part by structural considerations of movement of the sand container and the patterns of behavior established are controlled by many variables, including load level and load amplitude. Also the initial residual stress system locked in the pile as a result of installation is extremely important. It is quite clear to us that much more work has to be done before full understanding of pile behavior under slow repeated loading is available. The suggestion that the dividing line between distinct types of behavior is related to the value of the applied surcharge pressure is interesting. To date this has not been investigated.

Technical Papers

Original papers should be submitted in triplicate to the Manager of Technical and Professional Publications, ASCE, 345 East 47th Street, New York, N.Y. 10017. Authors must indicate the Technical Division or Council, Technical Committee, Subcommittee, and Task Committee (if any) to which the paper should be referred. Those who are planning to submit material will expedite the review and publication procedures by complying with the following basic requirements:

1. Titles must have a length not exceeding 50 characters and spaces.

2. The manuscript (an original ribbon copy and two duplicate copies) should be double-spaced on one side of 8-1/2-in. (220-mm) by 11-in. (280-mm) paper. Three copies of all figures and tables must be included.

3. Generally, the maximum length of a paper is 10,000 word-equivalents. As an *approximation*, each full manuscript page of text, tables or figures is the equivalent of 300 words. If a particular subject cannot be adequately presented within the 10,000-word limit, the paper should be accompanied by a rationale for the overlength. This will permit rapid review and approval by the Division or Council Publications and Executive Committees and the Society's Committee on Publications. Valuable contributions to the Society's publications are not intended to be discouraged by this procedure.

4. The author's full name, Society membership grade, and a footnote stating present employment must appear on the first page of the paper. Authors need not be Society members.

5. All mathematics must be typewritten and special symbols must be identified properly. The letter symbols used should be defined where they first appear, in figures, tables, or text, and arranged alphabetically in an appendix at the end of the paper titled Appendix.—Notation.

6. Standard definitions and symbols should be used. Reference should be made to the lists published by the American National Standards Institute and to the *Authors' Guide to the Publications of ASCE*.

7. Figures should be drawn in black ink, at a size that, with a 50% reduction, would have a published width in the *Journals* of from 3 in. (76 mm) to 4-1/2 in. (110 mm). The lettering must be legible at the reduced size. Photographs should be submitted as glossy prints. Explanations and descriptions must be placed in text rather than within the figure.

8. Tables should be typed (an original ribbon copy and two duplicates) on one side of 8-1/2-in. (220-mm) by 11-in. (280-mm) paper. An explanation of each table must appear in the text.

9. References cited in text should be arranged in alphabetical order in an appendix at the end of the paper, or preceding the Appendix.—Notation, as an Appendix.—References.

10. A list of key words and an information retrieval abstract of 175 words should be provided with each paper.

11. A summary of approximately 40 words must accompany the paper.

12. A set of conclusions must end the paper.

13. Dual units, i.e., U.S. Customary followed by SI (International System) units in parentheses, should be used throughout the paper.

14. A practical applications section should be included also, if appropriate.